National Aeronautics and Space Administration

Langley Research Center

Hampton, Virginia 23365

NASA RESEARCH GRANT NGR 31-001-221

Title: Investigation of Structure-Property Relationships in Systematic Series of Novel Polymers

Annual Report

Period Covered 3/1/73 - 2/28/74

Princeton University

Polymer Materials Program

Chemical Engineering Department

August 1974

J. K. Gillham

Principal Investigator

The following publications are included:

* *Thermomechanical Behavior of a Polynorbornadiene.* M. B. Roller, J. K. Gillham and J. P. Kennedy, Journal of Applied Polymer Science, Vol. 17, 2223-2233(1973). N73-14596

* *Low-Temperature Relaxations in Amorphous Polyolefins.* A. Hiltner, E. Baer, J. R. Martin and J. K. Gillham, Journal of Macromolecular Science-Physics, Vol. B(9), No. 2, 255-266(1974).

* *Thermomechanical Behavior of Amorphous Tactic Methacrylate Polymers.* E. Kiran, J. K. Gillham and E. Gipstein, Journal of Macromolecular Science-Physics, Vol. B(9), No. 2, 341-366 (1974).

* *Isothermal Transitions of a Thermosetting System.* J. K. Gillham, J. A. Benci, and A. Noshay, Journal of Applied Polymer Science, Vol. 18, 951-961 (1974).

Low Frequency Thermomechanical Spectrometry of Polymeric Materials: Computerized Torsional Braid Experiments - I. Overview. Y. Hazony, S. J. Stadnicki and J. K. Gillham, American Chemical Society, Polymer Preprints, Vol. 15, No. 1, 549-555(1974).

Low Frequency Thermomechanical Spectrometry of Polymeric Materials: Computerized Torsional Braid Experiments - II. Data Processing. S. J. Stadnicki, J. K. Gillham and Y. Hazony, American Chemical Society, Polymer Preprints, Vol. 15, No. 1, 556-561 (1974).

Low Frequency Thermomechanical Spectrometry of Polymeric Materials: Computerized Torsional Braid Experiments - III. Tactic Polymethylmethacrylates. J. K. Gillham, S. J. Stadnicki and Y. Hazony, American Chemical Society, Polymer Preprints, Vol. 15, No. 1, 562-569 (1974).

* PAPERS INTENTIONALLY OMITTED

American Chemical Society, Polymer Preprints, Vol.15, No.1, 549-555(1974).

LOW FREQUENCY THERMOMECHANICAL SPECTROMETRY OF POLYMERIC MATERIALS: COMPUTERIZED TORSIONAL BRAID EXPERIMENTS - I. OVERVIEW.

Y. Hazony, Computer Center, Princeton University, Princeton, N. J., and S. J. Stadnicki and J. K. Gillham, Polymer Materials Program, Department of Chemical Engineering, Princeton University, Princeton, N. J. 08540

INTRODUCTION. Torsional Braid Analysis (TBA), a variant of the torsional pendulum technique, is a low frequency (∿ 1 Hz) dynamic mechanical method for determining the thermomechanical spectra of polymers (1). A TBA experiment may run over the course of several days and generate more than 1000 damped sine waves. Manual data reduction techniques to obtain the frequency and damping constant for each analog wave, using a stopwatch and graduated scale or even a strip-chart recorder, are slow and limited in accuracy.

It is because of difficulties in the data acquisition and data reduction procedures that the torsional pendulum has not developed to the level of being regarded as a thermomechanical spectrometer. The usefulness of the technique has been limited mainly to the monitoring of transition temperatures and time-temperature hysteresis phenomena. It is apparent that further extension of the scope of research employing the torsional pendulum will require a breakthrough in methodology.

A technological breakthrough will permit a deeper and more extensive study of problems, such as: a) Characterization of the thermomechanical spectra in terms of analytical expressions. Such analytical formulae will introduce new parameters to better characterize the spectra, and make it possible to resolve the temperature dependent data in terms of contributions from primary and secondary transitions. These developments could lead to a better understanding of the underlying physics and chemistry of the observed transformations; b) Comparison of the thermomechanical spectra of systematic series of related polymeric materials. This will allow verification of the structural origin of the observed phenomena; c) Time-temperature hysteresis phenomena. In such experiments the time-temperature cycle may be used as a well controlled variable in order to sort out the time constants which characterize the kinetics of the physical and/or chemical transformations; d) Non-linear mechanical effects. Inspection of typical dynamic mechanical response curves reveals that the derived parameters are amplitude dependent. Study of the amplitude dependence would provide additional parameters to characterize the thermomechanical behavior of polymeric materials; and e) Frequency dependence of the response function. It is possible to alter the frequency range of measurements by at least an order of magnitude by changing the specimen geometry and the inertial mass. This will be required to represent the thermomechanical spectra in frequency-independent form.

A factor common to the above experiments is the need for the acquisition of a large volume of data in a meaningful way. That is, the resolving power of the sensor system as well as that of the control functions must be such that the observed small differences between different experimental sequences be significantly larger than the experimental errors. Further, in order to be able to pursue such experiments, the reduced data must be consulted prior to the termination of the current experiment so that a timely decision with regard to the next step may be made.

The present paper discusses the results of the on-line interface of the TBA experiment to an Hierarchical Computer System for data acquisition, data reduction and control of experimental variables (2). Some experimental results are demonstrated and the data reduction procedures are outlined. Several modes of presentation of the final computer-reduced data are discussed in an attempt to elucidate possible interrelations between the thermal variation of the rigidity and loss parameters.

OVERVIEW OF THE DATA PROCESSING SYSTEM. An important guideline for the implementation of a computer network for laboratory application is that the success of a research project in a particular field should not depend on the proficiency of the researcher in computer technology. The experimentalist can benefit from the advantage of the batch computer with a minimal acquaintance with a high-level programming language such as Fortran. The computer

can be used in a rather sophisticated multi-level data reduction operation without knowledge of the inner workings of the particular computer or of sophisticated coding in machine or even assembler language. The "non-expert" use of the batch computer is quite common in theoretical work and in the present paper such an application with a laboratory TBA experiment is discussed.

The Hierarchical Computer System is designed to interface the laboratory experiment to the tremendous power of the large scale batch computer (IBM 360/91) for the purpose of the "on-line" processing of large volume of data with no involvement of the researcher in this stage of the data handling (2). In order to accomplish this on-line interface, two additional computers are interconnected in the hierarchical fashion between the experiment and the batch computer (Figure 1). The actual data acquisition is performed by a small real-time computer (IBM System 7) which serves as a digital front-end for the system. The front-end computer is equipped with a 20 Kcps analog-to-digital converter and an analog multiplexer providing for the simultaneous monitoring of many analog signals from one or several experiments. The incoming signals are digitized and tested by the front-end computer for the purpose of scan rate optimization as well as for other criteria which are imposed by the requirements of the final data reduction procedures by the central batch computer. Following this preliminary optimization and trimming of the data, it is coded for the purpose of data management and shipped to the central facility. In order to interface between the vastly different timing requirements of the real-time and batch computers, a third intermediate computer is used for data buffering and timing matching. In the initial design of the network, this role has been played by an IBM 1800 computer which has been recently replaced by an IBM 370/155 (Fig. 1) operating as the buffer computer for the real-time applications (in addition to providing time sharing services).

The advantage of the Hierarchical Computer System, as compared with the application of a dedicated minicomputer, is twofold: 1) it allows for maximum flexibility in the further development of the procedures for data acquisition and experimental control by the digital front-end, and 2) it sets the power of the central batch computer as the ultimate limitation on the magnitude and sophistication of the data reduction procedures. By separation of the two distinctly different functions, a high degree of optimization in the utilization of the resources of the hierarchical system is achieved.

The obvious disadvantage of the use of a batch computer in the environment of laboratory experiments is the rather slow turn-around time. Typically, it takes from one to several hours before the reduced data are available for consultation and for a decision to be made with regard to the following step of the experiment. For faster decisions having to do with the control of the sequence of the experiment, processing procedures must be developed for use by the digital front-end. The front-end would be used in such an instance as a mini-computer. It is clear, however, that there is a definite conflict between the two modes of operation. The trade-off requires that the amount of data processing going on in the digital front-end be kept at a minimum in order to maintain its power and flexibility for data acquisition and control. In the present application, a minimal amount of data processing by the front-end is concerned with setting the scan-rate, phase angle and amplitude boundary conditions. These have been in effect dictated by the optimization requirements of the processing routines in the central batch computer. The interplay between the processing power of the front-end in real-time and that of the central computer in the batch mode is a most important feature of the hierarchical system and can have a substantial conceptual impact on the design of the experiment.

OVERVIEW OF THE DATA REDUCTION PROCEDURES. The response function of the torsional pendulum to mechanical excitation is described to a good approximation by

$$\theta(t) = \theta_o e^{-\alpha t} \cos\omega(t-t_o) \qquad (1)$$

which is a solution to the equation of motion

$$\ddot{\theta} + 2\alpha\dot{\theta} + (\omega^2 + \alpha^2)\theta = 0 \qquad (2)$$

where θ is the amplitude, α is the damping constant and ω is the frequency in radians/sec. Eqn. 2 may be recast in complex format

$$\ddot{\theta} + (G' + iG'')\theta = 0 \qquad (3)$$

where G' and G'' are the in-phase and out-of-phase shear moduli, respectively. These expressions do not include effects of experimental non-linearity of transducers and circuits, noise, drift, as well as possible amplitude-dependent terms. Equation 1 is commonly used in the analysis of torsional pendulum data, manually or by dedicated analog and digital systems. This is done by monitoring the maxima to determine the frequency and the amplitude ratios to determine the damping constant. In the environment of the batch computer it is possible to apply universal methods of nonlinear least mean squares fitting. These are susceptible to generalizations designed to incorporate in the fitting procedures contributions due to noise, drift and non-linearities. If the sampling rate is very much faster than the frequency of oscillation it is possible to substitute

$$\dot{\theta}_j = (\theta_{j+1} - \theta_{j-1})/2\Delta t \qquad (4)$$

and

$$\ddot{\theta}_j = (\dot{\theta}_{j+1} - \dot{\theta}_{j-1})/2\Delta t$$

$$= (\theta_{j+2} + \theta_{j-2} - 2\theta_j)/4(\Delta t)^2 \qquad (5)$$

into Eqn. 2, resulting in (n-4) linear equations in terms of the n observations of the amplitude θ_j (j = 1....n). These may be solved by standard methods of *linear* least mean squares fit for the parameters α and $(\omega^2 + \alpha^2)$. The obvious advantages of the linear procedure is that it does not require initial estimates, and that it eliminates the need for iterations. An enormous computational simplification is obtained by the elimination of the use of exponentials and trigonometric expressions (Eqn. 1) in the fitting procedure.

In both cases (Eqns. 1 and 2) the interplay between the use of the computational powers of the digital front-end and the central batch computer plays a crucial role in the application of the above procedures in a fully automated mass-production effort of data analysis. The digital front-end is responsible for the scan-rate optimization over the range of change of the frequency and loss during a complete experiment. In using Eqn. 2 a faster scan-rate is employed to ensure the validity of the substitution of the derivatives. The second method (Eqn. 2) provides a straight forward and a more economical (in computing costs) approach to the data reduction problem than the first one (Eqn. 1).

In order to minimize effects of non-linearity in the behavior of the pendulum and the optical transducer, the front-end ensures that the data is being recorded within the correct boundary conditions with respect to the vibrational amplitude. The front-end also verifies the correct phase relationship of the data taken (equivalent to setting the t_o value in Eqn. 1). This requirement, which has been found necessary empirically, might have to do with the approximate nature of the correction for the baseline drift as done by a more generalized version of Eqn. 2 [see part II (3) of this paper].

In the early development of the computerized experimental setup, the linear least mean squares fitting procedure produced unacceptable scatter in the thermal variation of the loss parameter. Attempts were made to eliminate this scatter both by analog filtering (signal conditioning by hardware) and by digital filtering, the latter being pursued in the batch computer. This problem was first solved by the digital method using an iterative process to optimize the sample size with regard to the signal to noise ratio. The optimal signal to noise ratio was obtained when the least mean squares analysis was performed over an integral number of oscillations. The number of data points used in the analysis was determined by the frequency obtained in the previous iteration. Typically, the iteration procedure converged after three

cycles producing results as shown in Fig. 2. Later, as a result of improvements in the data monitoring hardware, the quality of the primary signals had been upgraded to the point of eliminating the need for digital filtering. This interplay between the analog and digital filtering in the optimization of the signal-to-noise ratio is another demonstration of the power and flexibility of the Hierarchical Computer System for laboratory application.

At the completion of the first level of data analysis (which had been described above), the reduced data is available in the batch computer in the form of the temperature dependence of two variables: the damping constant, α, and the relative in-phase shear modulus, $G' \propto \omega^2 + \alpha^2$. This particular presentation derives from the use of Eqn. 2 in the data reduction procedure. Alternative modes of data presentation may be derived from the use of Eqns. 1 and 3 (Table I). The logarithmic decrement is defined as the natural logarithm of the ratio of two successive maxima of the damped cosine function (Eqn. 1). The relative rigidity of the composite specimen is a simplification of the relative in-phase shear modulus, G' (elastic shear modulus), the two parameters being equivalent for low damping values. Absolute values are not specified for the above parameters because the configuration of the polymer-impregnated glass braid precludes precise measurements of dimensions. It is the relative thermal variation of the two parameters which is being monitored by the TBA technique.

In addition to the above forms of data presentation, derivatives of the reduced data with respect to temperature are calculated and plotted. These are obtained by a least mean squares fit of a third order polynomial, over nine consecutive temperature points, centered at the point of evaluation. The respective derivatives are given by the calculated coefficients of the appropriate terms in the fitted polynomial. The first derivative of G' with respect to temperature is shown in Fig. 2 together with the G' curve. Figures 3-5 present the loss data in three of the four ways summarized in Table I. A plot of tanδ data is not presented because it is very similar to that for the logarithmic decrement.

DISCUSSION. The experimental data shown in Figs. 3-5 represent one experiment where a sample of syndiotactic polymethylmethacrylate (4) has been monitored on cooling from 473°K to 93°K at a rate of 2 degrees per minute. There are noticeable differences between the various loss curves (Figs. 3-5) as well as the first derivative of the elastic shear modulus with respect to temperature (Fig. 2). The out-of-phase shear modulus, G" (inelastic shear modulus) is best suited for the purpose of resolving the α and β peaks. This is because the two maxima are better resolved and there is less ambiguity in the assignment of the "base-line" of the curve for more quantitative analysis.

A more significant difference between the various presentations is that they indicate slightly different transition temperatures (Table I) as determined by the respective maxima in the curves. Since all are derived from the same experimental data, the notion of a discrepancy between the assigned transition temperatures as obtained from the rigidity and loss curves, is unacceptable. A description of the data in terms of the inelastic (G") and the derivative of the elastic (d(G')/dT) shear moduli, provides internally consistent values of the transition temperatures. Figure 6 provides an expanded view of the Tg region for various modes of data presentation.

Inspection of the mathematical descriptions of the different presentations of the loss data (Table I), points to the origin of the observed differences in the derived transition temperatures. Since the frequency of the torsional pendulum enters differently in the expressions, the fact that it varies dramatically across the temperature region in which the phase transformation occurs, results in the apparent shifts in the observed maxima in the data. The description of the data in terms of the complex shear moduli (Eqn. 3) provides a unique determination of the transition temperature Tg and T_β, indicating that this presentation is preferable in the context of future attempts at theoretical discussions of the physics of the phase transitions.

It is noteworthy that while the G" and dG'/dT curves are quite similar in their gross features and are internally consistent insofar as the

transition temperatures are concerned, they are substantially different in the details and contain therefore complementary rather than redundant information.

REFERENCES

1. Gillham, J. K., "Torsional Braid Analysis -- A Semimicro Thermomechanical Approach to Polymer Characterization", CRC Critical Reviews in Macromolecular Science , 1, 83 (1972).
2. Hazony, Y., "Hierarchical Computing in Laboratory Experiments: Potential and Pitfalls", Computer Phys. Comm. 4, 279 (1972).
3. Stadnicki, S. J., Gillham, J. K., Hazony, Y., "Low Frequency Thermomechanical Spectrometry of Polymeric Materials: Computerized Torsional Braid Experiments - II. Data Processing", ACS, Polymer Preprints (this volume).
4. Gillham, J. K., Stadnicki, S. J., Hazony, Y., "Low Frequency Thermomechanical Spectrometry of Polymeric Materials: Computerized Torsional Braid Experiments - III. Tactic Polymethylmethacrylates", ACS, Polymer Preprints (this volume).

ACKNOWLEDGMENT. This work was supported in part by the National Aeronautics and Space Administration (Grants NGR 31-001-200 and NGR 31-001-221), by the Chemistry Branch of the Office of Naval Research (Contract N00014-67-A-0151-0024, Task No. NR 356-504) and by the Air Force Materials Laboratory (Contract F33615-72-C-1590). It is our pleasure to thank Messrs. Robert Cassidy and Peter Olenick of the Princeton University Computer Center for the development of the necessary system software and Mr. Colin Bell of the Natural Rubber Research Products Association, U.K., for his contributions in the early stages of this work.

TABLE I. DIFFERENT MODES OF DATA PRESENTATION - SYNDIOTACTIC PMMA.

	T_g, °K	T_β, °K
A. Rigidity* (G')		
$\omega^2 + \alpha^2$	399	295
Relative rigidity = ω^2	399	295
$\omega^2 - \alpha^2$	399	295
B. Loss Parameter		
$G'' = 2\alpha\omega$	399	294
Damping coefficient = α	401	300
Log decrement = $\Delta = 2\pi\alpha/\omega$	403	303
$\tan\delta = 2\alpha\omega/(\omega^2 + \alpha^2)$	403	303

*T_g values obtained from dG'/dT; the theoretical basis for the different rigidity parameters is discussed in, Nielsen, L. E., *Mechanical Properties of Polymers*, Chapter 7, Reinhold Publishing Corp., New York, 1965.

TBA AND PYROLYSIS LABORATORY

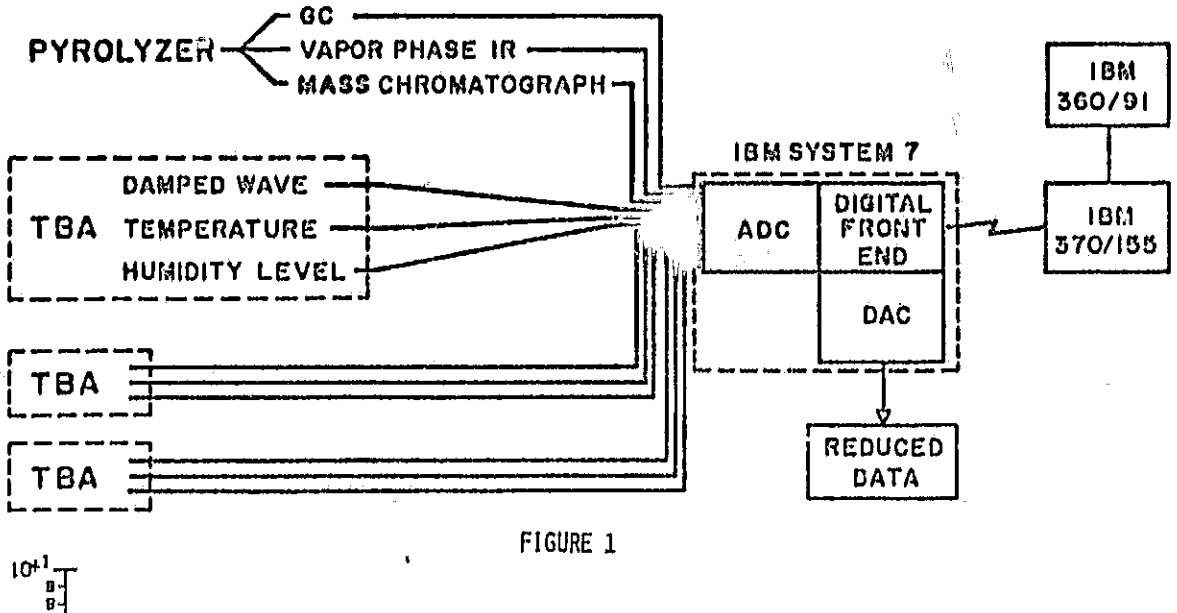

FIGURE 1

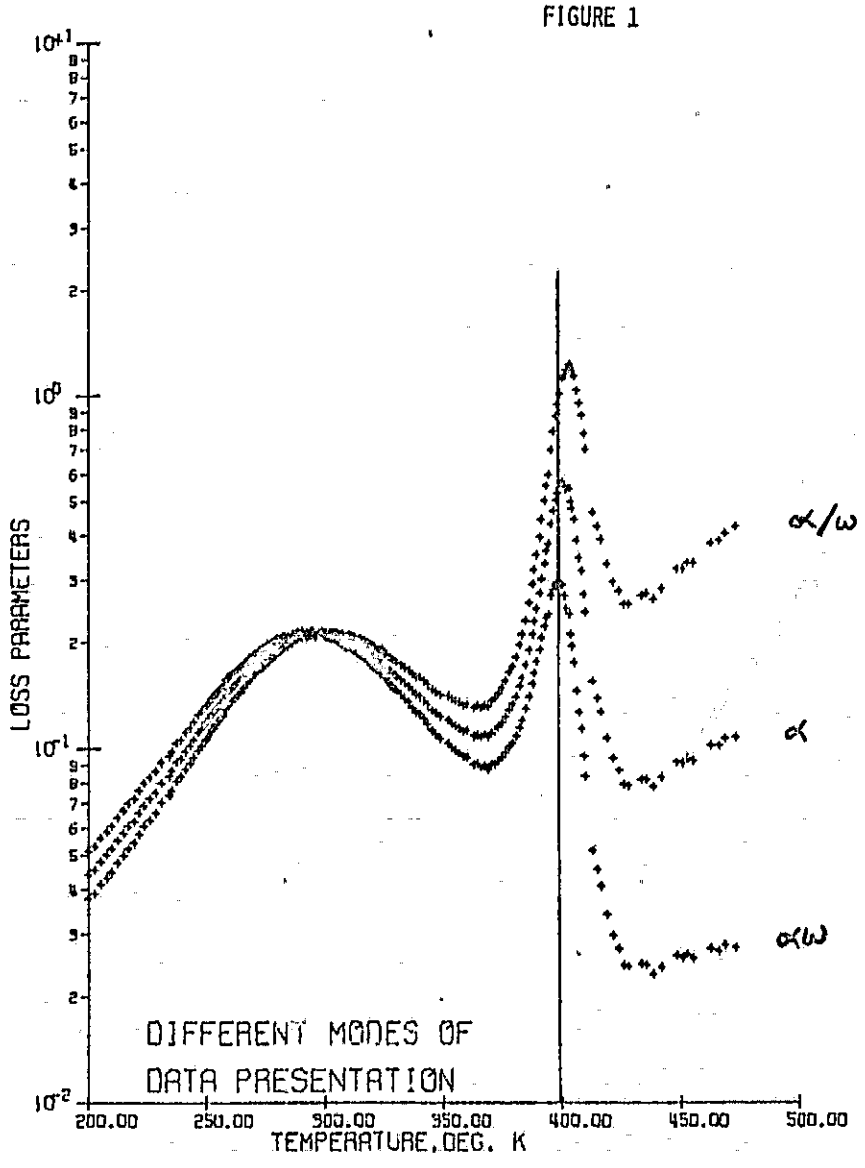

SYNDIOTACTIC PMMA

FIGURE 6

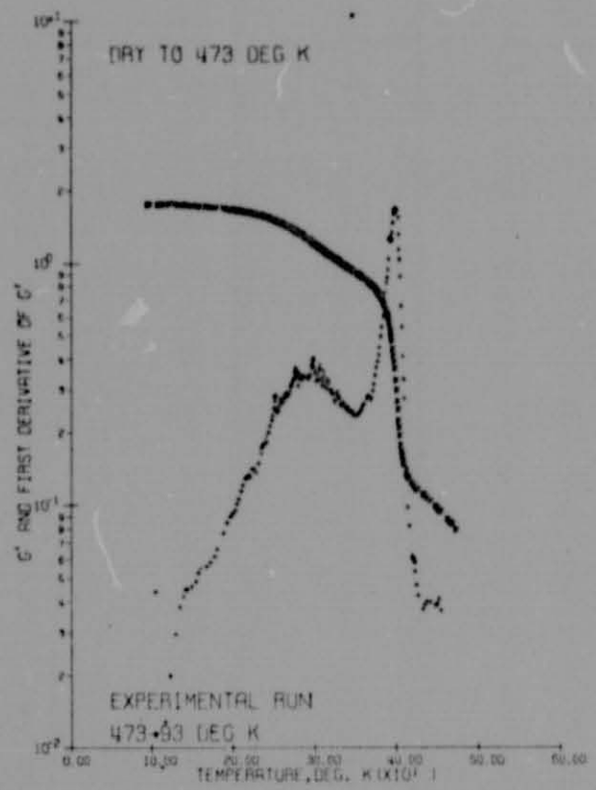

SYNDIOTACTIC PMMA

FIGURE 2

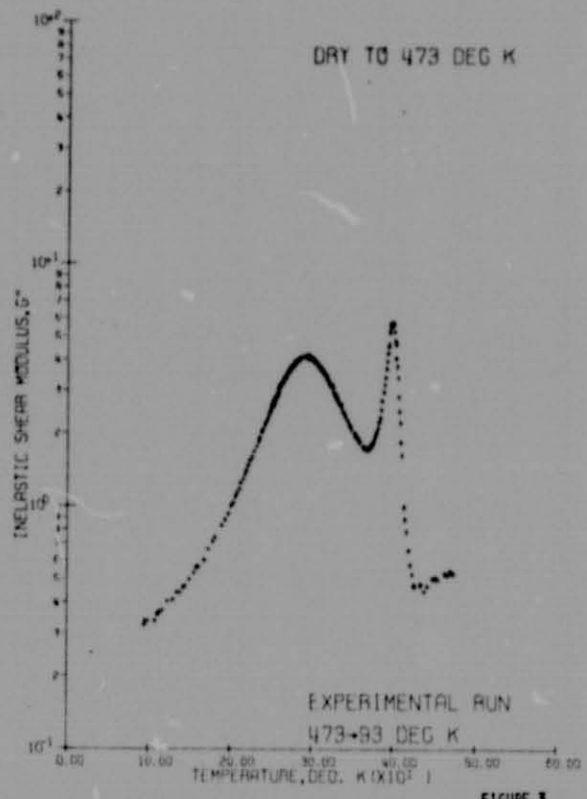

SYNDIOTACTIC PMMA

FIGURE 3

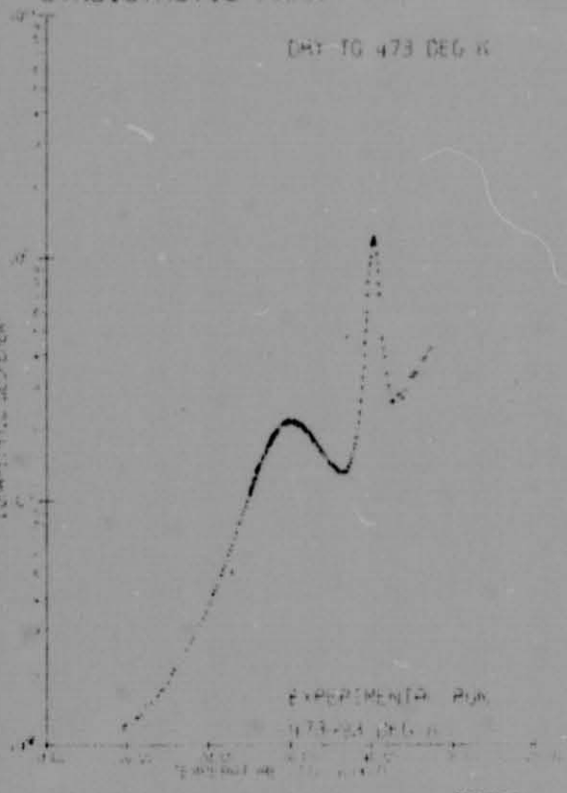

SYNDIOTACTIC PMMA

FIGURE 5

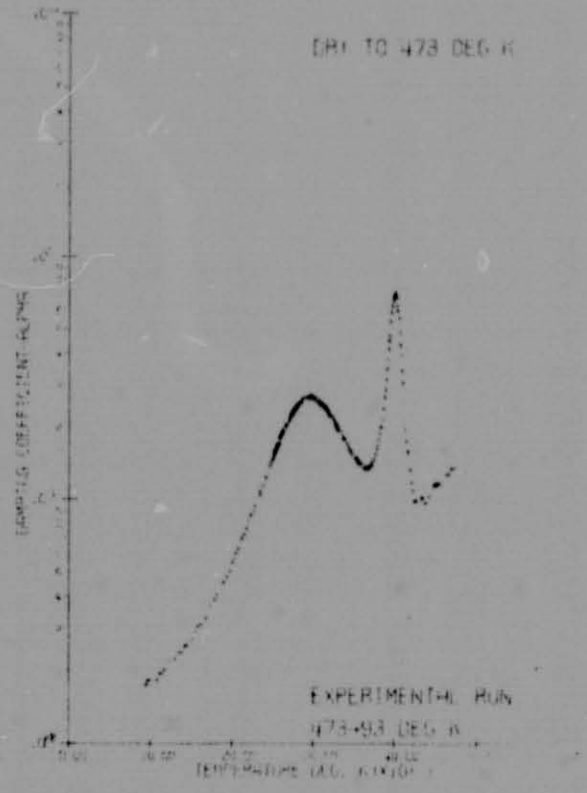

SYNDIOTACTIC PMMA

FIGURE 4

American Chemical Society, Polymer Preprints, Vol.15, No.1, 330-331(1974).

LOW FREQUENCY THERMOMECHANICAL SPECTROMETRY OF POLYMERIC MATERIALS: COMPUTERIZED TORSIONAL BRAID EXPERIMENTS - II. DATA PROCESSING.

S. J. Stadnicki and J. K. Gillham, Polymer Materials Program, Department of Chemical Engineering and Y. Hazony, Computer Center, Princeton University, Princeton, N. J. 08540.

INTRODUCTION. The effectiveness of torsional pendulum studies has been limited due to difficulties in processing large amounts of data. Manual data reduction techniques, to determine the rigidity and damping for each damped wave, using a stopwatch and graduated scale, or a strip-chart recorder, are slow and limited in accuracy. An overview of the Hierarchical Computer System used with a Torsional Braid Analysis (TBA) apparatus for fully automated data acquisition, reduction, and presentation has been described in Part I (1-3).The present manuscript deals with data processing.

On-line data acquisition and preprocessing are performed by a computer which is situated in the experimental laboratory. The data reduction program which employs a linear least mean squares fit of the data to the differential form of the equation of motion, is written in Fortran and is processed in a batch computer. An intermediate computer is employed for data buffering and for matching the time requirements of the batch computer. Evolution of the data reduction scheme is outlined.

INSTRUMENTATION. An IBM System/7 computer is employed in conjunction with a torsional braid apparatus for on-line data acquisition and preprocessing. At the time of this work, an Hierarchical Computer System was used with the data transmitted through an IBM 1800 computer (employed for data buffering) and then onto an IBM 360/91 batch computer for data reduction. The final presentation of the thermomechanical parameters as a function of temperature is obtained on a Calcomp Plotter. Presently,the data are sent by telecommunication from the System/7 directly to an IBM 370/155 computer which is attached to the IBM 360/91.

The capabilities of the present preprocessing facility are as follows:

1. Four digit analog to digital conversion.
2. Maximum scan rate of 20,000 samplings per second.
3. Running several simultaneous experiments.
4. Reduced data transmission directly to the laboratory.
5. Real time local control functions.

A summary of the data acquisition and preprocessing characteristics of the present procedure are as follows:

1. A data acquisition rate of 100 points per second (3). This scan rate is automatically adjusted to acquire a minimum of two complete cycles.
2. Acquisition of approximately 600 raw data points from each damped wave. (The reduction program at the batch computer utilizes all of these to obtain one reduced data point for each of the frequency and damping parameters.)
3. Standardization of phase angle and amplitude boundary conditions of the data to be acquired.

Figures 1A and 1B show typical preprocessed digital data (damped waves) obtained in the glassy state and glass transition regions, respectively.

THEORY OF DATA REDUCTION. The basic equation of motion for a "simple" torsional pendulum is given in Eq. (1), where θ is the angle of displacement from the neutral position (or the amplitude of the electrical analog), I is an inertial constant, η_{dym} is the dynamic viscosity,and G_{dym} is the dynamic modulus (4,5).

$$I \frac{d^2\theta}{dt^2} + \eta_{dym} \frac{d\theta}{dt} + G_{dym}\theta = 0 \qquad (1)$$

Equation (2) contains the same information in terms of the complex shear modulus.

$$I \frac{d^2\theta}{dt^2} + (G' + iG'')\theta = 0 \qquad (2)$$

The solution to Eq. (1) has the form of an exponentially damped cosine function

$$\theta = \theta_o e^{-\alpha t}\cos(\omega t + \phi) \tag{3}$$

with

$$\alpha = \eta_{dym}/2I$$

and

$$\omega = [G_{dym}/I - (\eta_{dym}/2I)^2]^{1/2}$$

where α is the damping coefficient and ω is the frequency in radians per second. A phase angle term, ϕ, has been introduced because of the timing of the initiation of data acquisition. Because the TBA specimen has a tendency to twist, especially during a transition, causing a drift in the baseline, the equation describing the actual amount of deflection at any point in time is more closely represented by Eq. (4).

$$\theta = \theta_o e^{-\alpha t}\cos(\omega t + \phi) + \beta t + C \tag{4}$$

The differential equation corresponding to Eq. (4) is used in the linear least mean squares analysis of the digitized data,

$$\frac{d^2\theta}{dt^2} + 2\alpha\frac{d\theta}{dt} + (\alpha^2 + \omega^2)\,\theta - C(\alpha^2 + \omega^2) - 2\alpha\beta - \beta(\alpha^2 + \omega^2)t = 0 \tag{5}$$

which may be simplified to

$$D = \frac{d^2\theta}{dt^2} + A_1\frac{d\theta}{dt} + A_2\,\theta + A_3 t + A_4 = 0 \tag{6}$$

where A_i are the parameters fitted by the analysis, and

$$\alpha = A_1/2$$

$$\omega = [A_2 - (A_1/2)^2]^{1/2}$$

(The significance of D will be discussed below.) The derivative values of θ at any point n were calculated numerically from an extension of Newton's Forward Formula, which utilizes 5 consecutive points to obtain the first and second derivatives (6). These derivative formulae are refinements of the expressions used in Part I of this paper (3) and are given by

$$\frac{d\theta_n}{dt} = (-\theta_{n+2} + 8\theta_{n+1} - 8\theta_{n-1} + \theta_{n-2})/12h \tag{7}$$

$$\frac{d^2\theta_n}{dt^2} = (-\theta_{n+2} + 16\theta_{n+1} - 30\theta_n + 16\theta_{n-1} - \theta_{n-2})/12h^2 \tag{8}$$

where h is the step size.

LINEAR LEAST MEANS SQUARES ANALYSIS. The linear least mean squares fitting of N experimental data to the differential form of the equation of motion involves minimization of the summation,

$$S = \sum_{n=3}^{N-2} v_n^2 = \sum_{n-3}^{N-2} (f_n - D_n)^2 \tag{9}$$

where v_n^2 are the squares of the approximation errors and f_n is derived from the experimental data,

$$f_n = \frac{d^2\theta}{dt_n^2} + A_1\frac{d\theta_n}{dt_n} + A_2\theta_n + A_3 t_n + A_4 \tag{10}$$

The respective derivatives are defined by Eqns. 7 and 8. t_n is n divided by the scan rate. D_n is identically zero by definition (Eqn. 6). The limits of the summation (n = 3 to N - 2) have been dictated by the method for obtaining the derivatives. From the requirement that S is minimized, it follows that,

$$\frac{\partial S}{\partial A_i} = 2 \sum_n v_n \frac{\partial v_n}{\partial A_i} = 0 \qquad (i = 1 \text{ to } 4) \qquad (11)$$

This results in four simultaneous linear equations which may be presented in matrix notation:

$$\begin{bmatrix} \sum_n \dot{\theta}_n^2 & \sum_n \dot{\theta}_n \theta_n & \sum_n \dot{\theta}_n & \sum_n \dot{\theta}_n t_n \\ \sum_n \dot{\theta}_n \theta_n & \sum_n \theta_n^2 & \sum_n \theta_n & \sum_n \theta_n t_n \\ \sum_n \dot{\theta}_n & \sum_n \theta_n & \sum_n 1 & \sum_n t_n \\ \sum_n \dot{\theta}_n t_n & \sum_n \theta_n t_n & \sum_n t_n & \sum_n t_n^2 \end{bmatrix} \begin{bmatrix} A_1 \\ A_2 \\ A_3 \\ A_4 \end{bmatrix} = \begin{bmatrix} -\sum_n \ddot{\theta}_n \dot{\theta}_n \\ -\sum_n \ddot{\theta}_n \theta_n \\ -\sum_n \ddot{\theta}_n \\ -\sum_n \ddot{\theta}_n t_n \end{bmatrix}$$

The above expression can be solved by a matrix inversion procedure to determine the values of the coefficients A_1. A_1 and A_2 contain the damping and frequency parameters (see above).

REFINEMENT OF DATA REDUCTION TECHNIQUE. Even with the use of low pass signal filters (cut-off frequency of 2 Hz), the initial automatic data reduction technique was found to produce data with unacceptable scatter in the damping, although the frequency data was acceptable (Figure 2). (The two rigidity curves in Figure 2 are the consequence of thermohysteresis - see below.) The first refinement involved truncation of the data so that an integral number of cycles was analyzed. The excess points were eliminated from further computation. Effectively this is a digital filtering technique which was empirically found to improve the signal-to-noise ratio. Frequency, damping, and the number of points comprising the maximum number of integral cycles are determined by an iterative process which typically converges after 3 cycles. Computer simulations have demonstrated that this operation is theoretically unnecessary for noise-free data.

Once this change had been incorporated into the data reduction program, the reduced data for the damping appeared to be on two distinct levels (Figure 3). This phenomenon was traced back to the fact that the incoming data at the initiation of data storage had either a zero degree or 180 degree phase angle associated with it, corresponding to a maximum and a minimum in the oscillations of the analog damped wave. After the data acquisition program was modified to accept data only at a phase angle of zero degrees, the reduced data were on a single curve (Figure 4). Upon even closer examination, the damping curve showed signs of small discontinuities which were traced back to the procedure used to adjust for the baseline drift due to specimen twisting. This corrective action is employed to compensate for the non-linearity of the response curve of the optical transducer. This instrumentation problem has been solved manually (Figure 5) and a technique for automatic drift compensation is being developed (7). Alternatively, the computer itself can be programmed to compensate for non-linearities which can be incorporated into the equation of motion. With the increased sensitivity of the system, it is now essential to control precisely the temperature programming as fluctuations in the data are observable in regions in which there are non-constant rates of temperature change. As an example of the resolution of the experimental results, a linear expansion of the modulus data through a secondary transition is presented in Figure 6. The two different sets of data for decreasing and increasing temperature (thermohysteresis) are attributed to properties of the polymeric specimen *per se*, and not to the methods used in processing the data. This phenomenon will be discussed elsewhere (8).

COMMENT. The present system provides a powerful tool for the study of thermomechanical properties of polymeric materials and its flexibility allows

for extensive conceptual evolution of the experimental design. While this report presents preliminary data, further refinements of the system are in progress. These include upgrading of the TBA instrumentation, refinement of the data reduction procedure, optimization of the data acquisition parameters, as well as development of data analysis techniques for more quantitative interpretations of the thermomechanical spectra.

REFERENCES

1. Gillham, J. K., "Torsional Braid Analysis -- A Semimicro Thermomechanical Approach to Polymer Characterization", CRC Critical Reviews in Macromolecular Science, 1, 83 (1972).
2. Hazony, Y., "Hierarchical Computing in Laboratory Experiments: Potential and Pitfalls", Computer Phys. Comm. 4, 279 (1972).
3. Hazony, Y., Stadnicki, S. J., Gillham, J. K., "Low Frequency Thermomechanical Spectrometry of Polymeric Materials - I. Overview", ACS, Polymer Preprints (this volume).
4. Tobolsky, A. V., *Properties and Structure of Polymers*, Chapter 3, John Wiley & Sons, Inc., New York, 1962.
5. Nielsen, L. E., *Mechanical Properties of Polymers*, Chapter 7, Reinhold Publishing Corp., New York, 1965.
6. Lapidus, L., *Digital Computation for Chemical Engineers*, Chapter 4, McGraw Hill Book Co., Inc., New York, 1962.
7. Bell, C. L. M., unpublished results.
8. Gillham, J. K., Stadnicki, S. J., and Hazony, Y., "Low Frequency Thermomechanical Spectrometry of Polymeric Materials - III. Tactic Polymethylmethacrylates", ACS, Polymer Preprints (this volume).

ACKNOWLEDGMENT. This work was supported in part by the National Aeronautics and Space Administration (Grants NGR 31-001-200 and NGR 31-001-221), by the Chemistry Branch of the Office of Naval Research (Contract N00014-67-A-0151-0024, Task No. NR 356-504) and by the Air Force Materials Laboratory (Contract F33615-72-C-1590). It is our pleasure to thank Messrs. Robert Cassidy and Peter Olenick of the Princeton University Computer Center for the development of the necessary system software and Mr. Colin Bell of the Natural Rubber Research Products Association, U.K., for his contributions in the early stages of this work.

FIGURE CAPTIONS

Figure 1A - Digitized damped wave for polymer specimen in the glassy region.
Figure 1B - Digitized damped wave for the same polymer specimen in a transition region.
Figure 2 - Syndiotactic PMMA. Unacceptable scatter in the data. Logarithmic decrement and relative rigidity vs. T. Prehistory: heat to 423°K. Experiment: 423 → 93 → 423°K. Rate: 2°K/min.
Figure 3 - Polyethylenecarbonate (β-peak). Corrections made for an integral number of cycles. Logarithmic decrement and relative rigidity vs. T. Prehistory: heat to 393°K. Data: 236→93→247°K. Rate: 2°K/min. Reference: Udipi, K., Gillham, J. K., and Tsuruta, T., "Poly(ethylene carbonate) and Poly(propylene carbonate): Transitions and Thermomechanical Spectra", J. Appl. Polym. Sci., (in press).
Figure 4 - Same experiment as for Figure 3. Corrections made for phase angle.
Figure 5 - Syndiotactic PMMA (new specimen). Corrections made manually for non-linearity of optical transducer. Logarithmic decrement and relative rigidity vs. T. Prehistory: heat to 473°K. Experiment: 473 → 93 → 473°K. Rate: 2°K/min.
Figure 6 - Same experiment as for Figure 5. Expanded scale - relative rigidity vs. T.

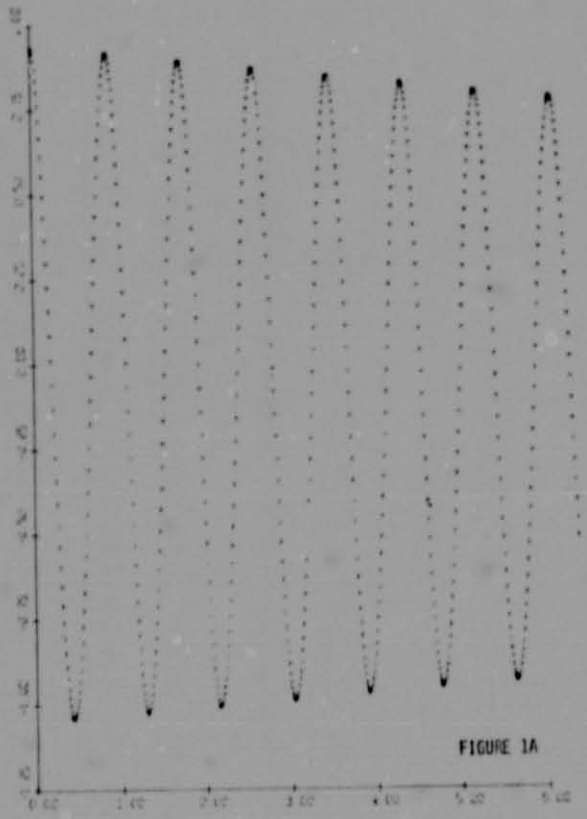

FIGURE 1A

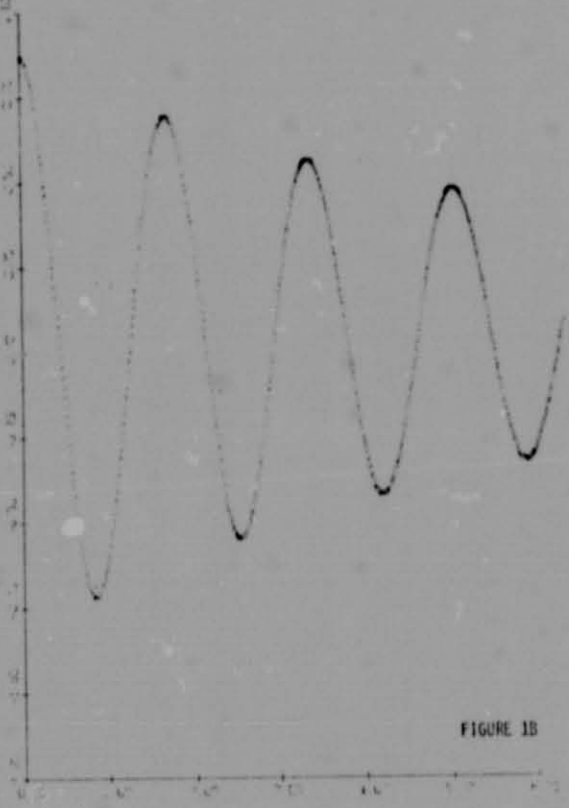

FIGURE 1B

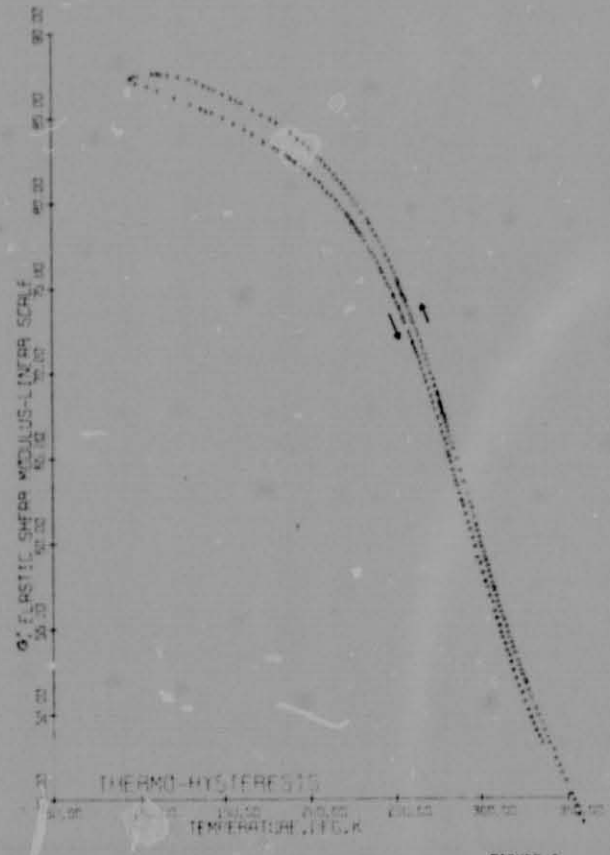

SYNDIOTACTIC PMMA

FIGURE 6

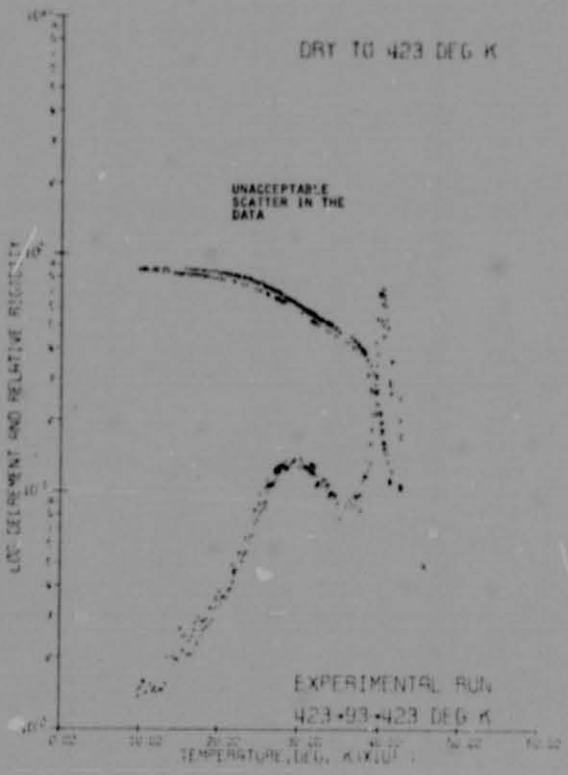

SYNDIOTACTIC PMMA

FIGURE 2

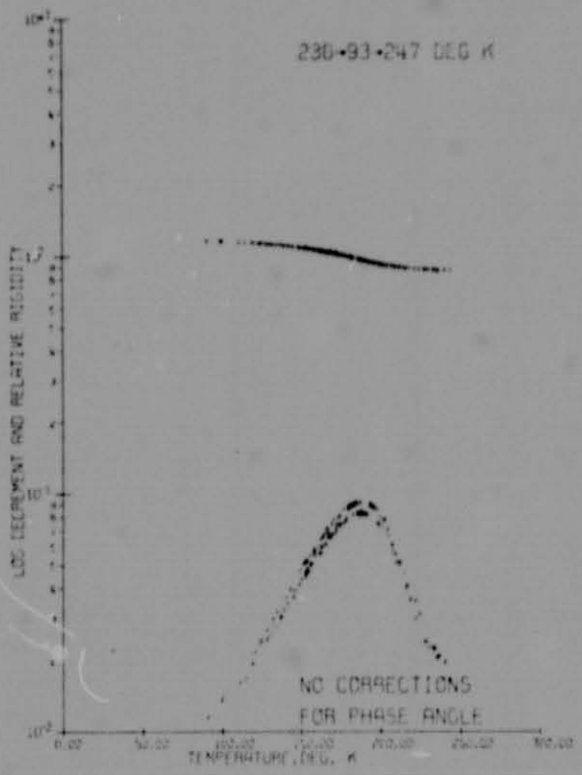

POLYETHYLENE CARBONATE (BETA PEAK)

FIGURE 3

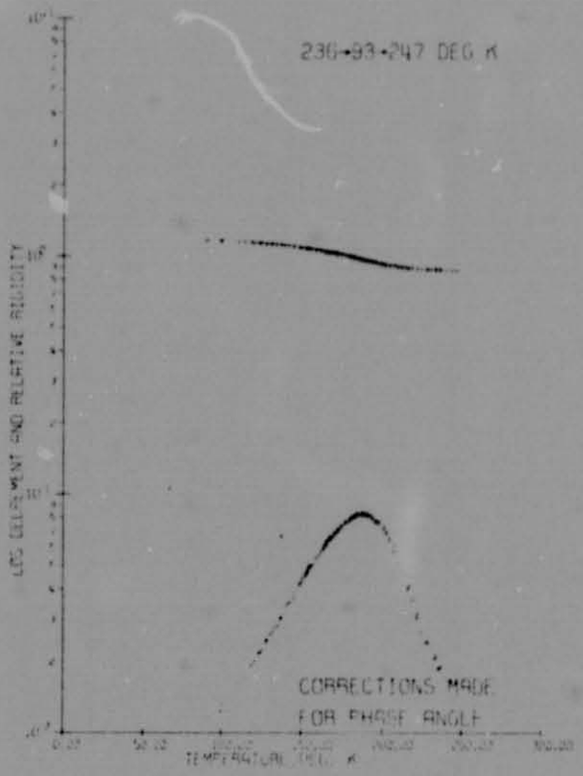

POLYETHYLENE CARBONATE (BETA PEAK)

FIGURE 4

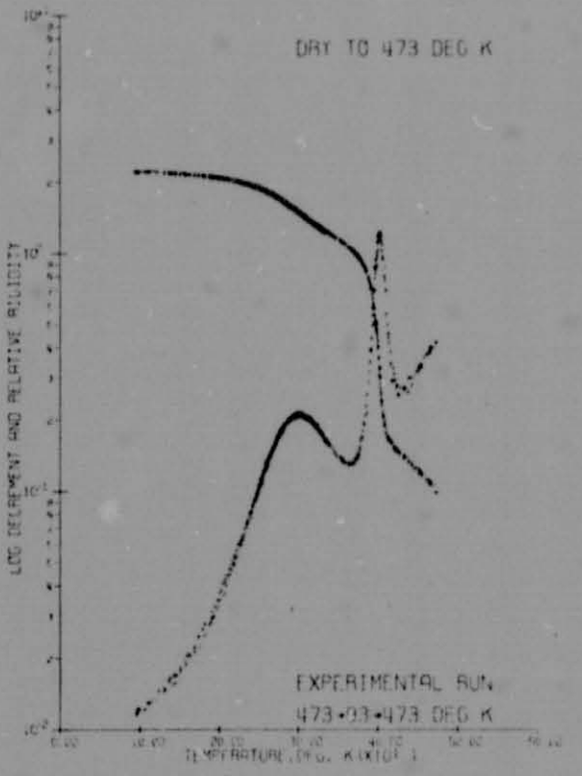

SYNDIOTACTIC PMMA

FIGURE 5

..., Polymer Preprints, Vol.15, No.1, 562-569(1974).

LOW FREQUENCY THERMOMECHANICAL SPECTROMETRY OF POLYMERIC MATERIALS: COMPUTERIZED TORSIONAL BRAID EXPERIMENTS. III. TACTIC POLYMETHYLMETHACRYLATES.

J. K. Gillham, and S. J. Stadnicki, Polymer Materials Program, Department of Chemical Engineering, and Y. Hazony, Computer Center, Princeton University, Princeton, N. J. 08540

INTRODUCTION. An automated instrument for torsional braid analysis (TBA), which includes on-line reduction of data (1,2), was used to characterize amorphous syndiotactic, atactic and isotactic polymethylmethacrylates at about 1 Hz in the temperature range 473 → 93°K. Manually reduced TBA data for the same polymers, together with documentation of the synthesis of the polymers, their average molecular weights ($\bar{M}w$ and $\bar{M}n$), and tactic contents (syndio-, hetero-, and iso-) have been reported previously (3). Characteristics of the stereoregular polymethylmethacrylates are summarized in Table I which includes assignments for the Tg and Tβ transitions made on the basis of the present data.

Polymer-braid composite specimens were prepared by impregnating multifilamented glass braids in 10 percent solutions of the polymers in tetrahydrofuran (THF, b.p. 66°C). Solvent was removed by heating the composite specimens to 473°K at the rate of 2°K/min. in flowing dry nitrogen gas (obtained from a Dewar of liquid nitrogen). The thermomechanical spectra were then obtained in a nitrogen atmosphere while cooling the solvent-free braid composites to 93°K and then heating to 473°K at a rate of 2°K/min. The spectra for the syndiotactic, atactic, and isotactic polymethylmethacrylates on cooling are presented in Figures 1, 2 and 3, respectively, in terms of the temperature dependence of the relative rigidity (∿ elastic shear modulus, G') and logarithmic decrement (Δ). This is the conventional mode for presentation of torsional pendulum data.

MODES OF DATA PRESENTATION. Whereas logarithmic decrement and relative rigidity as a function of temperature are presented in Figures 1-3, Figures 4-6 illustrate the same data in terms of G" and dG'/dT. This latter mode of data presentation has been found (1) to be the most consistent in the assignment of transition temperatures. A summary of the transition temperatures for all three PMMA samples as determined from the maxima of the various modes of data exposition is found in Table II. The assignment of transition temperatures appears to conform to the following trend:

$$T(\tan\delta) = T(\Delta) \geq T(\alpha) \geq T(G'') = T(dG'/dT).$$

EFFECT OF TACTICITY ON TRANSITIONS. The general characteristics of the TBA spectra compare well with published work (4), exhibiting two distinct loss peaks above 93°K. Temperatures below 93°K are not accessible with the present apparatus. The glass transition temperatures (as determined from G" and dG'/dT data) are assigned using the sharp loss peaks at 399°K (0.68 Hz), 384°K (0.67Hz), and 334°K (0.81 Hz) in syndiotactic, atactic, and isotactic PMMA, respectively. Each loss peak is accompanied by a large rise in rigidity with decreasing temperature. The glassy-state loss peaks (β-peaks) in syndiotactic and atactic PMMA are broad and centered at 294°K (1.25 Hz) and 297°K (1.24 Hz), respectively. The β relaxation in isotactic PMMA is ill-defined and appears as a shoulder at around 280°K (1. 4 Hz). The β-peak for each of these polymers is accompanied by a small but distinct rise in the rigidity with decreasing temperature. It should be noted that the absolute value of the relative rigidity at low temperatures (∿ 93°K) is about the same for all specimens, indicating an approximately equal amount of polymer in each composite specimen.

The secondary transitions appearing below Tg have been attributed to the motion of ester side groups which may include localized motions of the main polymer chain (3,4,5,6).

The fact that the glass transition temperature of syndiotactic PMMA is some 65°K higher than that of isotactic PMMA, despite a higher density for the latter in the glassy state, has been considered to be due to intermolecular geometrical interlocking of the syndiotactic chains (3,7), or alterna-

tively to differences in intramolecular chain stiffness (4). It should be noted that the molecular weight of the isotactic sample is some 30 times that of both the syndiotactic and atactic forms which, if anything, should have the effect of raising the glass transition temperature. The influence of molecular weight on the intensity of the β-peak is not known. The similarity of the thermomechanical spectra of atactic and syndiotactic PMMA was not unexpected due to the small difference between them in microtacticity content (50% versus 70% syndiotacticity).

EFFECT OF PREHISTORY. A problem of concern to the mechanical spectroscopist is the determination of the most suitable conditioning variables for specimen preparation. To obtain the relaxation spectrum of a polymer *per se*, it is necessary to prepare the specimen in a manner which removes all occluded volatiles (e.g., solvent and absorbed moisture) without causing crosslinking or degradation. Thermogravimetric analysis (TGA), often used to complement thermomechanical spectroscopy, is employed to determine temperature regions in which weight loss occurs. A more informative approach determines the volatile components upon heating by employing a pyrolyzer in series with a mass chromatograph (8) and an "on-the-fly" infrared spectrophotometer .

Thermogravimetric analysis of isotactic PMMA showed a 1-2% weight loss in heating to 473°K after predrying to 423°K. Mass chromatographic analysis of the volatile products of heating in the 433 to 473°K range indicated one major volatile component having a molecular weight of about 93. Monomer was not detected until above 523°K. A check of the synthesis procedure (3) indicated that petroleum ether (C_5s and C_6s) was used as one of the solvents for purification and was probably the volatile component in question.

Figure 7 shows the thermomechanical spectra (logarithmic decrement vs. temperature) of a single specimen of syndiotactic PMMA after preheating first to 423°K and then to 473°K, respectively, at the rate of 2°K/min. Plasticization by bound solvent is apparent. The glass transition temperature of the specimen dried more thoroughly is some 11 degrees higher. The secondary transition (298°K) does not appear to have been affected, but the observed differences in the loss levels at temperatures between T_β and T_g and also at ∿100°K are attributed to the presence of the small amount of diluent.

EFFECT OF THERMAL CYCLING. Figure 8 presents the thermomechanical spectra, G" and G' versus temperature for syndiotactic PMMA preheated to 473°K. Experimental data is displayed during cooling to 93°K and subsequent heating to 473°K at 2°K/min. The thermohysteresis in the G" loss data at low temperatures may be due either to inaccurate temperature assignment (thermal lag between the thermocouples and specimen) or to microcracking of the composite specimen. Correct temperature assignment is indicated at higher temperatures since the data lie on one curve. Figure 9 illustrates a portion of the elastic shear modulus curve, G', (shown in Figure 8) on an expanded linear scale. The irreversibility in the rigidity, upon first cooling to 93°K and then heating, is attributed to microcracking of the composite specimen. The mechanism leading to these cracks may involve the thermal stresses which arise from the different coefficients of contraction of the two phases of the specimen. Polymers with bulky side groups are observed to be susceptible to cracking (3) probably because there are weaker cohesive forces between chains, per unit cross-sectional area, than for more compact molecules (9, 10). The fracture mechanism may also involve penetration of trace amounts of water into small pores and its subsequent expansion upon freezing. The moisture content of the "dry" nitrogen atmosphere was measured to be about 5 PPM which corresponds to a frost point of about 207°K. In a similar manner, occluded solvent could form voids upon freezing which could be sites for initiation of cracks. Alternatively, cracks may originate from the stress applied to initiate pendulum oscillations, particularly at low temperatures where the side group motions are frozen out. In any case, the loss level would be expected to be higher after a crack, reflecting an increase in the ability of the composite specimen to dissipate energy on deformation. In a like manner, the elastic modulus curve would be expected to be at a lower level on heating after cracking, indicating a less rigid structure. Indeed,

this is what is found.

EFFECT OF H_2O. Atactic PMMA was conditioned overnight at RT in a flowing N_2 atmosphere containing 300 PPM H_2O (~1.2% R.H.). A hygrometer (Panametrics Model 2000), capable of measuring to less than 1 PPM, was used to monitor the water content continuously at the exit port of the TBA apparatus. The specimen was then taken through the temperature cycle, RT → 473 → 93 → 473°K at 2°K/min (Figure 10). The "wet" conditioning atmosphere was changed to a flowing dry atmosphere containing less than 5 PPM H_2O at 303°K during the cooling mode. The presence of this small amount of water had no effect on Tg, but a small γ-peak centered around 170°K had developed. The derivative form of the logarithmic decrement, $d\Delta/dT$, illustrates the presence of the γ-transition in another way (Figure 11).

DISCUSSION. Use of G" as the measure of loss in dynamic mechanical experiments has been shown herein to give values for transitions which are identical with those obtained from the maxima of the derivative of G' with respect to temperature. Use of G" rather than other loss parameters appears to be particularly effective for investigating secondary transitions by reducing the response of the Tg relaxation. The G" mode would also appear to be the logical function to use in comparing dynamic mechanical and dielectric loss (ε") data. A further advantage in its use appears to lie in the flat baseline of G" vs. temperature curves which could provide opportunities for comparing peak shapes and for resolving peaks quantitatively.

For example, the data of Figure 12, which compares G" vs. T plots for the syndiotactic, atactic and isotactic polymers, shows that the relative intensity of the β-peak decreases drastically with increasing isotactic content. The speculation could be made that completely isotactic polymer would not display a β-peak. The similar shape of the G" vs. T curves for the three polymers (Figure 12) indicates that the basic mechanism of the β-process is the same for the three polymers and supports the validity of extrapolating in this fashion. The absence of a β-peak is noted for polyisobutylene (11) which also has an anomalously low glass transition temperature. The latter has been ascribed to a lack of spacial sites for geometrical intermolecular interlocking along the molecule (7) and this reason has also been suggested to explain the low Tg of isotactic PMMA (3).

The data presented above are preliminary. Nevertheless the power of the computerized experiment and the scope of the investigation which may be undertaken have been demonstrated.

ACKNOWLEDGMENT. This work was supported in part by the National Aeronautics and Space Administration (Grants NGR 31-001-200 and NGR 31-001-221), by the Chemistry Branch of the Office of Naval Research (Contract N00014-67-A-0151-0024, Task No. NR 356-504), and by the Air Force Materials Laboratory (Contract F33615-72-C-1590). Gratitude is expressed also to Dr. E. Gipstein for providing the characterized polymers.

REFERENCES

1. Hazony, Y., Stadnicki, S. J., Gillham, J. K., "Low Frequency Thermomechanical Spectrometry of Polymeric Materials: Computerized Torsional Braid Experiments. I. Overview". ACS Polymer Preprints (this volume).
2. Stadnicki, S. J., Gillham, J. K., Hazony, Y., "Low Frequency Thermomechanical Spectrometry of Polymeric Materials: Computerized Torsional Braid Experiments. II. Data Processing". ACS Polymer Preprints (this volume).
3. Kiran, E., Gillham, J. K., Gipstein, E., "Thermomechanical Behavior of Tactic Amorphous Methacrylate Polymers", J. Macromolecular Science-Physics, (in press).
4. McCrum, N. G., Read, B. E., and Williams, G., *Anelastic and Dielectric Effects in Polymeric Solids*, John Wiley & Sons, New York, 1967.
5. Kawamura, Y., *et. al.*, J. Poly. Sci., A2, (7), 1559 (1969).

6. Ishida, Y., J. Poly. Sci., A2, (7), 1835 (1969).
7. Martin, J. R., Gillham, J. K., J. Appl. Poly. Sci., 16, 2091 (1972).
8. Kiran, E., Gillham, J. K., "Pyrolysis-Mass Chromatography of Polymers", ACS Polymer Preprints, 14, 1, 580 (1973).
9. Vincent, P. I., Nature, 233(40), 104 (1971).
10. Vincent, P. I., Polymer, 13, 588 (1972).
11. Hiltner, A., Baer, E., Martin, J. R., Gillham, J. K., "Low Temperature Relaxations in Amorphous Polymers", J. Macromolecular Science-Physics, (in press).

Table I
Characteristics of Stereoregular Polymethylmethacrylates

Molecular Weight (3)	Syndiotactic	Atactic*	Isotactic
$\overline{M}w$	83,200	105,000	2,780,000
$\overline{M}n$	62,700	48,000	1,200,000
$\overline{M}w/\overline{M}n$	1.33	2.15	2.29
Tactic Content (%) (3)			
syndio-	70.1	50.6	0
hetero-	26.1	41.7	8.5
iso	3.8	7.7	91.5
Transition Data			
Tg, °K†	399 (0.68)	384 (0.67)	334 (0.81)
T_β, °K (Hz)#	294 (1.25)	297 (1.24)	∿ 280 (1.4)
T_β/Tg	0.74	0.77	> 0.84
Ratio of Peak Heights of the Tβ to Tg Transition#	0.73	0.60	0.19
Synthesis (3)			
initiator	fluorenyl lithium	*	phenylmagnesium bromide
$T_{synthesis}$, °C	-70		0

†Determined from G" and dG'/dT loss data (decreasing temperature).

#Determined from G" loss data (decreasing temperature).

*Source: Cellamer Associates (3).

Table II
Transition Data of Stereoregular Polymethylmethacrylates*

PMMA	dG'/dT	G"		Δ		tanδ		α	
	Tg	Tg	Tβ	Tg	Tβ	Tg	Tβ	Tg	Tβ
Syndiotactic	399	399	294	403	298	403	298	400	298
Atactic	384	384	297	388	297	388	297	384	297
Isotactic	334	334	∿280	336	∿285	336	∿285	336	∿285

*Loss maxima in °K (decreasing temperature data).

FIGURE CAPTIONS

Figure 1. Syndiotactic PMMA.
Figure 2. Atactic PMMA.
Figure 3. Isotactic PMMA.

Logarithmic decrement and relative rigidity vs. T. Prehisotry: heat to 473°K. Experiment: 473 → 93°K. Rate: 2°K/min.

Figure 4. Syndiotactic PMMA.
Figure 5. Atactic PMMA.
Figure 6. Isotactic PMMA.

G'' (upper) and dG'/dT (lower) vs. T. Same experiments as for Figures 1, 2 and 3, respectively.

Figure 7. Syndiotactic PMMA. Effect of thermal prehistory.

Logarithmic decrement vs. T.
Prehistory: heat to 423°K (x) and 473°K (+), (same specimen).
Experiment: cool to 93°K. Rate: 2°K/min.

Figure 8. Syndiotactic PMMA. Thermohysteresis.

G'' and G' vs. T. Prehistory: heat to 473°K. Experiment: 473 → 93 → 473°K. Rate: 2°K/min.

Figure 9. Syndiotactic PMMA. Thermohysteresis.

G' vs. T (linear scale). Same experiment as for Figure 8.

Figure 10. Atactic PMMA. Effect of H_2O (300 PPM).

Logarithmic decrement and relative rigidity vs. T. Prehistory: see text. Experiment: 473 → 93 → 473°K. Rate: 2°K/min.

Figure 11. Atactic PMMA. Effect of H_2O (300 PPM). Derivative of logarithmic decrement vs. T. Same experiment as for Figure 10 using data for 93 → 473°K.

Figure 12. Syndiotactic, Atactic and Isotactic PMMA. G'' vs. T.
Prehistory: RT → 473. Experiment: 473 → 93°K.
Rate: 2°K/min.

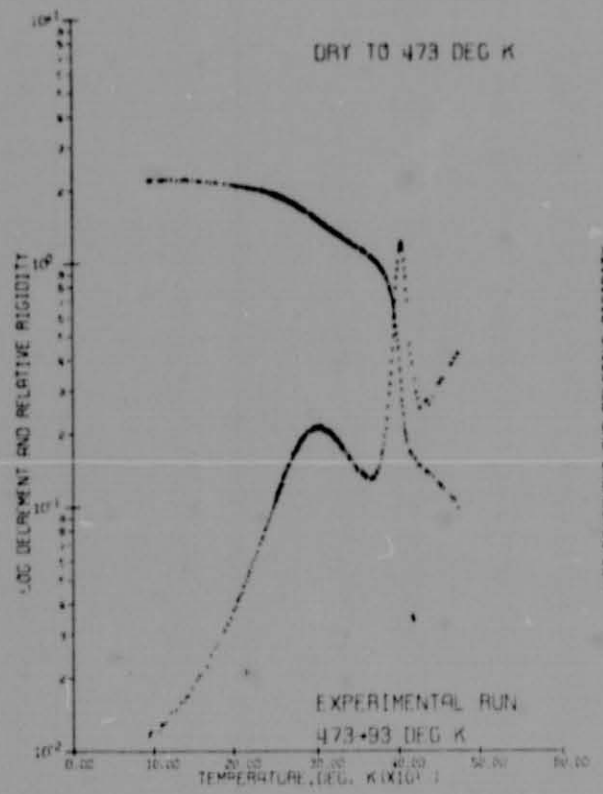

SYNDIOTACTIC PMMA

FIGURE 1

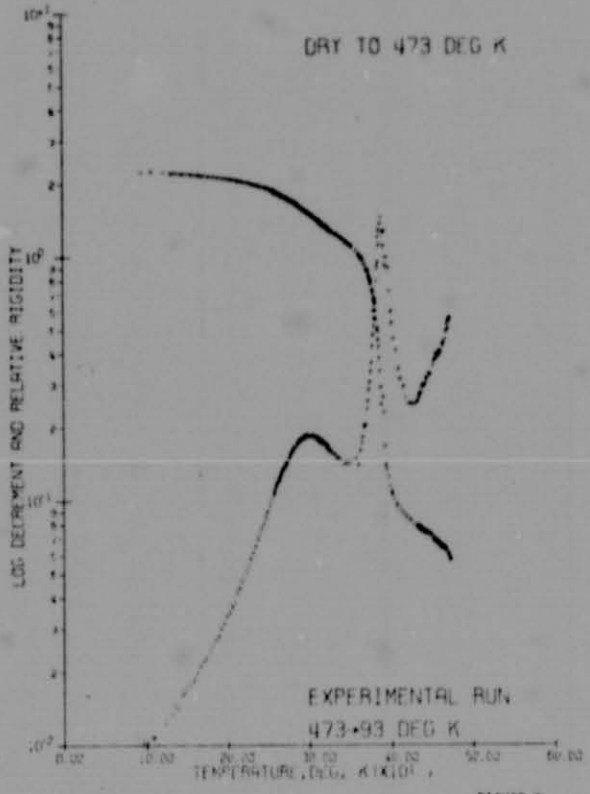

ATACTIC PMMA

FIGURE 2

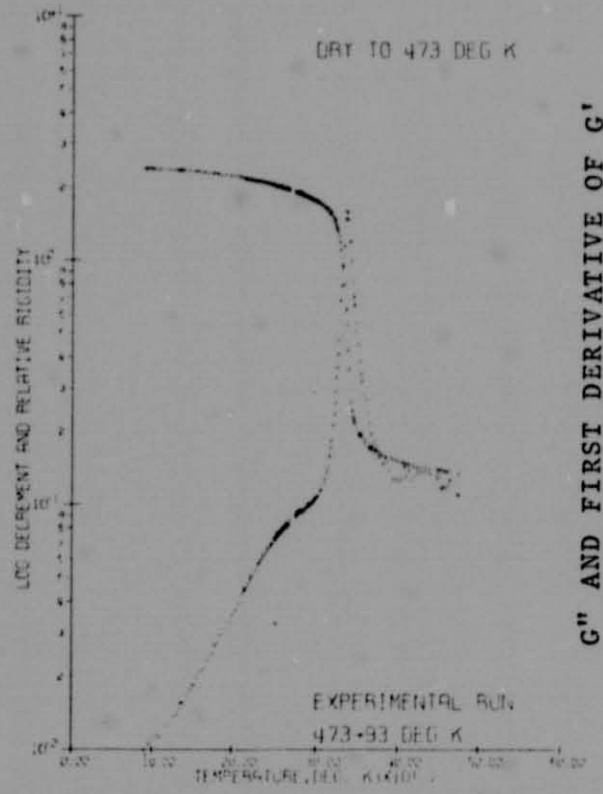

ISOTACTIC PMMA

FIGURE 3

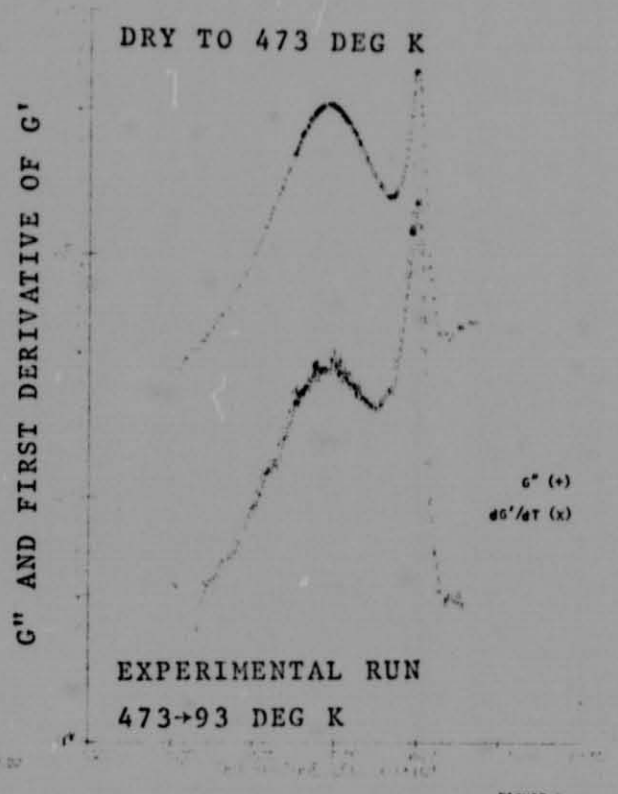

SYNDIOTACTIC PMMA

FIGURE 4

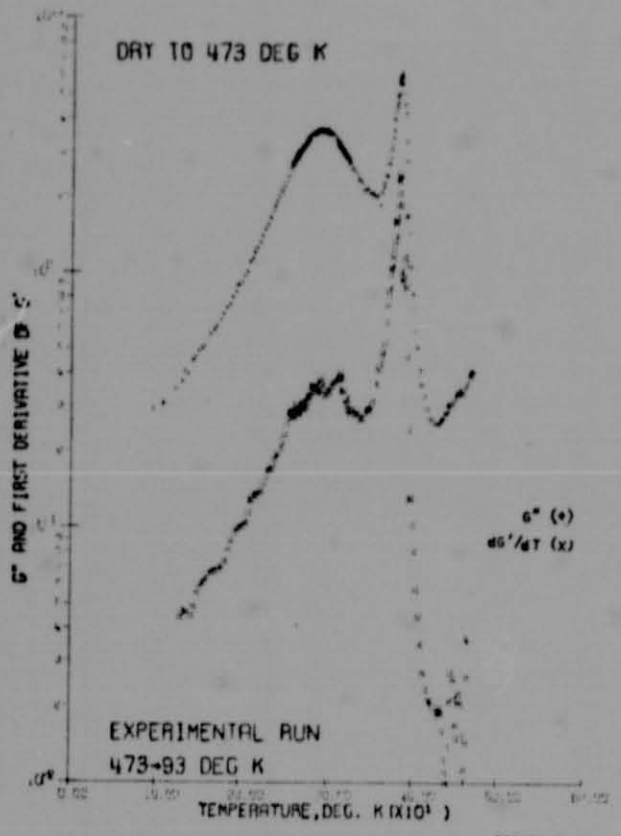

ATACTIC PMMA

FIGURE 5

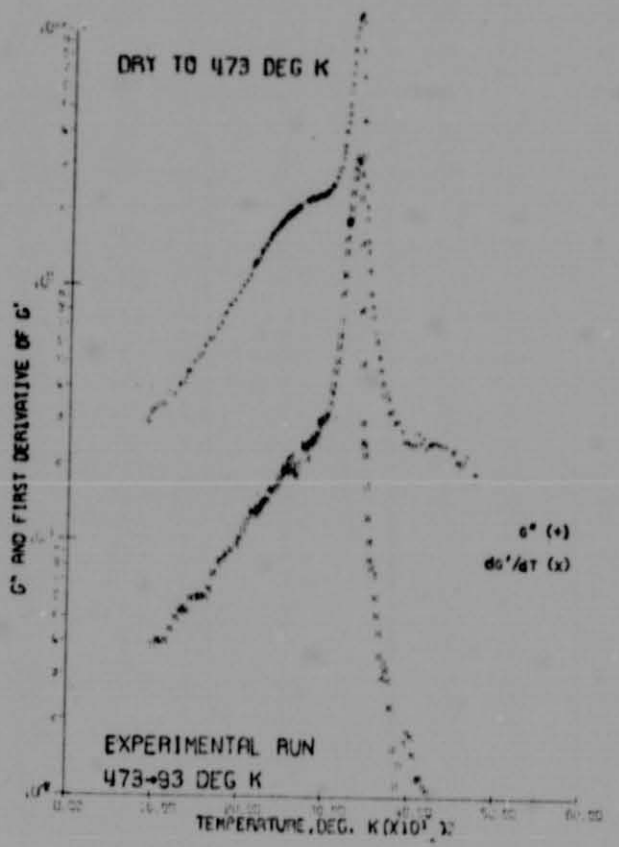

ISOTACTIC PMMA

FIGURE 6

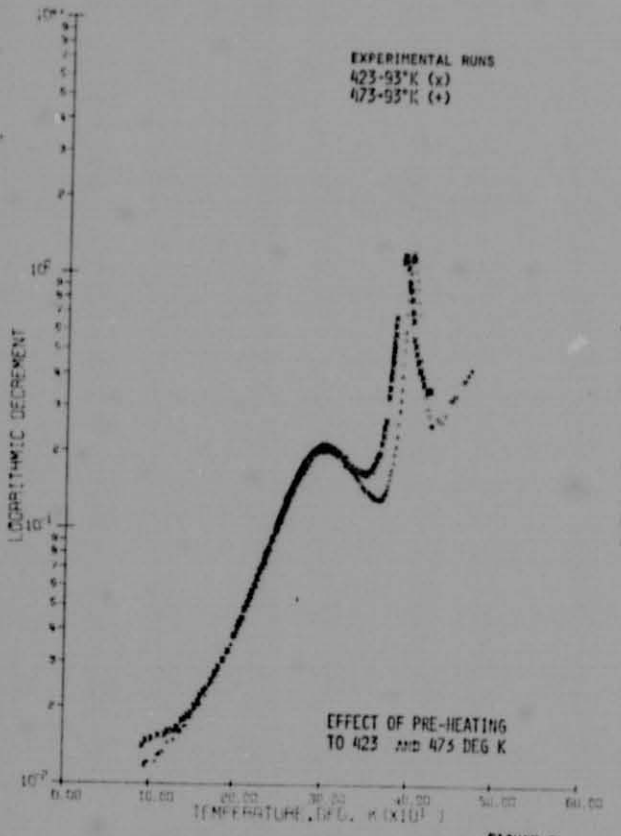

SYNDIOTACTIC PMMA

FIGURE 7

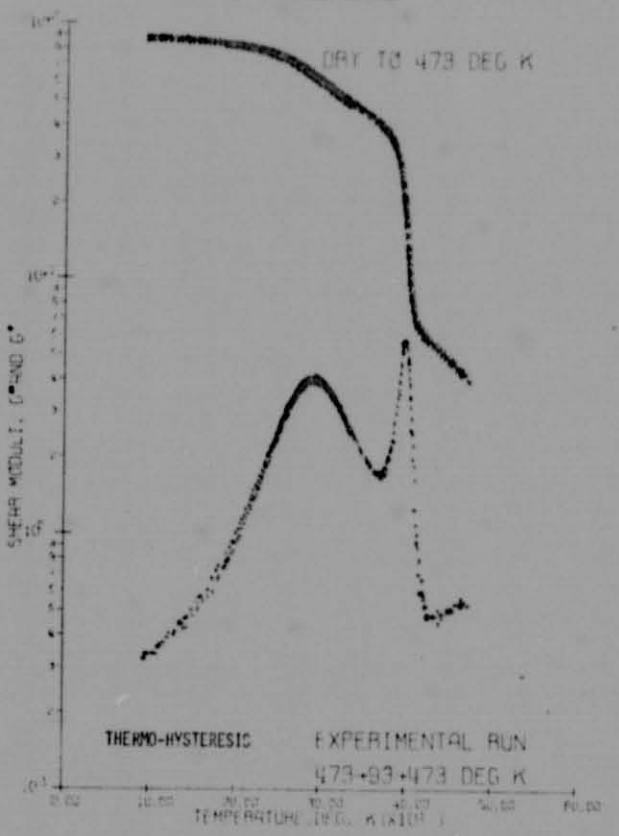

SYNDIOTACTIC PMMA

FIGURE 8

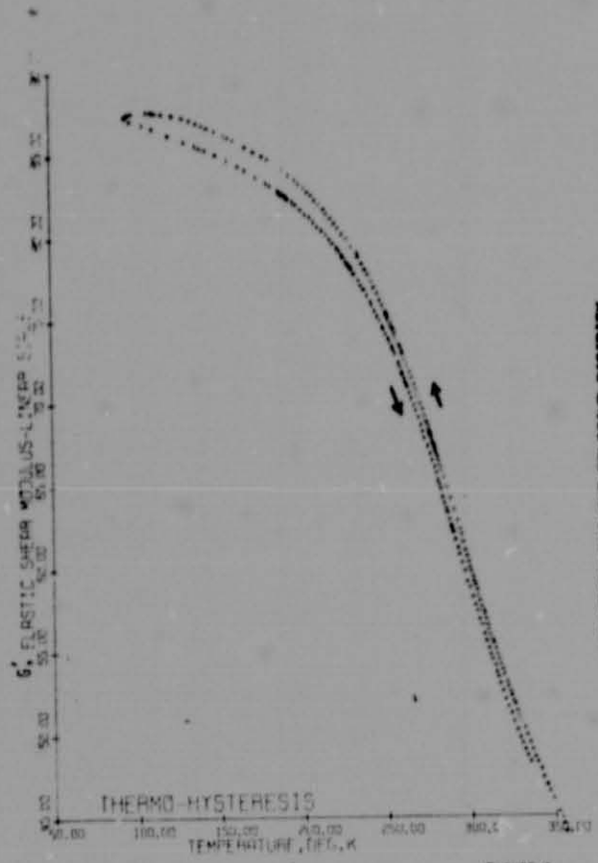

FIGURE 9

SYNDIOTACTIC PMMA

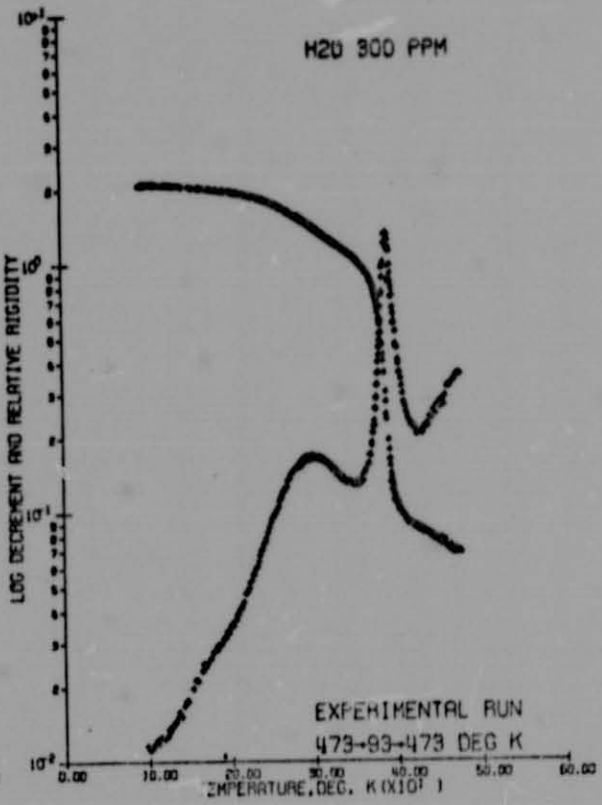

FIGURE 10

ATACTIC PMMA

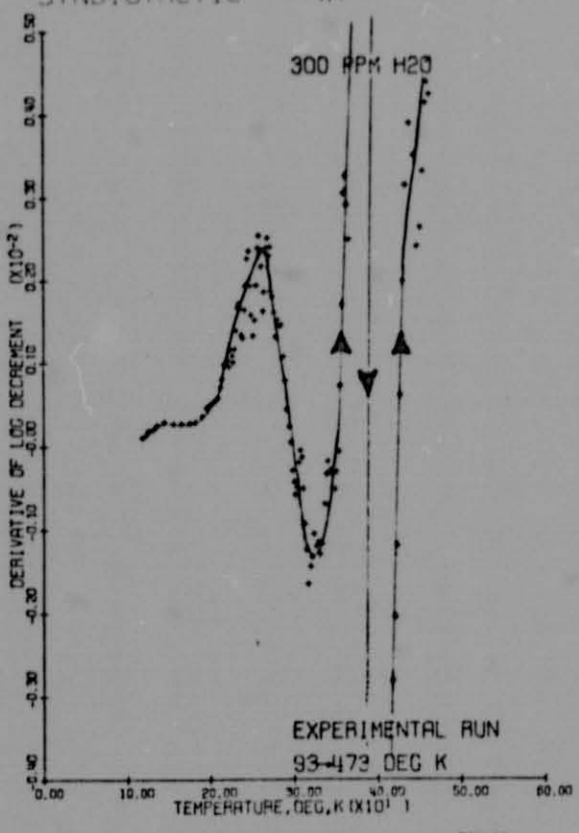

ATACTIC PMMA

FIGURE 11

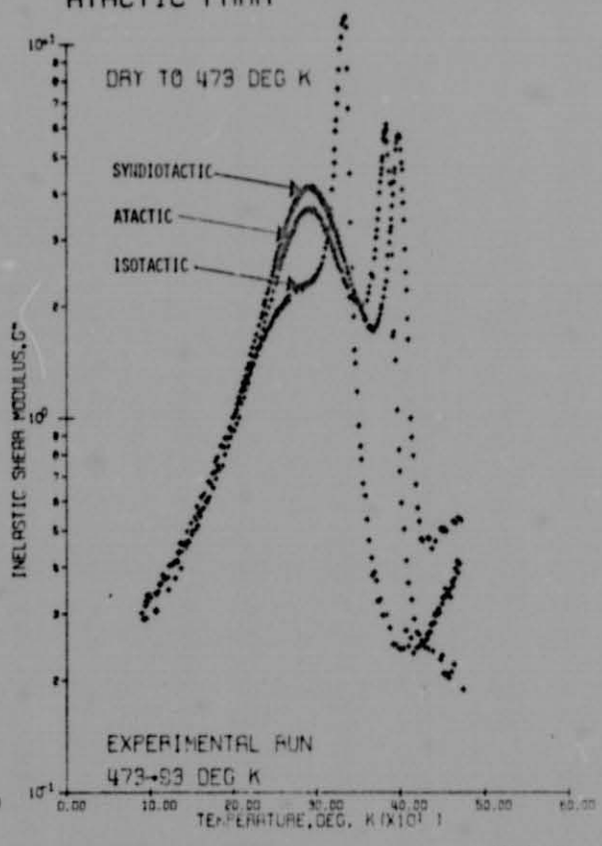

TACTIC PMMAS

FIGURE 12

JOURNAL OF APPLIED POLYMER SCIENCE VOL. 18, PP. 951–961 (1974)

Isothermal Transitions of a Thermosetting System

J. K. GILLHAM and J. A. BENCI, *Polymer Materials Program, Department of Chemical Engineering, Princeton University, Princeton, New Jersey 08540*, and A. NOSHAY, *Chemicals and Plastics Division, Union Carbide Corporation, Bound Brook, New Jersey 08805*

Synopsis

A study of the curing reactions of a cycloaliphatic epoxy resin/anhydride system by torsional braid analysis showed the existence of two critical isothermal temperatures. These are $T_{g\infty}$ (the maximum glass transition temperature of the thermoset system) and T_{gg} (the glass transition temperature of the material at its gel point). Two rheologically active kinetic transitions occur during isothermal cure which correspond to gelation and vitrification. Three types of isothermal behavior occur: if $T_{\text{cure}} > T_{g\infty}$, only gelation is observed; if $T_{g\infty} > T_{\text{cure}} > T_{gg}$, both gelation and vitrification are observed; if $T_{\text{cure}} < T_{gg}$, only vitrification is observed. T_{gg} corresponds to the isothermal cure temperature at which gelation and vitrification occur simultaneously. Methods for determining the time to gel and the time to vitrify, and also $T_{g\infty}$ and T_{gg}, have been developed. The time to gel obeyed the Arrhenius relationship, whereas the time to vitrify passed through a minimum. Application of these results to thermosetting systems in general is discussed in terms of the influence of molecular structure on the values of $T_{g\infty}$ and T_{gg}.

INTRODUCTION

A previous study[1] of the thermosetting reactions of the diglycidyl ether of bisphenol A with four aromatic diamines led to conclusions which appeared to be generalizations not limited to the specific systems studied. In particular, it was demonstrated that three types of rheological behavior occur on isothermal cure depending on the temperature of cure relative to two critical transition temperatures which were designated T_{gg} and $T_{g\infty}$. To test the generalizations further, the present investigation examined another type of thermosetting system, i.e., a cycloaliphatic epoxy resin/anhydride formulation. Since the results of the present work fitted the earlier generalizations which are summarized in the present conclusions, they are not repeated in this introduction. The technique which permitted the monitoring of the rheological changes which occur during the complete cure of a reactive system as it changes from liquid to solid was torsional braid analysis.[2]

EXPERIMENTAL

Reactants and Chemistry

The components used in the cure reaction of the epoxy resin/anhydride system were: (1) the epoxy resin 3,4-epoxycyclohexylmethyl-3,4-epoxy-

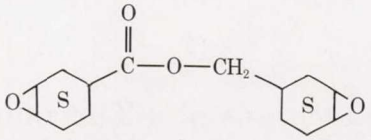

cyclohexane carboxylate (Bakelite Resin ERL-4211), (2) the hardener hexahydrophthalic anhydride, (3) the initiator ethylene glycol, and (4) the catalyst benzyldimethylamine. The names, codes, formulae, molecular weights, boiling points, and formulation of these chemicals are listed in Table I. All chemicals were obtained from the Union Carbide Corporation.

A summary of the mechanism and cure chemistry of the cycloaliphatic epoxy resin/hexahydrophthalic anhydride system appears in a technical bulletin which was published by the manufacturer.[3] The principal reaction between the epoxy resin and hardener leads to the following polyester structure:

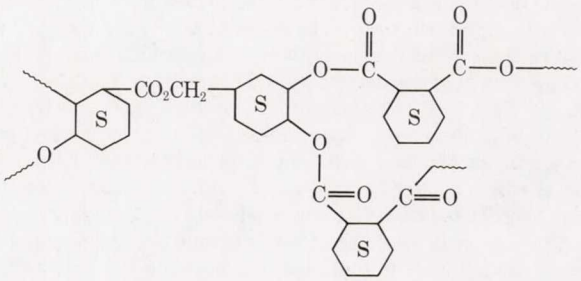

A certain amount of epoxide homopolymerization occurs in competition with the formation of polyester linkages and leads to a polyether structure:

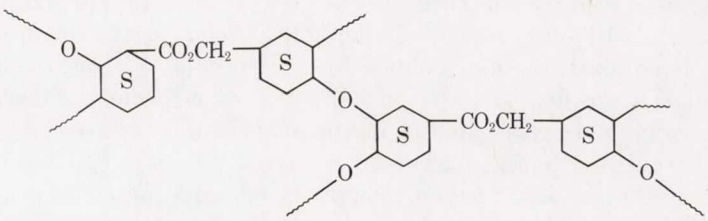

In both structures, the crosslinks of the molecular network are provided by the tetrafunctional epoxide. The anhydride reaction is initiated by active hydrogen which is provided by ethylene glycol, and is catalyzed by base which is provided by benzyldimethylamine. The mole ratios of epoxide and hexahydrophthalic anhydride components used in formulations reflect the relative amounts of the competing reactions which occur for the given amounts of initiator and catalyst and give rise to optimum thermophysical properties in the cured resins.

The chemicals were combined at room temperature as liquids in the order epoxy (first), anhydride (at 55°C), ethylene glycol, and benzyldimethylamine (last). No solvent was required since the viscosity was low. The reactive mixture was stored under nitrogen in a freezer. The mixture

TABLE I
Cycloaliphatic Epoxy Resin System: Chemicals and Formulation

Chemical	Molecular weight	Boiling point at 760 mm Hg, °C	Formulation	
			Wt. used, g	Equivalents used
3,4-Epoxycyclohexylmethyl-3,4-epoxycyclohexane carboxylate (ERL-4221) 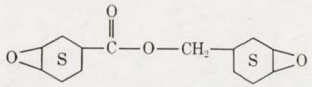	252.3 (theoretical) specification equivalent weight (per epoxy group) = 137 (average)	354	10.0002	0.073
Hexahydrophthalic anhydride	154.2	284 (at 750 mm Hg)	10.0065	0.0649
Ethylene glycol	62.1	198	0.2989	0.00964(OH)
Benzyldimethylamine	135.2	178–180	0.1002	0.00074

was used to prepare specimens for torsional braid analyses by intermittently warming to room temperature.

Torsional Braid Analysis

The low strain isothermal dynamic mechanical data were obtained at about 1 cps by the technique of torsional braid analysis (TBA).[2] This adaptation of the torsional pendulum involves a free-hanging composite specimen consisting of a multifilamented (~3600) glass braid and the polymer system which is the subject of investigation. A specimen was prepared in a dry box by impregnating a glass fiber braid with the reactive mixture for 30 min at room temperature. The specimen was then mounted in the TBA apparatus which was being maintained at a predetermined constant temperature (±0.5°C). The remainder of the reactive mixture was saved for successive experiments. Monitoring of changes in dynamic mechanical behavior began within 2 min after introducing the specimen into the TBA specimen chamber. The same specimen could be used for determination of transitions in the cured polymer (while cooling to −180°C and then heating) and for observing the effects of additional cure (by heating to 300°C followed by cooling). Flowing dry nitrogen gas was used as the environment in all experiments.

Details of the theory, technique, methods of data reduction, and conventions for presentation of data for torsional braid analysis have been published.[2]

Results and Discussion*

Dynamic mechanical behavior of the epoxy resin/anhydride system during isothermal cure at different temperatures is presented in Figure 1. The curves are arranged in order of increasing cure temperature for the purpose of easy comparison. Stacking the curves in this manner on a logarithmic scale does not alter the shapes of the curves (since $\Delta \log [(\text{constant})X] = \Delta \log X$).

Analysis of the results presented in Figure 1 reveals the occurrence of three different types of dynamic mechanical behavior. The first type of behavior occurs at low temperatures and is characterized by the occurrence of a single damping peak, B, which is accompanied by a one-step increase in rigidity. As the temperature of cure is increased, a second damping peak, A, becomes resolvable as shown by the 80°C cure isotherm. The relative rigidity curves then show a two-step increase in rigidity corresponding to damping peaks A and B. This represents the second type of behavior on isothermal cure. Increasing the temperature further results in a broadening of damping peak B, and the first step of the two-step increase in rigidity becomes relatively more dominant. Above a certain temperature, only a single damping peak, A, and a corresponding one-step increase in rigidity

* Complications due to volatility of constituents of the reaction mixture have been neglected in this analysis. Stoichiometry can be upset by selective volatilization of components from specimens with large surface to volume ratios.

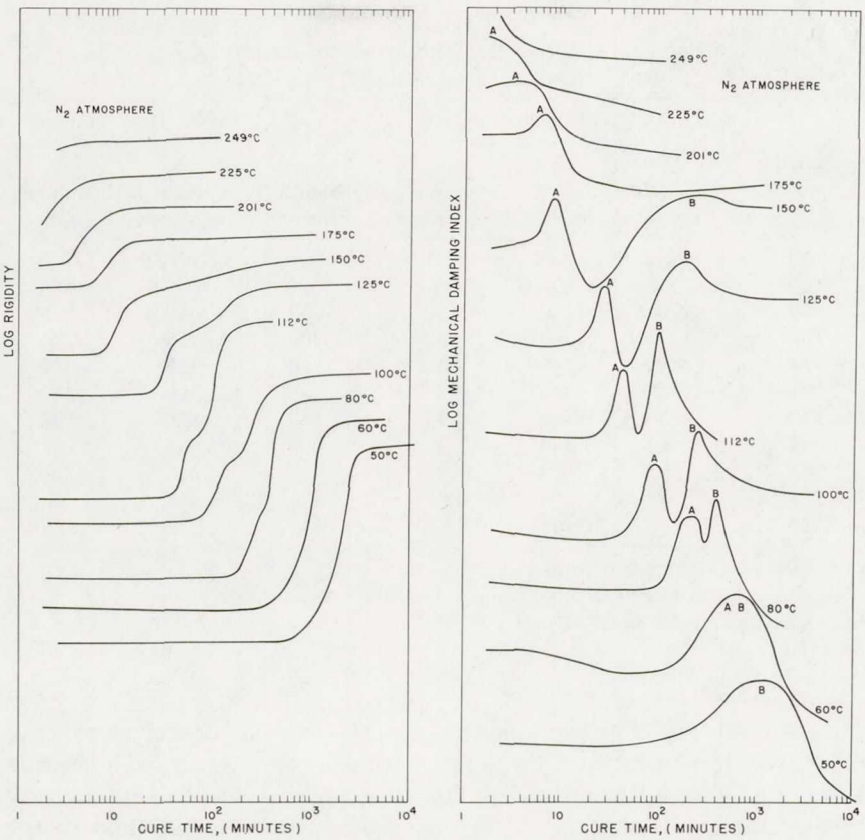

Fig. 1. Rigidity and mechanical damping vs. time during isothermal cure of the cycloaliphatic epoxy system in the temperature range of 50° to 249°C.

are observed. This corresponds to the third type of behavior on isothermal cure. At still higher cure temperatures, damping peak A is not completely definable owing to the high rate of reaction (i.e., when peak A occurs at a time less than 1 min after lowering the specimen into the TBA apparatus).

Damping peak A and its corresponding increase in rigidity are associated with the gel point of the reactive system, whereas damping peak B and its corresponding increase in rigidity are associated with vitrification (transition to the glassy state).

The first type of behavior is a result of an increase in molecular weight of the prepolymer which causes its transformation from the fluid to the glassy state before the onset of gelation. This behavior is apparent until the temperature of isothermal cure is equal to the glass transition temperature of the reactive system at its gel point, T_{gg}. At this point, the processes of vitrification and gelation occur together. This follows since vitrification occurs when the glass transition $T_g(t)$ of the reacting system equals the temperature of cure and since (for a given reactive system) gelation occurs at a constant conversion which is independent of temperature.

TABLE II
Gelation and Vitrification Times Versus Isothermal Cure Temperatures as Determined by Three Methods

Cure temp., °C	Gelation time, min			Vitrification time, min		
	Rigidity intercept	$^1/_2\Delta$ (log rigidity)	Damping peak	Rigidity intercept	$^1/_2\Delta$ (log rigidity)	Damping peak
50	n.a.	n.a.	n.a.	—[b]	1,950	1,250
60	n.a.	n.a.	n.a.	—[b]	950	650
80	175	230	215	350	420	395
100	73	102	91	205	275	255
112	42	47	43	90	106	100
125	25	31	27	95	160	180
150	7.4	9.6	8.4	105	650	245
175	5.5	8.4	6.5	n.a.	n.a.	n.a.
201	3.1	4.7	3.8	n.a.	n.a.	n.a.
225	—[a]	2.6	—[a]	n.a.	n.a.	n.a.
249	—[a]	—[a]	—[a]	n.a.	n.a.	n.a.

[a] Difficult to measure experimentally.

[b] Rigidity intercept method ambiguous because unique linear extrapolation of log rigidity vs. log time not possible.

n.a. Not applicable.

The second type of behavior occurs when the temperatures of cure exceed T_{gg}, at which temperatures the reactive system can pass through gelation before vitrifying. Vitrification is due to an increase in crosslink density after gelation. In this region, the materials pass from the fluid to the rubbery and then to the glassy state.

The results also show (Table II) that the time of occurrence of gelation decreases with increasing temperature. This is due to the increased rate of reactions at higher temperatures. The time of occurrence of vitrification reflects the competition between the increased rate of cure with increased temperature and the increased degree of cure necessary for vitrification at higher temperatures. Vitrification time is observed to pass through a minimum value at 112°C. The occurrence of a minimum is presumably the consequence of a decrease in reaction rate at high conversion.

The gelation and vitrification times were measured in the three ways illustrated in Figure 2. These are designated rigidity intercept, $^1/_2\Delta$ (log rigidity), and damping peak maximum methods. The times for gelation and vitrification for each of the isothermal experiments as measured by the three methods are tabulated in Table II. It is noted for both gelation and vitrification at any isothermal temperature that the time of a transition depends on the method of measurement and that the value of the time generally increases thus: rigidity intercept time < damping peak time $<^1/_2\Delta$ (log rigidity) time.

Since the chemical conversion at the gel point is constant for a given reactive thermosetting system, it follows that the gelation time, t_g, is a

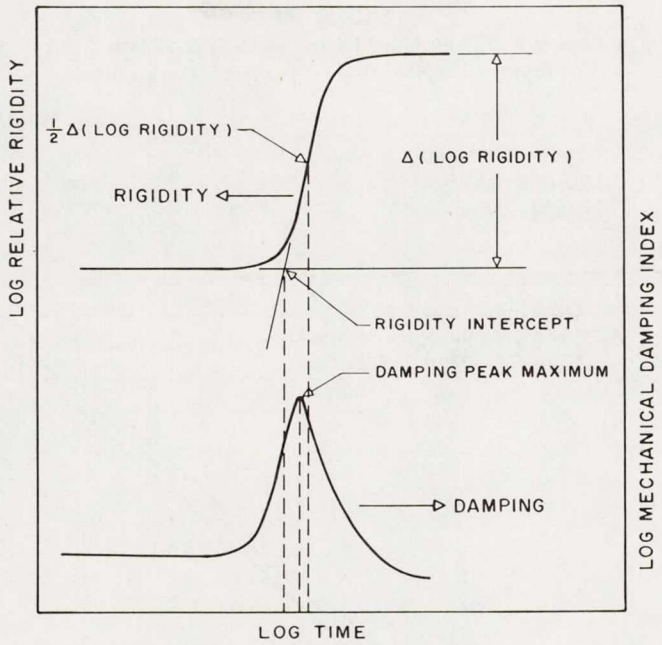

Fig. 2. Methods for determining time to gel and time to vitrify: top, rigidity intercept and $^1/_2\Delta$ (log rigidity) from relative rigidity curve; bottom, damping peak maximum from damping curve.

direct inverse measure of the overall rate of the reaction. The Arrhenius relationship can be used to relate gelation time to temperature by plotting the logarithm of the gelation time versus the reciprocal of the absolute temperature since t_g = constant $\times$ $e^{E/RT}$, where E is the activation energy. The plot of logarithm gelation time, measured by the three methods, versus $1/T°K$ is displayed in Figure 3. Three lines with the same slope appear to fit the data. The apparent overall activation energy calculated from the slope is 12.2 kcal/mole, a value which agrees with those obtained for other epoxy systems.

Plots displaying the times to gelation and times to vitrification, measured by the three methods, versus cure temperature are shown in Figure 4. The gelation curves were extrapolated (dashed lines) to low temperatures by using the Arrhenius relationship (see above). At cure temperatures below the minimum in the vitrification time, the vitrification curves were extrapolated linearly (dashed lines). The intersection of each pair of the extrapolated gelation and vitrification curves (paired according to the method used for determining the transitions) is designated T_{gg}. The values are tabulated in Table III. The values which result for T_{gg} differ but little, in part because of the steep slope of the exponential gelation time versus cure temperature relationship in the vicinity of T_{gg}. The procedure, therefore, results in an accurate method for determining T_{gg}.

TABLE III
Values of T_{gg} Determined by Intersection of Gelation and Vitrification Times Versus Cure Temperature Curves

Method	T_{gg}, °C
Rigidity intercept	58
$^1/_2\Delta$ (log rigidity)	58
Damping peak	57

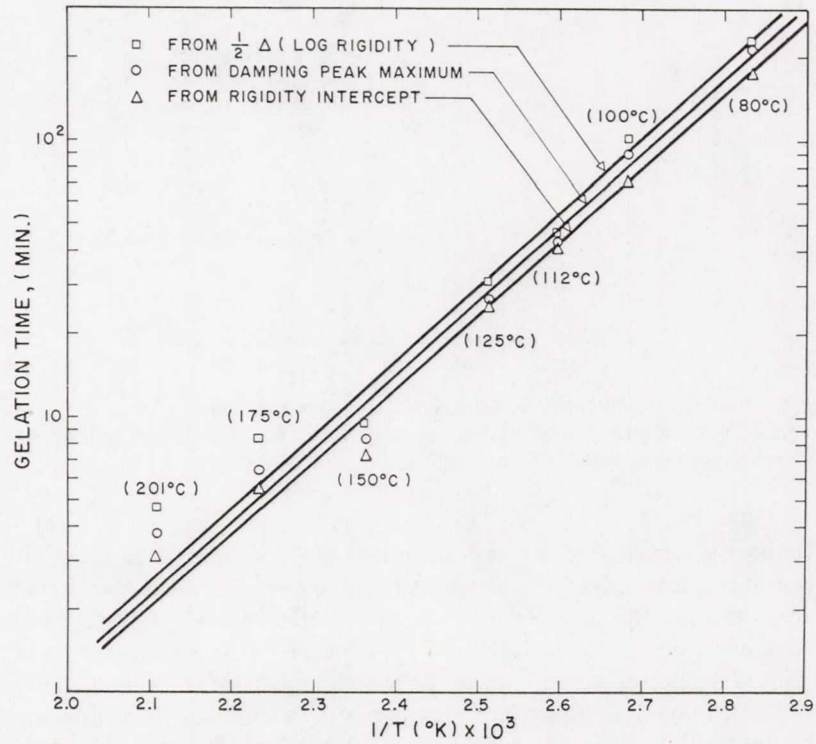

Fig. 3. Arrhenius plot of log (time to gel) vs. T^{-1} (°K). Gelation time was obtained by three methods: (1) rigidity intercept; (2) $^1/_2\Delta$ (log rigidity); (3) damping peak maximum.

The data points listed in Table II for vitrification times for isothermal cure temperatures of 60° and 50°C do not appear in Figure 4 and do not lie on the linear extrapolations of Figure 4. These data points are treated differently for the reason that above T_{gg} (and below $T_{g\infty}$) the measures of vitrification time involve measuring a change from a rubbery network to a glassy structure, whereas below T_{gg} measurements of vitrification time involve measuring a change from a liquid to glassy structure.

CONCLUSIONS

The significance of the presently reported and of the earlier research[1] lies in the generalities which appear to have been developed for reactive thermo-

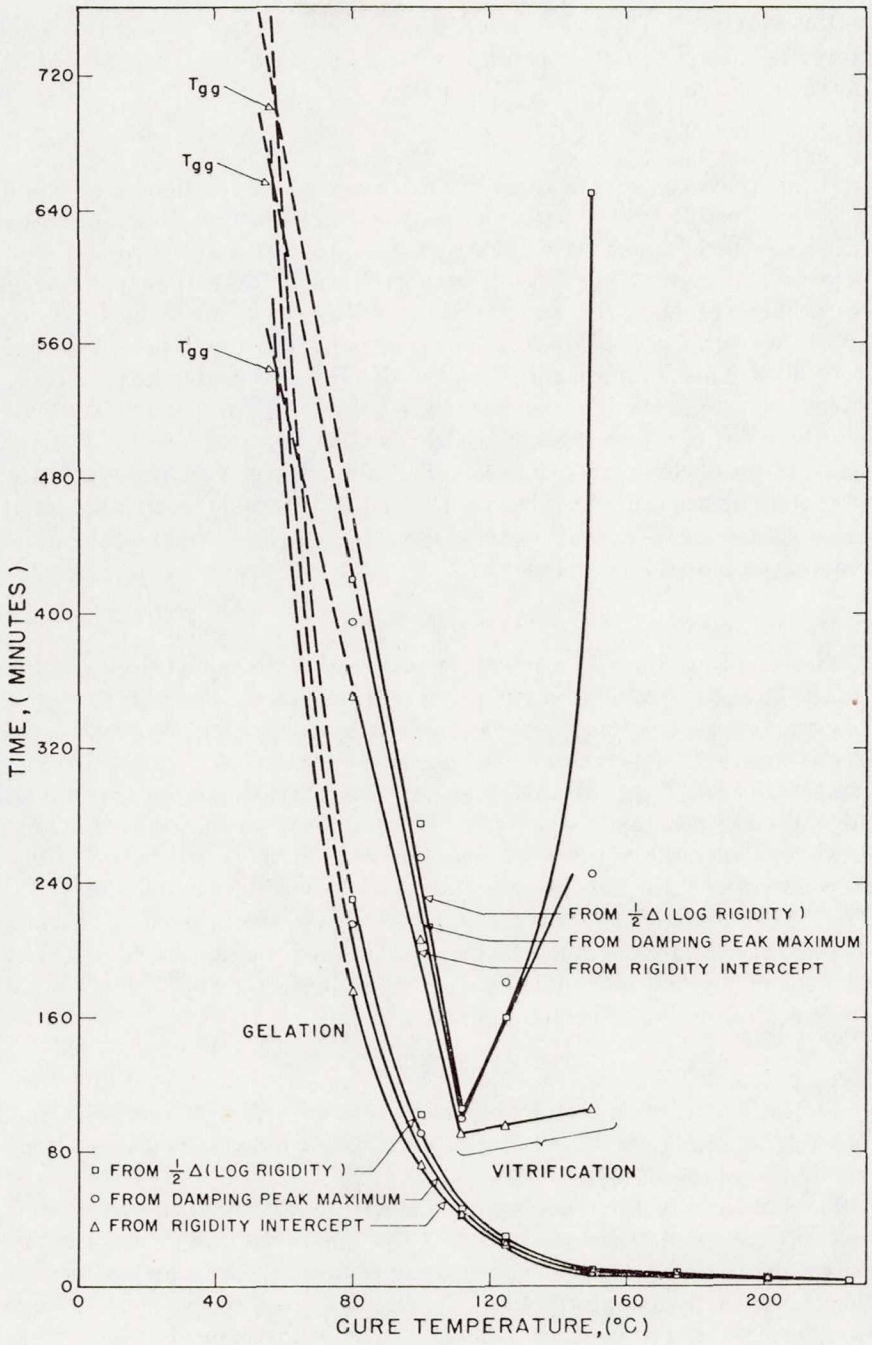

Fig. 4. Time to gelation and time to vitrification vs. temperature of isothermal cure of the cycloaliphatic epoxy system. Gelation and vitrification times were obtained by three methods: (1) rigidity intercept; (2) $^1/_2\Delta$ (log ridigity); (3) damping peak maximum.

setting systems. These depend on the existence of two critical temperatures, T_{gg} and $T_{g\infty}$, for isothermal cure. Three types of behavior can be obtained on cure:

1. $$T_{\text{cure}} < T_{gg}$$

Before the occurrence of vitrification, the rate of the reaction in the liquid state presumably fits the Arrhenius relationship with the activation energy which can be obtained by measuring times to gelation at isothermal temperatures of cure above T_{gg}. After vitrification, the rate of reaction is essentially quenched. A reactive thermosetting system should be stored at temperatures well below T_{gg} so as to avoid gelation and provide a long shelf-life. This is presumably the basis of "B-stage" technology.

An accurate method for determining T_{gg} is reported which involves finding the point of intersection of the vitrification and gelation times versus temperature of cure curves (Fig. 4). The method arose from the realization that the vitrification and gelation times should coincide at an isothermal temperature of cure which is equal to the glass transition temperature of the reacting system at its gel point.

2. $$T_{gg} < T_{\text{cure}} < T_{g\infty}$$

The rates of isothermal reaction are presumably the same before gelation (in the fluid state) and up to the time of vitrification (in the rubbery state). The reaction is essentially quenched on vitrification which occurs when the glass transition temperature of the reactive system, $T_g(t)$, equals the temperature of cure, T_{cure}. A consequence of this is that the system can only be fully cured by reacting above $T_{g\infty}$. This is shown schematically in Figure 5, which shows the anticipated relation between the temperature of isothermal cure, T_{cure}, and the resultant glass transition temperature, T_g. The value for the glass transition temperature of the fully cured thermosetting system, $T_{g\infty}$, is obtained most easily after curing above $T_{g\infty}$. A convenient method for obtaining $T_{g\infty}$ is to obtain the thermomechanical spectra after curing or postcuring above $T_{g\infty}$.

3. $$T_{\text{cure}} > T_{g\infty}$$

The rates of reaction presumably obey the same Arrhenius relationship as for $T_{\text{cure}} < T_{g\infty}$ (before vitrification). Gelation occurs, but there is no vitrification process.

The influence of the reactants on the nature of the cure is determined not only by the inherent reactivity of the functional groups, but also by the geometry and polarity of the growing chain segments which determine the transition temperatures (T_{gg}, T_g, $T_{g\infty}$) of the reactive systems and therefore the type (1, 2, and 3) of dynamic mechanical behavior experienced in isothermal cure. For example, for highly crosslinked or rigid chain polymeric systems $T_{g\infty}$, or even T_{gg}, can be above the limits of decomposition, and then only type 1 and type 2, or only type 1, behavior would be observed. Only type 3 behavior can be observed at $T \geq$ room

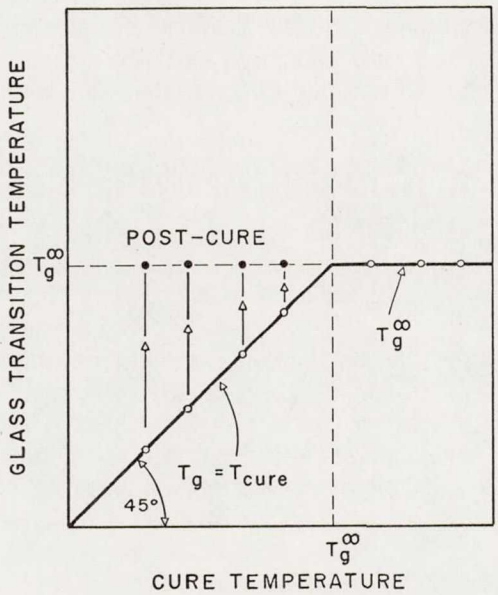

Fig. 5. Schematic diagram of glass transition temperature, T_g, to be expected from curing at isothermal temperature, T_{cure}. Note that the maximum value of the glass transition temperature, $T_{g\infty}$, is obtained only after heating to above $T_{g\infty}$.

temperature for reactive prepolymer systems if $T_{g\infty}$ is below room temperature (as for elastomers).

The financial support provided by the National Aeronautics and Space Administration (Grant NGR-31-001-221) and the Chemistry Branch of the Office of Naval Research (Contract Number N00014-67-A-0151-0024) are acknowledged. Appreciation is also extended to the Newark Section of the Society of Plastics Engineers for an undergraduate research grant which was administered by the Plastics Institute of America and awarded to Mr. J. Benci.[4]

References

1. P. G. Babayevsky and J. K. Gillham, *J. Appl. Polym. Sci.*, **17**, 2067 (1973).
2. J. K. Gillham, *Crit. Rev. Macromol. Sci.*, **1**, 83 (1972).
3. Technical Bulletin, *Bakelite*$^{(R)}$ *Cycloaliphatic Epoxides*, Union Carbide Corporation, Park Avenue, New York, N.Y., 1970.
4. J. A. Benci, Dynamic Mechanical Analysis of the Catalyzed Cure Reaction of a Cycloaliphatic Epoxide with Hexahydrophthalic Anhydride, Senior Thesis, Department of Chemical Engineering. Princeton University, Princeton, N.J., June 1973.

Received July 24, 1973

J. MACROMOL. SCI.—PHYS., B9(2), 255-266 (1974)

Low-Temperature Relaxations in Amorphous Polyolefins

A. HILTNER and E. BAER
Department of Macromolecular Science
Case Western Reserve University
Cleveland, Ohio 44106

J. R. MARTIN* and J. K. GILLHAM
Polymer Materials Program
Department of Chemical Engineering
Princeton University
Princeton, New Jersey 08540

Abstract

The dynamic mechanical relaxation behavior (1cps) of two series of amorphous polyolefins, $-(CH_2)_mC(CH_3)_2-$ and $-(CH_2)_mC(CH_3)(CH_2CH_3)-$ where m = 1, 2, 3 was investigated from 4.2°K to the glass transition. Most of the polymers show a damping maximum or pleateau in the 40 to 50°K region. Various mechanisms which have been suggested for cryogenic relaxations in amorphous polymers are considered as they might relate to the polyolefins. Two secondary relaxation processes above 80°K are distinguished. A relaxation at about 160°K (β) in the second and third member of each series is associated with restricted backbone motion. This process requires a certain degree of chain flexibility since it is not observed in the first member of each series. A lower Temperature process (γ) is observed in each member of the second series and is attributed to motion of the ethyl side group.

*Present address: Textile Research Institute, Princeton, N.J.

INTRODUCTION

This study presents an investigation of the dynamic mechanical relaxation behavior at 1 cps of two series of amorphous polyolefins, —$(CH_2)_mC(CH_3)_2$—and—$(CH_2)_mC(CH_3)$ (CH_2CH_3)—where m = 1, 2, 3. The intramolecular flexibility of the polymer molecules is varied by increasing the number of in-chain—CH_2—units between substituted carbon atoms. Because of the absence of polar forces the results of the dynamic mechanical study must be interpreted solely in terms of geometric effects other than tacticity and crystallinity which are absent. A previous study using a modified torsional pendulum (1 cps) [1,2] has characterized the glass transition temperatures and also indicated complex secondary relaxation behavior. Since these form an important class of polymers, the mechanical relaxation measurements have been extended down to 4.2°K in order to further elucidate the secondary relaxation processes.

EXPERIMENTAL

The polymers were synthesized using the procedures of Kennedy [3]. Because the polymers are not self-supporting at room temperature, and some members of the series were available only in small quantities, the torsional braid technique [2] was used. Characterization of the polymers and preparation of the composite polymer/braid specimens have been described previously [1-3]. High-resolution NMR measurements of polymer solutions show that the first two members of each series are structurally pure. The structural purity of the third member of the first and second series has been estimated to be 65% and 92%, respectively [4]. Dynamic mechanical measurements were made with a free-oscillating, inverted torsional pendulum at about 1 cps [5] over the temperature range from 4.2°K to the increase in damping which marks the beginning of the glass transition region.

RESULTS AND DISCUSSION

All the polymers show a damping maximum or plateau in the 40 to 50°K region (δ process) with the possible exception of the third member of the first series (Fig. 1). This process is more intense for members of the second series than for the first. A plateau at about 20°K is also observed for the first member of each series. Various mechanisms have been suggested for cryogenic relaxations

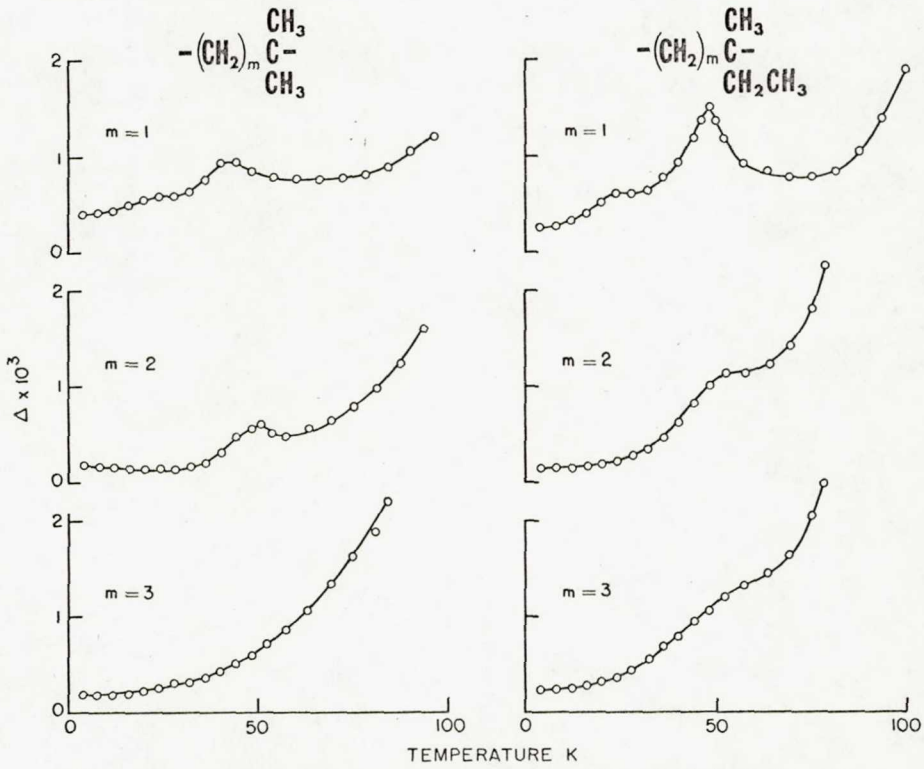

FIG. 1. Relaxation behavior of amorphous polyolefins below 80°K, Series 1 and 2.

in amorphous polymers, and some are considered below as they might relate to the polyolefins.

It is generally thought that classical rotation of methyl groups not attached directly to the main chain can produce a mechanical relaxation below 80°K [6]. Few polymers with methyl groups attached directly to the backbone have been studied at cryogenic temperatures. Poly(dl-propylene oxide) exhibits a broad shoulder in mechanical measurements at about 80°K (10,000 cps). From correlation of the mechanical with dielectric and wide-line NMR data, this shoulder has been associated with methyl group rotation [7]. Wide-line NMR measurements indicate the onset of methyl group rotation in polypropylene at about the same temperature [8]. The corresponding mechanical loss peak should be located at about 80°K (10,000 cps), but this has not been observed [9]. A T_1 minimum in the wide-line NMR of the first member of the first series has also been identified with methyl group motion [10], and extrapolation of the Arrhenius

plot indicates the process would occur at about 95°K at 1 cps.* The reason for the apparent absence of a mechanical methyl group process at the predicted temperature is not understood. However, it would appear that the δ peaks can not be attributed to such a mechanism.

Several other types of processes can also give rise to cryogenic relaxations. Polypropylene, the singly substituted analog of the first member of the first series, shows a plateau of about 20°K (10,000 cps) [9] in mechanical measurements which has been attributed to quantum mechanical tunneling of the methyl group in amorphous regions about the rotational axis of symmetry [11]. A similar plateau observed at about 20°K in two of the polymers in this study may involve a similar tunnelling process.

Another mechanistic possibility does not involve specific side group motion. Relaxations observed in the 40 to 50°K range in some linear semi-crystalline polymers have been attributed to motion of defects in the crystalline or ordered regions [12]. It has also been suggested [13] that certain types of disclinations which may be present in amorphous polymers can give rise to mechanical relaxations.

Finally, cryogenic relaxations have been observed in some silicates [14], and the possibility that the δ peaks observed in this study arise either from the glass support, or from the composite nature of the specimens, can not be ignored.

Above 80°K, the first member of the first series shows no secondary peaks while the second and third members each show a single peak at 168 and 156°K, respectively (Fig. 2). The third member of this series is not pure, and the shoulder at about 100°K may be attributed to the isobutyl and isopropyl side groups which are present as structural impurities [4]. In the second series, the first member has a single peak at 144°K and the second and third members each have two peaks (Fig. 3). The purity of the third member of this series is estimated at about 92% and it is felt that the assignment of two separate processes is justified. The earlier study [1], which extended only down to 80°K, reported similar results with the exception of the third member of the second series where only a single temperature was assigned.

Although the relaxation spectra appear complex, an interpretation consistent with the relaxation behavior of other polyolefins can be made. It is proposed that the single peak for the second and third members of the first series and the higher temperature of the peaks in the corresponding members of the second series (labeled β) can be associated with restricted backbone motion. The single peak in the

*Pertinent to this discussion is the observation of a dielectrically active and yet mechanically inactive low-temperature relaxation for the second member of the first series at 108°K (1 cps) [1].

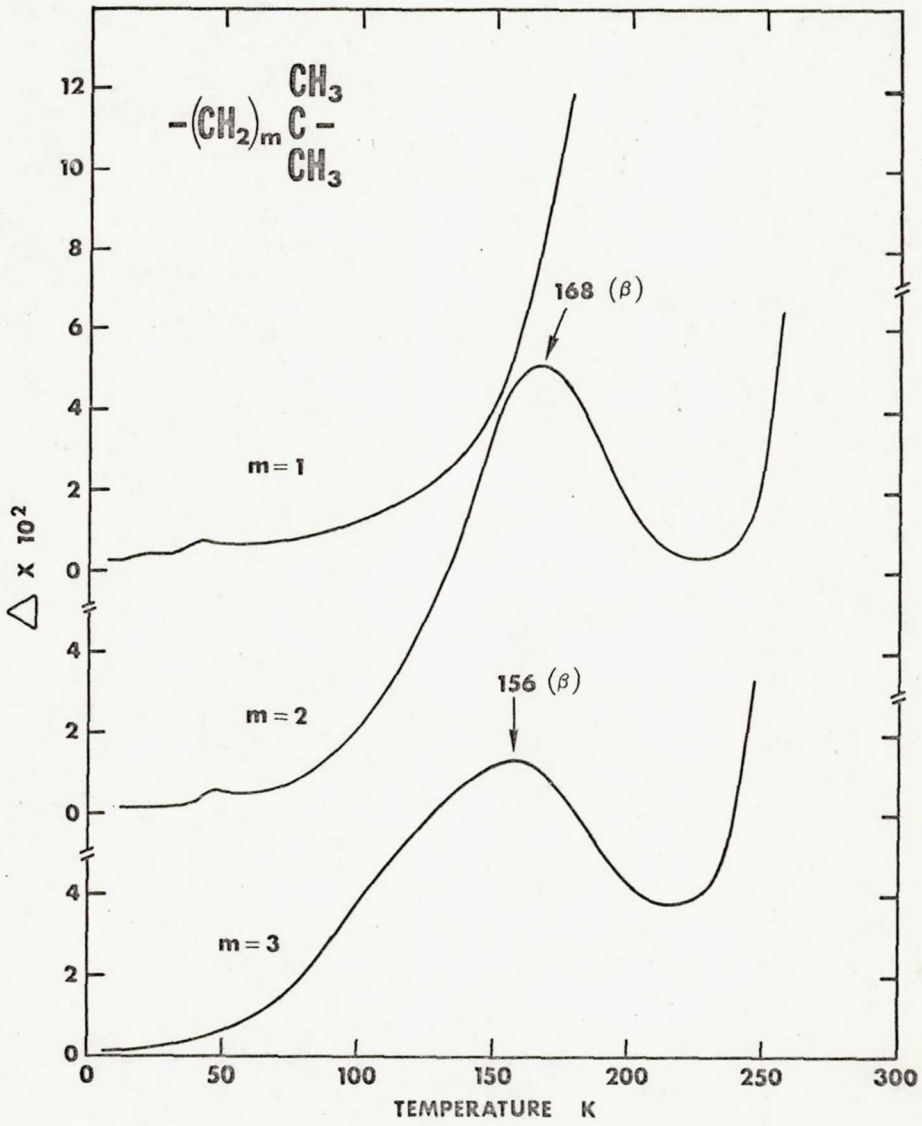

FIG. 2. Relaxation behavior of amorphous polyolefins, Series 1.

first member of the second series and the lower temperature peak in the higher members of this series (labeled γ) are attributed to motion of the ethyl side group. The temperature of the γ process in the first member is comparable to the process in polybutene-1 at

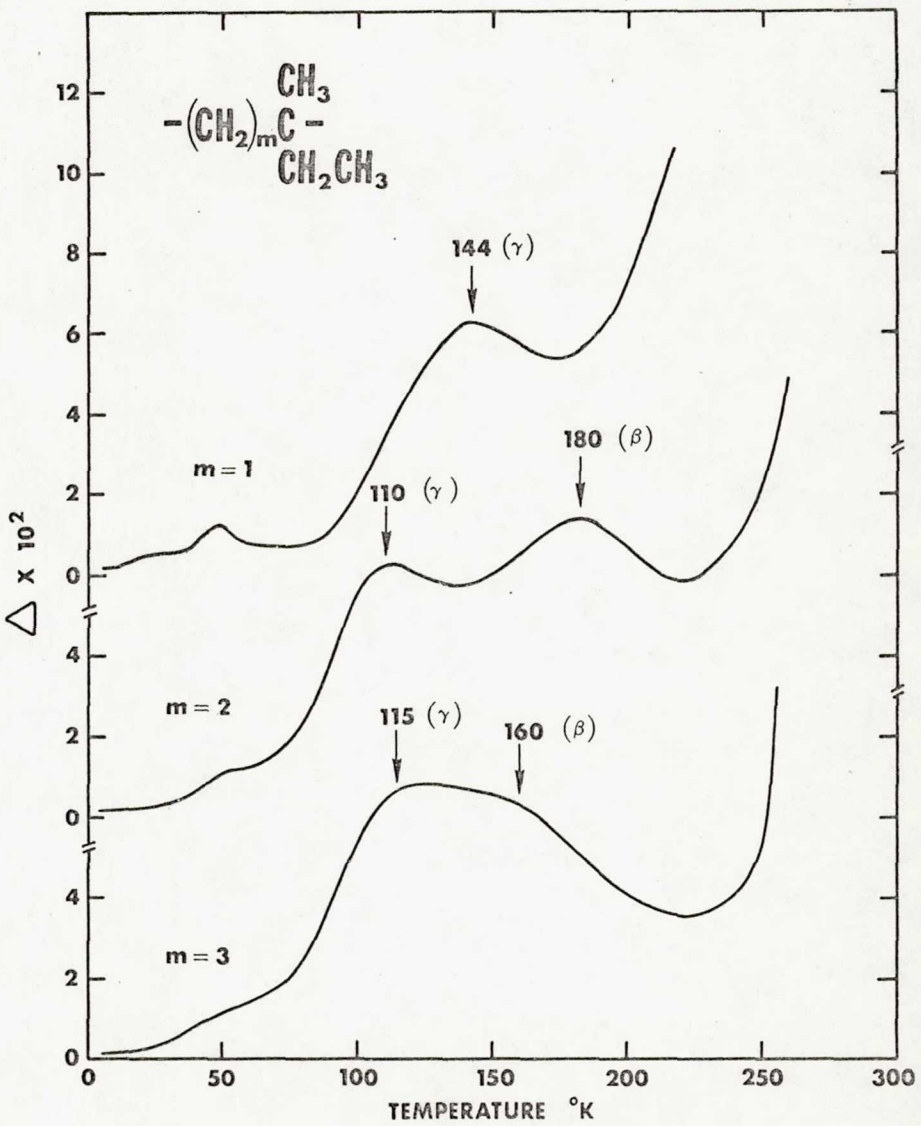

FIG. 3. Relaxation behavior of amorphous polyolefins, Series 2.

133°K (200 cps) [15] and is higher than for the second and third members of the series as a result of steric hindrance. Side group motion in the second and third members is less hindered, and the γ

temperature is closer to that suggested for terminal ethyl groups (about 105°K, 200 cps) [15].

The members of the first series do not exhibit a peak analogous to the γ which can be associated with the methyl side group. As mentioned above, extrapolation of the wide-line NMR data for the first member of the first series predicts such a relaxation should be observed at about 95°K at 1 cps. However no peak is observed in the mechanical measurements at this temperature. The reason why a methyl side group process is absent in mechanical measurements is not understood, although the symmetry of methyl group rotation may be important. Other polyolefins with methyl side groups such as polypropylene and hydrogenated hevea [15] also show no mechanical side group relaxation.

It is proposed that the β peak, which is only observed in the second and third member of both series, should be associated with restricted backbone motion. Although the formal crankshaft motion [15] is forbidden in these polymers and also in—$(CH_2)_2CH[C(CH_3)_3]CH_2$—which exhibits a process at about 160°K [16], certain minimum chain flexibility requirements must be necessary since the process is not observed in the first members of the series. The constant ratio of the β temperature to the glass transition temperature for all four polymers (Table 1) is further evidence that backbone motion is involved and suggests that the β process is a precursor to the glass transition. For example, the glass transition can be considered as a freeing of the localized β motions permitting the entire chain to move cooperatively. The absence of a secondary process below the glass transition in the first member of the first series, polyisobutylene (PiB), would seem to contradict this interpretation. To find an explanation it is necessary to consider more closely the nature of the glass transition in PiB and the other polymers.

Two factors which are usually considered of prime importance in determining the glass temperature of a polymer are intramolecular steric hindrance and intermolecular interaction of dipolar groups. Since the polyolefins are nonpolar the former should be the predominant factor. The first member of each series is highly hindered sterically and from intramolecular considerations would be expected to have the highest glass temperature. However in both series the glass temperature of the first member is lower than that of the second and third members. Another anomaly is encountered in the comparison of vinylidene polymers—(CH_2CR_2)—with their more flexibly vinyl counterparts—(CH_2CHR)—. Thus the glass temperature of PiB (208°K at 1 cps [2]) is much lower than that of polypropylene (273°K at 1 cps [17]). A comparison of PiB and polypropylene with their chlorinated analogs, poly(vinylidene chloride) (T_g = 288°K

TABLE 1

Relaxation Temperatures for Amorphous Polyolefins

	Polymer	M_v^*	T_g^*	T_β	T_γ	T_β/T_g
$-(CH_2)_m-\underset{\displaystyle CH_3}{\overset{\displaystyle CH_3}{\overset{|}{\underset{|}{C}}}}-$	m = 1	200,000	208°K (22 kcal/mole)	—	—	
	m = 2	30,000	266 (48 kcal/mole)	168	—	0.63
	m = 3	460,000	258 (44 kcal/mole)	156	—	0.60
$-(CH_2)_m-\underset{\displaystyle CH_2CH_3}{\overset{\displaystyle CH_3}{\overset{|}{\underset{|}{C}}}}-$	m = 1	18,500	253 (28 kcal/mole)	—	144	
	m = 2	25,100	278 (44 kcal/mole)	180	110	0.65
	m = 3	268,000	258	160	115	0.62
$-(CH_2CH_2)_n-$	Polyethylene		240**	160**	—	0.67

*Ref. 2.
**Refer to text.

[18]) and poly(vinyl chloride) (T_g = 347°K [19]) is interesting. The polar nature of these polymers should cause higher glass temperatures but steric factors should be similar since the—Cl atom and the—CH_3 group are almost the same size. Again the glass temperature of the more hindered polymer (i.e., that with two substituents on alternate C atoms) is about 60° lower than that of the singly substituted polymer. Similarly the glass temperature of poly(vinylidene fluoride) (233°K [20]) is much lower than that of poly(vinyl fluoride) (314°K [18]). One possible explanation of these anomalies has been suggested by Boyd and Breitling [21]. The pendant methyl groups on alternate C atoms of PiB are severely crowded. This crowding is best alleviated when pairs of backbone bonds are distorted slightly (about 20°) from either trans or gauche. The calculated barriers to transitions between trans and gauche states were found to be too high (much higher than the trans $\rightleftharpoons$ gauche barrier in polyethylene, for example) to figure significantly at the observed glass temperature. Backbone motions associated with the glass transition of PiB are therefore thought to be very restricted compared to most polymers, and the authors suggest that transitions between secondary minima associated with the distorted trans or gauche conformations may be important.

It was suggested earlier that the glass transition could be considered as a freeing of local backbone motions (β process) permitting long segments of the chain to move cooperatively. Goldstein [22] has predicted on theoretical grounds that a glass transition should have a $T_\beta < T_g$ process. Matsuoka and Ishida [23] have shown empirically that T_β/T_g is a constant for many polymers including polypropylene, poly(vinyl chloride) and poly(vinyl fluoride) [24]. It is shown here that the second and third members of both polyolefin series also fit this category. The validity of such a relationship strongly supports the idea of a common glass transition mechanism. Exceptions to the constant T_β/T_g relationship include PiB, poly(vinylidene chloride) and poly(vinylidene fluoride). No secondary process is observed in PiB or poly(vinylidene chloride) although a low temperature shoulder on the glass peak has been reported for poly(vinylidene fluoride) [20]. This "anomaly" in the secondary relaxation behavior also points to a different glass transition mechanism in the vinylidene polymers. If molecular motion associated with the glass process in the vinylidene polymers is very restricted, as suggested above, the barriers to motion over long chain segments may not differ greatly from the barriers to local motion, and therefore the local processes would be observed at temperatures very close to the glass temperature.

It is of interest to extend the ideas developed above to a discus-

sion of the glass transition temperature in polyethylene (PE). PE does not have the steric hindrance of the vinylidene polymers and hence would be expected to exhibit a secondary amorphous relaxation. The mechanical γ peak in PE can be resolved into at least two components [25]. The lower temperature component at about 120°K (1 cps) is associated with the crystalline phase and is thought to involve chain reorientation at defects [26,27]. The more intense component at 160°K (1 cps) is from the amorphous phase. Measurements down to 4.2°K have revealed no additional amorphous relaxations below 160°K although several crystalline peaks were observed [28]. If the 160°K process is then taken as T_β, a glass transition would be predicted in the vicinity of 240°K ($T_\beta/T_g = 0.67$, 1 cps) for amorphous PE. This coincides with the temperature of the so-called β peak observed in low density, branched PE and is in agreement with the glass temperature of PE suggested by Illers [25] and others [29,30].

The question of the glass transition temperature also arises in other highly crystalline polymers. Like PE, polyoxymethylene (POM) has a complex γ relaxation that can be separated into at least two components at 180° and 205°K (1 cps) with the higher temperature component associated with the amorphous regions [31]. Admittedly some modification of the empirical relationship between T_β and T_g may be appropriate for polymers without the C—C backbone. However as described above, the relationship predicts the glass transition of POM to be around room temperature, possibly corresponding to the so-called β process at about 270°K (1 cps).

Previous considerations of the glass transitions for the two series of polyolefins has led to a theory [1] in which intermolecular interlocking was proposed to be a dominant factor affecting the glass transitions for the second and third members of each series, but not for the first. Dielectrically obtained activation energies for the glass transitions of these polymers also indicated a different mechanism for T_g in the first member of each series [1]. The results presented here provide additional evidence for mechanistic differences in the first member of each series through the absence of a major secondary relaxation (β process). In addition, extrapolation of the constant T_β/T_g ratio (observed for m = 2 and 3) to m = ∞ predicts a T_g for PE of 240°K. If this extrapolation is valid, it would indicate that T_g decreases only slightly with increasing values of m. Thus, the concept of intermolecular interlocking could be brought into question since the theory predicts a T_g for PE considerably lower than the other members of the series as a result of the supposition that PE would not be expected to display intermolecular interlocking. However, criticism of the interlocking mechanism, and conclusions regarding the glass transition of PE, depend on the validity of the extrapolation of the T_β/T_g ration to m = ∞.

CONCLUSIONS

The mechanical relaxation behavior of two series of amorphous polyolefins with the structures—$(CH_2)_mC(CH_3)_2$— and —$(CH_2)_mC(CH_3)(CH_2CH_3)$—where m = 1,2,3, has been described. In the absence of other structural variables such as polar forces, tacticity and crystallinity, the results can be interpreted solely in terms of the molecular flexibility in the bulk state:

I. Only members of the second series, which contain an ethyl side group, appear to show a side group relaxation. No mechanical relaxation peak is observed which can be attributed to the methyl group.

II. For $m \geq 2$, the polyolefins exhibit a β relaxation which is associated with local backbone motion. The temperature of the β process is such that T_β/T_g is a constant, and from his relationship the predicted glass transition temperature of polyethylene ($m = \infty$) is about 240°K.

III. For m = 1, the β peak is absent. This observation, together with the unusually low glass temperature of these polymers, suggests that a different glass mechanism is operative.

Acknowledgment

This research was generously supported by the Atomic Energy Commission, University of California Lawrence Radiation Laboratory, and the National Aeronautics and Space Administration Grant NGR-31-001-221.

REFERENCES

[1] J. R. Martin and J. K. Gillham, *J. Appl. Polym. Sci.*, 16, 2091 (1972).
[2] J. K. Gillham, *Crit. Rev. Macromol. Sci.*, 1, 83 (1972).
[3] J. P. Kennedy, in *Encyc. Polym. Sci. Tech.* (N. Bikales, ed.), Vol. 7, Wiley-Interscience, New York, 1967, p. 754.
[4] J. R. Martin, Doctoral Thesis, Princeton University, 1972.
[5] C. D. Armeniades, I. Kuriyama, J. M. Roe, and E. Baer, *J. Macromol. Sci.—Phys.*, B1, 777 (1967).
[6] A. Hiltner and E. Baer, *Crit. Rev. Macromol. Sci.*, 1, 215 (1972).
[7] J. A. Sauer and R. G. Saba, *J. Macromol. Sci.—Chem.*, A3, 1217 (1969).
[8] J. G. Powles and P. Mansfield, *Polymer*, 3, 339 (1962).
[9] A. E. Woodward, *J. Polym. Sci., Part C*, 14, 89 (1966).
[10] W. P. Slichter, *J. Chem. Ed.*, 47, 193 (1970).
[11] A. Eisenberg and S. Reich, *J. Chem. Phys.*, 51, 5706 (1969).
[12] A. Hiltner and E. Baer, *Polym. J.*, 3, 378 (1972).
[13] J. C. M. Li and J. J. Gilman, *J. Appl. Phys.*, 41, 4248 (1970).
[14] W. W. Scott and R. K. MacCrone, *Phys. Rev.*, B1, 3515 (1970).

[15] T. F. Schatzki, *Polym. Preprints*, 6(2), 646 (1965).
[16] T. F. Schatzki, *Bull. Amer. Phys. Soc.*, 16, CK-4 (1971).
[17] J. M. Crissman, *J. Polym. Sci., Part A-2*, 7, 389 (1969).
[18] K. Schmieder and K. Wolf, *Kolloid Z.*, 134, 149 (1953).
[19] N. G. McCrum, B. F. Read, and G. Williams, *Anelastic and Dielectric Effects in Polymeric Solids*, Wiley, New York, 1967, Chap. 11.
[20] H. Kakutami, *J. Polym. Sci., Part A-2*, 8, 1177 (1970).
[21] R. H. Boyd and S. M. Breitling, *Macromol.*, 5, 1 (1972).
[22] M. Goldstein, *J. Chem. Phys.*, 51, 3728 (1969).
[23] S. Matsuoka and Y. Ishida, *J. Polym. Sci., Part C*, 14, 247 (1966).
[24] R. F. Boyer, *Polym. Preprints*, 13(2), 1124 (1972).
[25] K. H. Illers, *Kolloid Z. Z. Polym.*, 231, 622 (1969).
[26] K. M. Sinnott, *J. Polym. Sci., Part C*, 14, 141 (1966).
[27] J. D. Hoffman, G. Williams, and E. Passaglia, *J. Polym. Sci., Part C*, 14, 173 (1966).
[28] Y. S. Papir and E. Baer, *J. Appl. Phys.*, 42, 4667 (1971).
[29] S. S. Chang, *Bull. Amer. Phys. Soc.*, 18, GD-5 (1973).
[30] G. T. Davis and R. K. Eby, *J. Appl. Phys.*, 44, 4274 (1973).
[31] Y. S. Papir and E. Baer, *Mater. Sci. Eng.*, 8, 310 (1971).

Received by Editor November 28, 1972
Accepted by Editor December 15, 1972

JOURNAL OF APPLIED POLYMER SCIENCE VOL. 17, PP. 2223–2233 (1973)

Thermomechanical Behavior of a Polynorbornadiene

M. B. ROLLER* and J. K. GILLHAM, *Polymer Materials Program, Department of Chemical Engineering, Princeton University, Princeton, New Jersey 08540*, and J. P. KENNEDY, *Institute of Polymer Science, The University of Akron, Akron, Ohio 44325*

Synopsis

A high-temperature linear amorphous hydrocarbon polymer synthesized cationically from 2,5-norbornadiene (bicyclo[2.2.1]hepta-2,5-diene), was studied thermomechanically with respect to physical transitions and stability in nitrogen. The glass transition temperature was determined to be 320°C (at less than 1 cps), which is probably the highest known for a linear hydrocarbon addition polymer. The thermomechanical technique of torsional braid analysis, together with thermogravimetric analysis, differential thermal analysis, infrared analysis, and solubility studies, was used to investigate the sequential events of the glass transition and degradation. The polymer is of particular interest since it is a high-temperature plastic which in the bulk form would probably need to be processed at high speeds in the vicinity of T_g in an inert atmosphere. The presence of tertiary hydrogen atoms should render it amenable to degradation by the earth's environment.

INTRODUCTION

The cationic polymerization of 2,5-norbornadiene (bicyclo[2.2.1]hepta-2,5-diene) (structure I below) has been interpreted to lead predominantly to structure IV.[1,2] Ultraviolet, infrared, and proton magnetic resonance spectroscopy have been used for structure determination.[1,2] The proposed cationic reaction mechanism involves a transannular rearrangement (II → III) of the initially formed intermediate (II), prior to the addition of another norbornadiene monomer[1,2]:

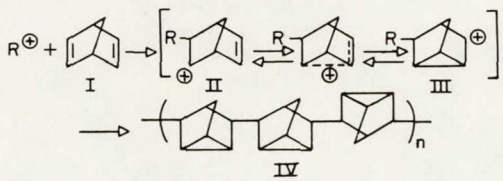

Probably for steric reasons, 1,2-enchainment does not occur. The product was found to be amorphous on the basis of x-ray examination[1,2]; the mechanism was therefore considered not to be stereospecific. An examination of models leads to the expectation that the bonds between cages would be

* Present address: Bell Laboratories, Whippany, New Jersey.

equatorial-to-equatorial. The nortricyclene cage structure in the backbone confers a high degree of chain stiffness on the molecule and therefore a high glass transition temperature on the material. The highly strained substituted cyclopropane ring in the cage would be expected to reduce the overall thermal stability of the structure while the presence of tertiary hydrogens would be expected to provide sites for oxidative attack.

The present report presents a preliminary examination of the thermomechanical behavior and thermal stability of the polymer. The techniques used were torsional braid analysis (TBA) for the thermomechanical spectra,[3–5] differential thermal analysis (DTA) to monitor heat effects, thermogravimetric analysis (TGA) to study weight loss, infrared analysis (IR) to monitor chemical changes, and solubility studies to monitor crosslinking and/or chain stiffening. All the studies were carried out with a heating rate of 2°C/min, with the exception of DTA ($\Delta T/\Delta t$ = 20°C/min), and all were performed in a dried nitrogen atmosphere. TGA was also studied in air.

EXPERIMENTAL

Synthesis

Norbornadiene (bicyclo[2.2.1]hepta-2,5-diene) monomer (Matheson, Colman and Bell) was distilled before use. Gas-chromatographic analysis indicated greater than 98% purity and the presence of four or five minor impurities.

Polymerizations were carried out in a dry box in stirred glass reactors using a published procedure for obtaining noncrosslinked polymer.[1] The catalyst, aluminum chloride, was dissolved in ethyl chloride (2.5% solution) and was added slowly (1–2 ml every 2–3 min) to the reactor which initially contained a homogeneous solution of norbornadiene (19.8 g) in ethyl chloride (130 ml) at −127°C. The temperature of the reaction medium increased to no higher than −125.5°C during the course of the synthesis (>1 hour). Polymerization started immediately after introduction of

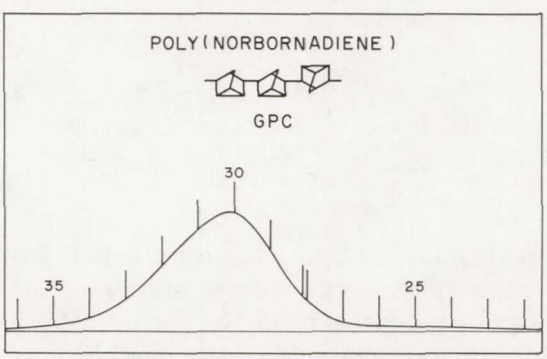

Fig. 1. Gel permeation chromatogram of polynorbornadiene in tetrahydrofuran solvent.

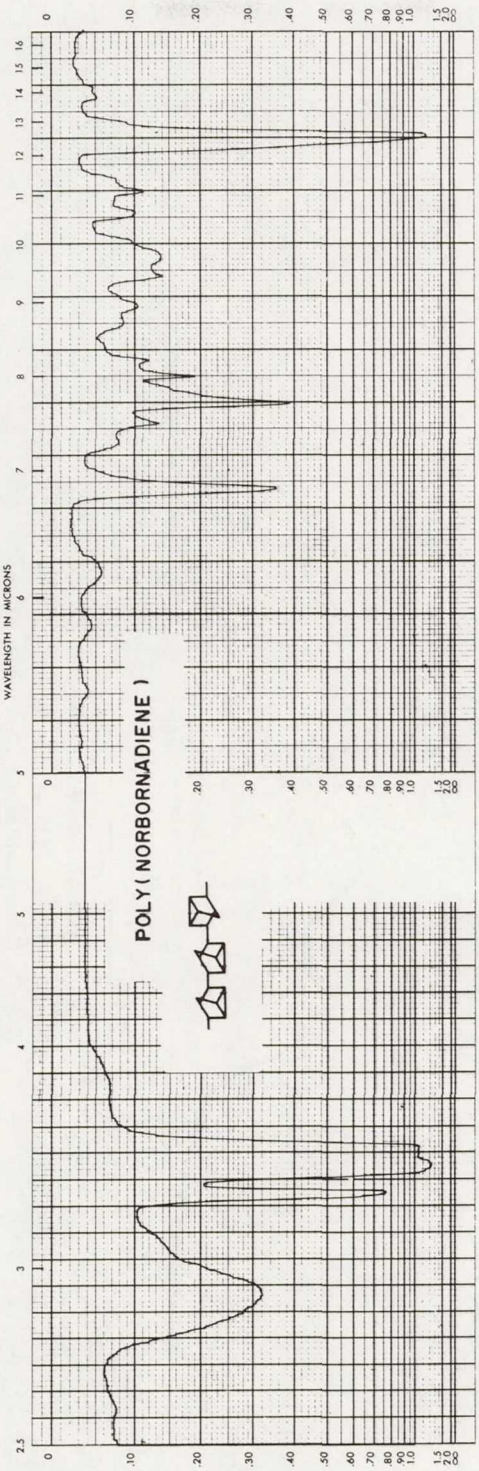

Fig. 2. Infrared spectrum of polynorbornadiene. Specimen was prepared by casting from a benzene solution at 50°C and forming a KBr pellet. Water present in the latter gives rise to absorption at 2.8 and 6.15 microns.

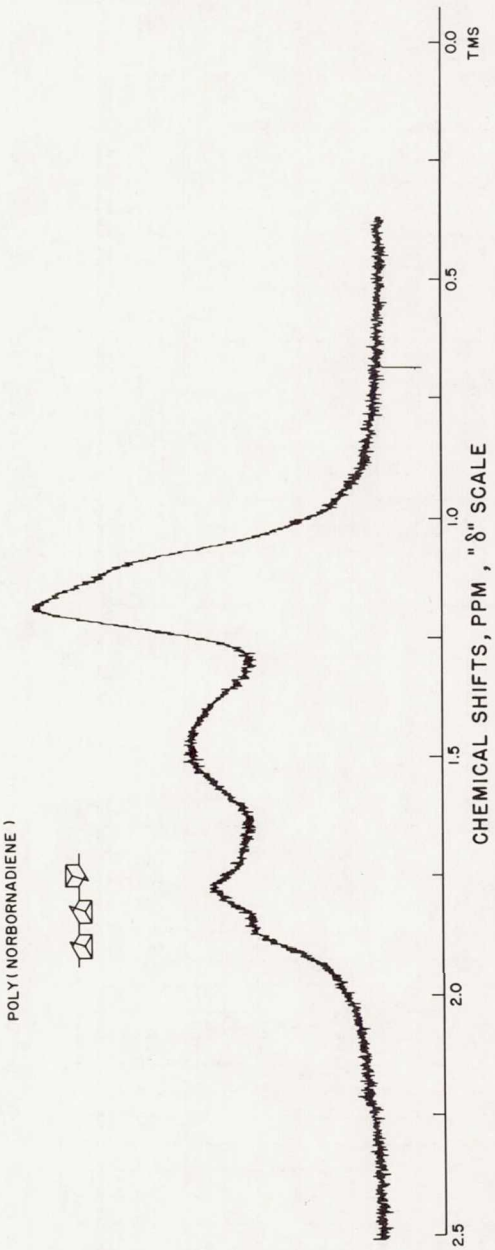

Fig. 3. NMR spectrum (100 MHz) of polynorbornadiene in hexachlorobutadiene (20%) at 90°C (lock signal, benzene). There was scarcely any absorption in the vinyl region (off scale).

catalyst, as detected by the development of haze. The reaction was terminated by introducing precooled *n*-propanol. The product was washed thoroughly with methanol, filtered, and dried under nitrogen at 50°C. The yield was 12.5% (2.5 g). The material was soluble in toluene, benzene, ether, and carbon tetrachloride. Its number-average molecular weight was 9850, as measured by vapor pressure osmometry, which corresponded to a degree of polymerization of about 100. Gel permeation chromatography (GPC) data are shown in Figure 1; when treated as polystyrene, $\bar{M}_n = 14970$ and $\bar{M}_w/\bar{M}_n = 3.73$. The infrared and nuclear magnetic resonance spectra of the polymer are shown in Figures 2 and 3, respectively.

Techniques

The low-strain thermomechanical data were determined at less than 1 cps throughout the range −180° to +500°C by the technique of torsional braid analysis.[3–5] The torsional braid analyzer is a free-hanging torsional pendulum with the specimen consisting of a multifilamented (~3600) glass braid impregnated with the sample polymer. The specimen is fabricated *in situ* by removing solvent from a braid that has been soaked in a polymer solution before mounting. The specimens for the pendulum were made by using a 10% (wt/vol) solution of the polymer in benzene. Solvent was removed from the composite specimens by heating in nitrogen to at least 200°C (see later) and cooling ($\Delta T/\Delta t = \pm 2$°C/min). Attached to the lower clamp is a polarizer disc, the inertial mass, which when coupled with another polarizer over a photocell, acts also as a "linear with angle" transducer to convert the mechanical oscillations into electrical signals.[5] The mechanical oscillations and the analogue signals approximate damped sine waves. The mechanical parameters are deduced from the character of the analogue signals. For isotropic, homogeneous specimens subject to small stains,

$$G' = K(1/P^2)$$

where G' is the in-phase elastic modulus, P is the period of oscillation, and K is a constant dependent upon the geometry. The logarithmic decrement, a measure of the ratio of energy dissipated to maximum energy stored on mechanical deformation, is defined as

$$\Delta = \ln (A_1/A_2) = \ln(A_2/A_3) \ldots = \ln(A_i/A_{i+1})$$

where A is the amplitude of deformation. Due to the composite nature, the small size, and the irregular geometry of the specimens, the data discussed herein are presented in terms of the relative rigidity ($=1/P^2$) replacing G'. The logarithmic decrement (Δ) is presented as the mechanical damping index, $1/n$, where n is the number of oscillations between two fixed but arbitrary boundary amplitudes in each wave (e.g., $A_i/A_{i+n} = 20$), taken constant over any thermomechanical experiment; and $1/n$ is directly proportional to the logarithmic decrement ($\Delta = 1/n \ln[A_i/A_{i+n}]$).

The thermogravimetric analyses were performed in nitrogen and in air using a du Pont 950 thermogravimetric analyzer. The differential thermal analyses were run on a Mettler thermoanalyzer at 20°C/min in nitrogen.

The infrared study was performed on a single film held between two sodium chloride plates. The holder, salt plates, and film were suspended in the TBA oven in a nitrogen atmosphere and were heated at 2°C/min to various "quench points," at which they were removed from the oven to a nitrogen chamber held at room temperature, without being exposed to air. The quenched specimen was examined at room temperature using a Perkin-Elmer Model 237B grating infrared spectrophotometer at low scan rate and normal slit opening. The specimen was returned to the nitrogen quench stream and purged before being returned to the oven at the quench point, after which the oven temperature was taken at 2°C/min to the next quench point. The quench points were taken as significant temperatures in the thermomechanical spectra.

The solubility studies used separate film specimens, each being taken at 2°C/min from room temperature to its quench point before being immersed in solvent. The behavior of the thermally treated films in excess benzene at 25°C was observed visually.

RESULTS AND DISCUSSION

Thermal Analyses (TGA and DTA)

A sample of the solution which was used to fabricate TBA specimens was examined by thermogravimetric analysis in nitrogen and air. After drying in nitrogen by heating at 2°C/min to 200°C, the specimen was cooled to room temperature and run at 2°C/min to 500°C. The thermogram in nitrogen shown in Figure 4 is essentially the same as those obtained in runs made on the dry, powdered, "as received" specimen. A small, slow weight loss started at 250°C and reached 6% by 370°C. The specimen started to lose weight rapidly at about 410°C and was reduced to about 29% of its original weight by 500°C where the rate of loss had diminished. In air, an initial gain in weight began at 150°C, reached a maximum weight of 102% of the original at 240°C, and returned to 100% by 275°C. The presence of the weight mximum was due to the competitive effects of the addition of oxygen (presumably due to the formation of hydroperoxides at the tertiary hydrogen sites) and the removal of both low molecular weight oligomers and of low molecular weight decomposition products. Just above 280°C there was an increase in the rate of oxidative weight loss which preceded a region of moderating rate. At about 425°C, there was another increase in rate of loss which approximately corresponds to the thermal degradation which was observed in nitrogen. The specimen was completely oxidized by 500°C and left no residue.

Differential thermal analyses (results not shown) were performed in nitrogen in two stages. The dry powder was first taken at 2°C/min to

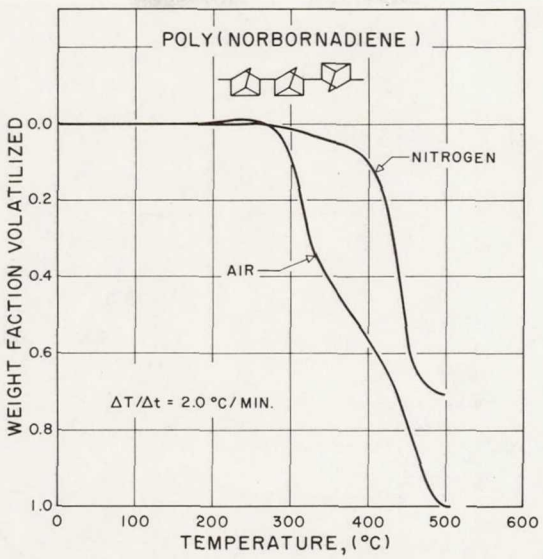

Fig. 4. Thermogravimetric analysis of polynorbornadiene in nitrogen and in air from 0° to 500°C at 2°C/min.

200°C (to simulate the drying step in the TBA analysis) and then, after cooling, was taken at 20°C/min to 500°C. An endothermic dip typical of the glass transition temperature was evident in the vicinity of 300°C. The exact position of the glass transition temperature was difficult to determine. A large exotherm began at 420°C. The data were somewhat ambiguous due to the large baseline drift and therefore are not shown. It is noteworthy that at 20°C/min, the glass transition temperature and the degradation processes were distinguishable.

Thermomechanical Analysis

The thermomechanical behavior of the polymer in dried nitrogen was determined over the range −180° to +500°C. Figure 5 shows the behavior of the specimen from −180° to 350° to 25°C after it had been preheated to 200°C in order to remove the benzene solvent and then precooled to −180°C. The data for the latter precooling (not shown) and subsequent reheating were not absolutely reproducible, although changes occurred at the same temperatures. In the low-temperature region, there were multiple damping peaks with maxima at −60° (see Fig. 6) and −140°C which were accompanied by changes in the slope of the rigidity curve. A shoulder in the broad glass transition damping peak at 225°C was also accompanied by a drop in modulus. The glass transition (T_g) was characterized by the large drop in rigidity and intense damping maximum at 320°C. The previously cited DTA study indicated an endothermic shift in this region which is typical of T_g. The glass transition temperature region was rendered even more pronounced after heating to 350°C, as is shown by the cool-

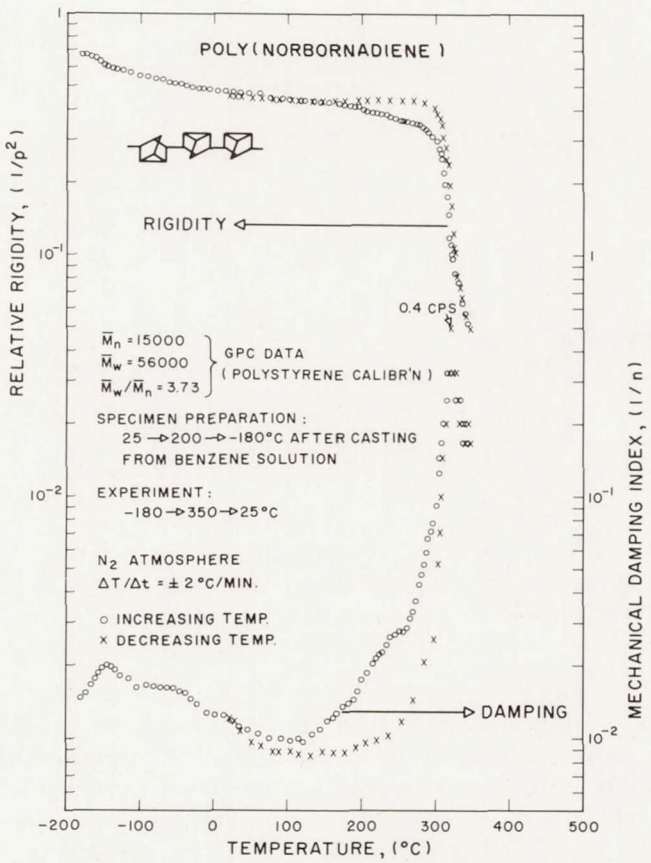

Fig. 5. Thermomechanical spectra of polynorbornadiene in nitrogen.

ing curves in Figure 5. Preheating the polymer to 350°C simplified the pre-T_g region by eliminating the damping shoulder and increasing the modulus in the 200–250°C temperature range. Later studies, involving the low-temperature casting of films, showed that the polymer was a poor film former; heating above T_g probably altered the morphology and perhaps improved the material properties of the polymer. A new specimen was heated to 350°C in nitrogen and data were taken from +350° to −180° to +500°C (Fig. 6, curves 1). Unlike the previous specimen, the data were reversible on cooling from 350°C and subsequent reheating. On heating above 350°C, the rigidity began to increase at about 370°C, displayed a small maximum at 415°C, a large sigmoidal rise between 435° and 470°C, and then decreased slightly to 500°C. The increase in rigidity at 435°C was accompanied by a damping peak at 453°C after which the damping decreased sharply. The stiffening reactions were also detected as a large exotherm by DTA (described above). Visual examination of the cooled pyrolyzed specimen indicated that the polymeric material had been converted to a smooth, glossy, black and opaque coating on the braid.

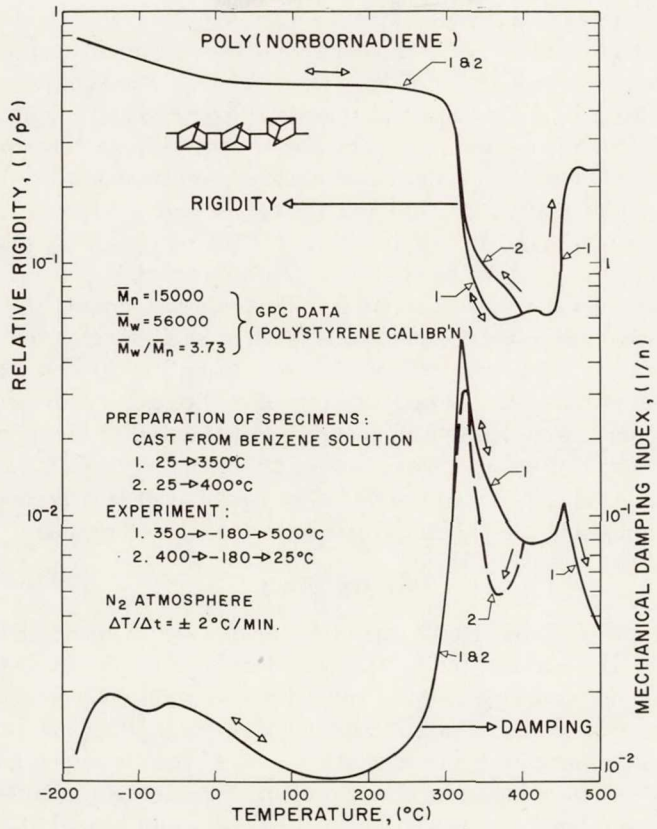

Fig. 6. Thermomechanical spectra of polynorbornadiene in nitrogen.

Curve 2 in Figure 6 represents the cooling behavior of another specimen after heating to 400°C. Note that preheating to 400°C shifted the glass transition up 7°C to 327°C, and the damping peak was rendered narrower and less intense than for the previous specimen which had been preheated to 350°C. The region below T_g was unaffected. Increase in the temperature of the glass transition and decrease in the intensity of the damping peak are typical of the effect of increasing crosslink density in a polymeric system. Narrowing of the damping peak is not typical but need not be unexpected if some of the skewness of the peak was due to reactions occurring in the vicinity of the glass transition temperature. The region below T_g was unaffected, presumably for the reason that the crosslink density, although sufficient to affect the longer-range motions associated with the glass transition, was insufficient to affect the more localized motions which are revealed by the damping pattern below T_g.[5,6]

Solubility Study

A study was undertaken to determine the temperature region to which a film of the polymer must be heated in order to become insolubilized by

chemical reactions (e.g., crosslinking or chain stiffening). Seven solutions were prepared in small vials. The benzene in the solutions was removed at reduced pressure overnight at 50°C. One specimen was kept as a control. The other dried films were suspended in the TBA oven and taken, one at a time, at 2°C/min from room temperature to various quench temperatures in nitrogen. The quench temperatures were room temperature (control), 100°, 180°, 260°, 320°, 360°, and 400°C. These temperatures correspond to significant points on the TBA, DTA, or TGA plots. After quenching, excess benzene was added to the vials, and after standing for a day the contents of the vials were compared. The colorless control and 100°C specimens were virtually the same. Thereafter, a yellow color developed in the liquid which intensified with degree of heating to 320°C, without the formation of visible gel. A small amount of swelled gel was evident in the 360°C specimen, indicating that chemical crosslinking or chain stiffening occurred above T_g. A major portion of the 400°C specimen had gelled and a brownish char was also visible. The fractions of polymer which had been insolubilized by the thermal treatment were not determined.

Infrared Study

A qualitative infrared study was undertaken so as to correlate chemical changes with those monitored by the other techniques. A film of the polymer, formed by predrying slowly from a benzene solution to prevent bubbling before being further dried at reduced pressure at 50°C, was placed between two sodium chloride plates which were held together in an aluminum holder. After obtaining an infrared spectrum (which was similar to that of Fig. 2), the specimen was placed in the TBA oven and heated at 2°C/min in nitrogen to quench points: 100°, 180°, 260°, 320°, 370°, 440°, and 500°C. Each infrared scan (not shown) was made after heating from the previous quench point to the new one. There were no apparent changes in the scans until 440°C, when the 3050 cm^{-1} band, the 2875 cm^{-1} shoulder, the 1730 cm^{-1} band, the 1300 cm^{-1} band, and the 800 cm^{-1} band decreased significantly relative to the 2925 cm^{-1} band. Several bands in the 1200 to 850 cm^{-1} region also appeared to be less intense. A new band appeared in the 1600 cm^{-1} region and indicated unsaturation.[7] The 800 cm^{-1} band has been attributed to the 2,6-disubstituted nortricyclene structure.[8–10] The changes observed at the 440°C quench point show that a major break down in the original nortricyclene structure had occurred, but the large-peak remaining in the 2925 cm^{-1} region suggests that a hydrocarbon structure still remains. The 500°C specimen scan displayed an almost total disappearance of all but the most prominant of the original peaks which were rendered weak.

CONCLUSIONS

The thermomechanical spectra of poly(bicyclo[2.2.1]hepta-2.5-diene), or polynorbornadiene, reveal the glass transition temperature of 320°C (at

less than 1 cps). This is probably the highest known T_g for a linear, soluble, and fusible addition-type hydrocarbon polymer. It is also noteworthy that by utilizing suitable heating rates, the glass transition and subsequent degradation reactions can be separated. The onset of degradation at temperatures just above T_g is not unusual for high-temperature plastics where the submolecular motions (and therefore diffusive processes), which are characteristic of polymeric materials, increase by orders of magnitude.[5,6]

The presence of low-temperature glassy-state relaxations indicates that some mechanism of energy dissipation is active at these low temperatures. Yet, the types of submolecular motions (crankshaft, rotations, oscillations) which are currently considered to be the intramolecular origin of these relaxations must be limited in such a structure.

The polymer is of particular interest since it might be a high-temperature plastic processible at high speeds in an inert atmosphere, provided that it could be prepared at sufficiently high molecular weights with satisfactory mechanical properties. The presence of tertiary hydrogen atoms in its structure should render it amenable to degradation by the earth's environment.

The support of the program on trosional braid analysis by NASA (Research Grant NGR 31-001-221) and the Chemistry Branch of the Office of Naval Research (N00014-67-A-0151-0024, NR 356-504) is acknowledged.

References

1. J. P. Kennedy and J. A. Hinlicky, *Polymer*, **6**, 133 (1965).
2. R. J. Cotter and M. Matzner, *Ring Forming Polymerizations*, Part A, Academic Press, New York, 1969, p. 47.
3. A. F. Lewis and J. K. Gillham, *J. Appl. Polym. Sci.*, **6**, 422, 1962.
4. J. K. Gillham, *Polym. Eng. Sci.*, **7**, 225 (1967).
5. J. K. Gillham and M. B. Roller, *Polym. Eng. Sci.*, **11**, 295 (1971).
6. J. K. Gillham, K. D. Hallock, and S. J. Stadnicki, *J. Appl. Polym. Sci.*, **16**, 2595 (1972).
7. R. C. Weast, Ed. *Handbook of Chemistry and Physics*, 48th ed., The Chemical Rubber Co., Cleveland, 1967.
8. L. Schmerling, J. P. Luvisi, and R. W. Welch, *J. Amer. Chem. Soc.*, **78**, 2819 (1956).
9. N. L. Zutty, *J. Polym. Sci.*, **A1**, 2231 (1963).
10. J. D. Roberts, *J. Amer. Chem. Soc.*, **72**, 3116 (1950).

Received June 20, 1972
Revised December 11, 1972

J. MACROMOL. SCI.—PHYS., B9(2), 341-366 (1974)

Thermomechanical Behavior of Amorphous Tactic Methacrylate Polymers

ERDOĞAN KIRAN AND JOHN K. GILLHAM
Polymer Materials Program
Department of Chemical Engineering
Princeton University
Princeton, New Jersey 08540

EDWARD GIPSTEIN
IBM Research Laboratory
San Jose, California 95114

Abstract

Dynamic mechanical spectra ($-180 \rightleftarrows > 140°\triangle$. ~1 cps) of amorphous stereoregular poly(methyl methacrylate)s and poly(t-butyl methacrylate)s with assigned microtacticities are presented and discussed. An intermolecular argument ("interlocking") is invoked to account for the higher T_g of syndiotactic vis à vis isotactic PMMA, in spite of the higher density of the latter at 30°C. An argument is presented to show that the T_β/T_g ratio is not only a measure of the degree of coupling of the T_β and T_g processes, but also of the degree to which intermolecular factors influence these processes. The greater extent of the low-temperature irreversibilities observed in the thermomechanical spectra of poly(t-butyl methacrylate)s is attributed to the brittle character induced by the bulky side groups which presumably weaken cohesive forces. Furthermore, internal stress generation and brittleness of the polymers are shown to be connected to freezing out of side group motions.

INTRODUCTION

A large number of investigations has been carried out to establish correlations between polymer microstructure and relaxation phenomena [1]. Amorphous polymers display at least two types of

dispersion processes which generally have been assumed to result from segmental motions of the main chain, and from the motion of side groups and/or more localized relaxation modes of the main chain, respectively. Crystalline polymers display, in addition to the relaxation processes associated with the amorphous regions, processes which are associated with the crystalline regions. The exact molecular mechanism of the relaxation processes, however, is not well understood and continues to be controversial even for the most extensively studied polymer systems such as the poly(methyl methacrylates)s.

The thermomechanical behavior, as obtained by torsional braid analysis [2], of atactic, syndiotactic and isotactic poly(methyl methacrylate)s (PMMAs) and poly(t-butyl methacrylate)s (P-t-BMAs), all with assigned microtacticities, is presented and discussed in the present communication.

EXPERIMENTAL

Purification of Monomers

Methyl methacrylate monomer (Rohm and Haas Co.) was passed through a column containing alumina (neutral grade, Woelm, W-200) to remove the inhibitor (10 ppm methylethylhydroquinone) and was collected over calcium hydride. The fraction boiling at 40°C and 100 mm Hg pressure was collected and stored at 0°C under helium.

Tertiary butyl methacrylate monomer (Polysciences, Inc.) containing 100 ppm hydroquinone inhibitor was washed with 10% aqueous sodium carbonate until a clear, colorless liquid was obtained. The monomer was dried over sodium sulfate, then passed through a column containing alumina (neutral grade) and collected over calcium hydride. The fraction boiling at 60°C and 51 mm Hg pressure was collected and stored at 0°C under helium.

Purification of Solvents

Toluene of spectrograde quality was distilled from and stored over calcium hydride. Tetrahydrofuran (THF) (Fisher Scientific Co.) was refluxed for 24 hr over potassium metal and was then distilled from lithium aluminum hydride.

Preparation of Initiators

Phenyl magnesium bromide (Alfa Inorganics), 3 M in diethyl ether, was used without further purification. N-Butyllithium (Foote

Mineral Co.), 1.6 M in hexane, was used as received. Fluorenyllithium was prepared by the metalation of fluorene in THF with n-butyllithium [3]. Sodium naphthalene was prepared from sodium metal and naphthalene in THF solvent [3].

Polymerization Procedures

Poly(methylmethacrylate)s

The atactic polymer was obtained from Cellomer Associates, Rochester, New York. The syndiotactic and isotactic polymers were synthesized by procedures described in the literature [3,4].

Syndiotactic poly(methyl methacrylate). A mixture containing 1.66 g (0.01 mole) fluorene and 6.1 ml (0.0097 mole) n-butyllithium in 500 ml of THF in a 1-liter 3-necked reaction flask was stirred 1 hr under argon at ambient temperature. The mixture was then cooled to −70°C in a Dry Ice-acetone bath and 83 g (0.83 mole) methyl methacrylate was added. The polymerization was carried out for 6 hr to give a viscous solution which, after addition of 5 ml methanol, was poured into 2500 ml cold petroleum ether to precipitate the polymer. The polymer was filtered, dissolved in benzene, reprecipitated in petroleum ether, collected and vacuum dried 78 hr at 50°C to give 82.7 g (99.7% yield) white product.

Isotactic poly(methyl methacrylate). Argon gas was bubbled through 32 g (0.32 mole) methyl methacrylate monomer dissolved in 425 ml toluene in a 1-liter 3-necked reaction flask. The mixture was cooled to 0°C and 3.6 ml phenylmagnesium bromide initiator was added. The mixture was stirred 4 hr to give a viscous solution which was added to 2 liters vigorously stirred petroleum ether to precipitate the polymer. The filtered polymer was washed with acidified methanol, then dissolved in benzene and reprecipitated in petroleum ether. The polymer was vacuum dried 72 hr at 50°C to give 24.7 (82.3% yield) product.

Poly(t-butyl methacrylate)s

The three tactic polymers were synthesized by published procedures [5].

Atactic poly(t-butyl methacrylate). The polymerization was carried out in a 250-ml 4-necked flask under a continuous flow of argon. Benzoylperoxide initiator (0.12 g, 4.9×10^{-4} mole) was added to a stirred mixture of t-butyl methacrylate (71.1 g, 0.5 mole) in dry

toluene (72 ml) at 70°C, and the polymerization was continued for 15 hr. The viscous mixture was poured into 6 liters of vigorously stirred water to precipitate a white polymer. The polymer was purified by repeated precipitation from acetone/water, then collected and dried under vacuum at 50-60°C for 72 hr to give 56 g (78.8% yield) product.

Syndiotactic poly(t-butyl methacrylate). The polymerization of syndiotactic poly(t-butyl methacrylate) was carried out in a 500-ml 3-necked flask at −50 ± 2°C inside a dry box under helium atmosphere. A stirred solution of 33.5 g (0.24 mole) t-butyl methacrylate in 250 ml dry THF solvent was cooled to −50°C and 0.56 g (3.75×10^{-3} mole) of freshly prepared sodium naphthalene initiator was added. The polymerization was terminated after 4 hr by pouring the mixture into 3 liters of rapidly stirred water to precipitate a white polymer. The polymer was purified by repeated precipitation from acetone/water to give 19.5 g (54.9% yield) of product after drying at 50-60°C for 48 hr under vacuum.

Isotactic poly(t-butyl methacrylate). A 1-liter 4-necked reaction flask was heated above 100°C prior to the introduction of solvent and monomer. Oxygen was excluded by maintaining a continuous flow of purified argon over the solution during the polymerization. A solution of 32.5 g (0.23 mole) of t-butyl methacrylate monomer in 500 ml dry toluene was cooled to −50°C and 0.16 g (2.5×10^{-3} mole) of 1.6 M n-butyllithium initiator was added. The mixture was stirred 30 min, warmed to room temperature and poured into 3 liters of vigorously stirred water to precipitate the polymer. The polymer was purified by repeated precipitation from acetone/water followed by vacuum drying at 50-60°C for 72 hr to give 24.5 g (75.4% yield) of white product.

The theoretical elemental content of p-t-BMA, calculated for $+C_8H_{14}O_2+_n$, is 67.57% carbon, 9.93% hydrogen, and 22.50% oxygen. The elemental analyses showed 67.19, 67.42, 67.47% carbon; 9.82, 9.78, 9.84% hydrogen; and 22.75, 22.15, 22.68% oxygen in atactic, syndiotactic, and isotactic p-t-BMA polymers, respectively.

Molecular Weight Distribution

Molecular weight distribution and molecular weight averages (number and weight averages) were obtained with a modified Water's Associates GPC-200 Gel Permeation Chromatograph. The chromatograph was run under ambient conditions using THF at 1 ml/min flow rate through columns packed with 10^6, 10^5, 10^4, 10^3, 250, and 60 Å polystyrene. $\bar{M}_w$ and $\bar{M}_n$ values, corresponding to chain extended

molecular sizes based on polystyrene, were determined by a computer-programmed analysis of the chromatograms.

Glass Transition Temperatures

Glass transition temperatures were measured with a du Pont 941 Thermomechanical Analyzer (TMA), a Perkin-Elmer 1B Differential Scanning Calorimeter (DSC), and a Torsional Braid Analyzer (TBA) [2].

Stereochemical Assignments

The stereochemical assignments for the methacrylate polymers were determined by a published procedure [6]. The three P-t-BMA polymers were hydrolyzed for five days in 96% sulfuric acid to polymethacrylic acids which were then esterified to polymethyl methacrylates with diazomethane [7]. The NMR spectra of the methacrylate polymers were then obtained in o-dichlorobenzene at 148°C with a Varian HA-100 spectrometer using hexamethyldisiloxane as an internal standard. The peak areas due to the α-methyl protons in the isotactic, heterotactic, and syndiotactic triads at δ = 1.22, 1.05, and 0.91 ppm, respectively, were measured with a planimeter and by a weighing technique.

Dynamic Mechanical Spectra

Thermomechanical spectra were obtained by torsional braid analysis (TBA) [2]. Polymer-braid composite specimens were prepared by impregnating multifilamented glass braids in 10% solutions of the polymers in THF (bp 66°C). The solvent was removed by heating ($\Delta T/\Delta t$ = 2°C/min) the composite specimen to 200°C [for poly(methyl methacrylate)s] or 145°C [for poly(t-butyl methacrylate)s] in flowing dried nitrogen. These temperature limits were determined using TGA runs which were carried out under flowing nitrogen (75 ml/min) at 2°C/min heating rate using a du Pont 950 TGA unit. The thermomechanical spectra were obtained in a nitrogen atmosphere while cooling the solvent-free braid composites to −180°C and then heating to 200°C or 145°C at a rate of 2°C/min.

RESULTS AND DISCUSSION

Molecular weight averages ($\overline{M}_w$, $\overline{M}_n$), tacticities, and glass transition temperatures of the polymers investigated in this study are shown in Table 1. Quotation marks have been used to emphasize the fact that the polymers are not completely the designated tactic forms.

TABLE 1

Properties of Tactic Poly(methyl methacrylate)s and Poly(t-butyl methacrylate)s

Polymer	Molecular weights			Tactic content, %			Glass-transition temp., °C		
	$\overline{M}_w$	$\overline{M}_n$	$\overline{M}_w/\overline{M}_n$	i	h	s	TMA*	DSC*	TBA**
PMMA									
"Atactic"	105,000	48,000	2.15	7.7	41.7	50.6	102	105	115
"Syndiotactic"	83,200	62,700	1.33	3.8	26.1	70.1	117	124	127
"Isotactic"	2,780,000	1,200,000	2.29	91.5	8.5	0	49	56	55
P-t-BMA									
"Atactic"	359,950	177,580	2.03	1	43	56	95	118	124
"Syndiotactic"	20,940	16,220	1.49	19	51	30	97	86.5	115
"Isotactic"	300,000	252,000	1.19	82	16	2	75.5	77	112

*Measurements were made on specimens prepared by pressing the polymer powders into pellets following synthesis.
**See text.

The results of thermogravimetric and torsional braid analyses are shown in Figs. 1-9.

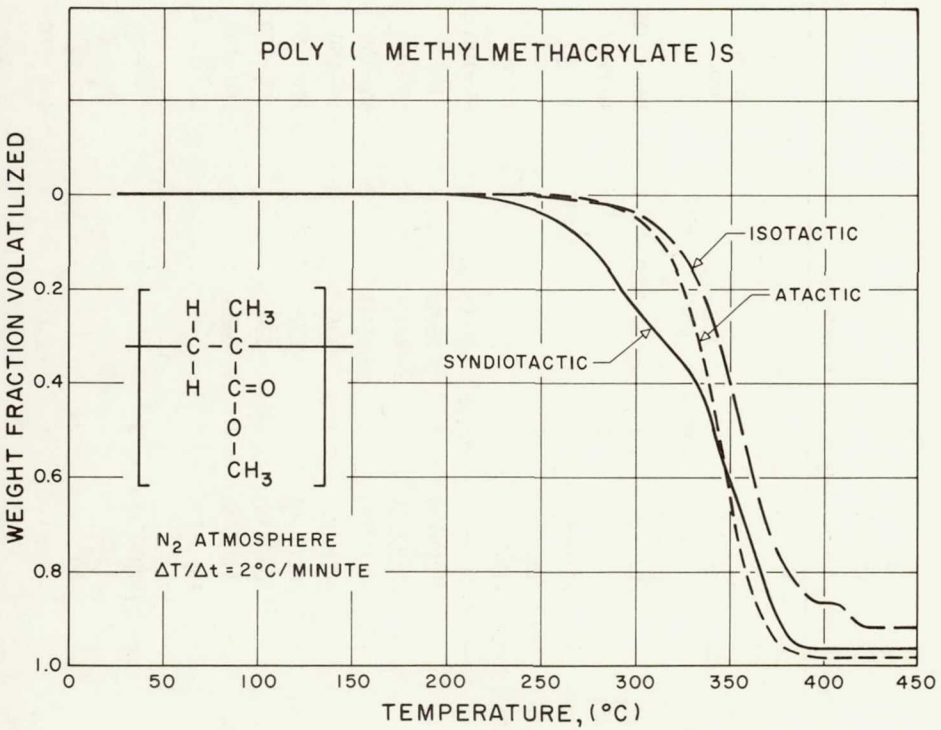

FIG. 1. Thermogravimetric analyses of poly(methyl methracylate)s.

Poly(methyl methacrylate)s

Relaxation phenomena in PMMA polymers have been studied by a number of investigators. Table 2 is a summary of some of their findings with respect to designation, microtacticity, density, melting point (T_m), glass transition (T_g) and glassy-state transition temperature (T_β). The table covers investigations carried out primarily at low frequencies and in particular includes studies reported after 1967. More extensive reviews of the literature up to 1967 can be found elsewhere [1,8]. The designations have been taken directly from the literature; when not accompanied with explicit microtacticity assignments, they are based on procedures used in synthesis; for example, authors have designated a polymer obtained by conventional free-radical polymerization as atactic.

TABLE 2

Transitions in Poly(methyl methacrylate)s: Literature Data

Designation*	Microtacticity	Density in g/cc, (°C)	Transition temperature					Temp. range, °C	Ref.
			T_m, °C	T_g, °C, (cps)	Method	T_β, °C, (cps)	Method†		
a	—	1.19(—)	—	119(—)	1	~60(~200)	1	−196→~120	39
a	—	1.169(25)	—	105(—)	2	—	—	−40→150	40
a	—	1.188(30)	—	104(—)	2	—	—	—	9,10
i**	—	1.22(30)	160	45(—)	2	—	—	—	9,10
s**	—	1.19(30)	>200	115(—)	2	—	—	—	9,10
a	—	—	—	—	—	~25(1)	1	−50→100	41
a	—	—	—	~130(60)	3	~50(60)	3	0→150	41
a	—	—	—	~125(28)	3	~40(28)	3	−40→150	15
s	—	—	—	~130(28)	3	~35(28)	3	−40→150	15
i	—	—	—	~70(28)	3	~30(28)	3	−40→150	15
a	—	1.188(25)	—	108(0.39)	1	~15(—)	1	−160→100	32
s	—	1.195(25)	—	105(0.48)	1	~32(0.9)	1	−160→100	32
i	—	1.23(25)	—	42(0.44)	1	absent	—	−160→100	32
a	—	—	—	105(—)	2	—	—	—	27
s	—	—	—	115 122***(—)	2	—	—	—	27
i	—	—	—	43— 50***(—)	2	—	—	—	27
a	~85% Syndiotactic	—	—	~130(1)	1	~25(1)	1	−180→200	29

i	∿95% Isotactic	—	—	~75(1)	1	~0(1)	1	−180→200	29
i	1.0(i), 0(h), 0(s)	—	—	48(—)	4	—	—	—	16
i	0.73(i), 0.16(h), 0.11(s)	—	—	56(—)	4	—	—	—	16
i	0.62(i), 0.20(h), 0.18(s)	—	—	59(—)	4	—	—	—	16
r	0.10(i), 0.31(h), 0.59(s)	—	—	114(—)	4	—	—	—	16
s	0 (i), 0.36(h), 0.64(s)	—	—	126(—)	4	—	—	—	16
i	$92(i+^{h}/2)$: $8(s+^{h}/2)$	—	—	~70(50)	3	20(50)	3	−50→150	12,17
s	$24(i+^{h}/2)$; $76(s+^{h}/2)$	—	—	~125(50)	3	50(50)	3	−50→150	12,17
i	96(i), 4(h), 0(s)	—	—	38(—)	2	—	—	—	18
i	78(i), 16(h), 6(s)	—	—	44(—)	2	—	—	—	18
i	51(i), 19(h), 30(s)	—	—	58(—)	2	—	—	—	18
r	6(i), 36(h), 58(s)	—	—	101(—)	2	—	—	—	18
s	4(i), 20(h), 76(s)	—	—	103(—)	2	—	—	—	18
s	0(i), 5(h), 95(s)	—	—	105(—)	2	—	—	—	18

*Designation: a, atactic; s, syndiotactic; i, isotactic; r, random; h, heterotactic.
**Assignments based on X-ray fiber diagrams.
***Variation depends on synthesis temperature.
†Methods: 1, mechanical; 2, volume-temperature; 3, dielectric; 4, differential thermal analysis;

Assignments for isotactic and syndiotactic forms were first based on X-ray analysis of fiber diagrams [9,10] and later, by high-resolution nuclear magnetic resonance of solutions. Polymers have often been designated isotactic or syndiotactic depending upon only the details of the synthesis.

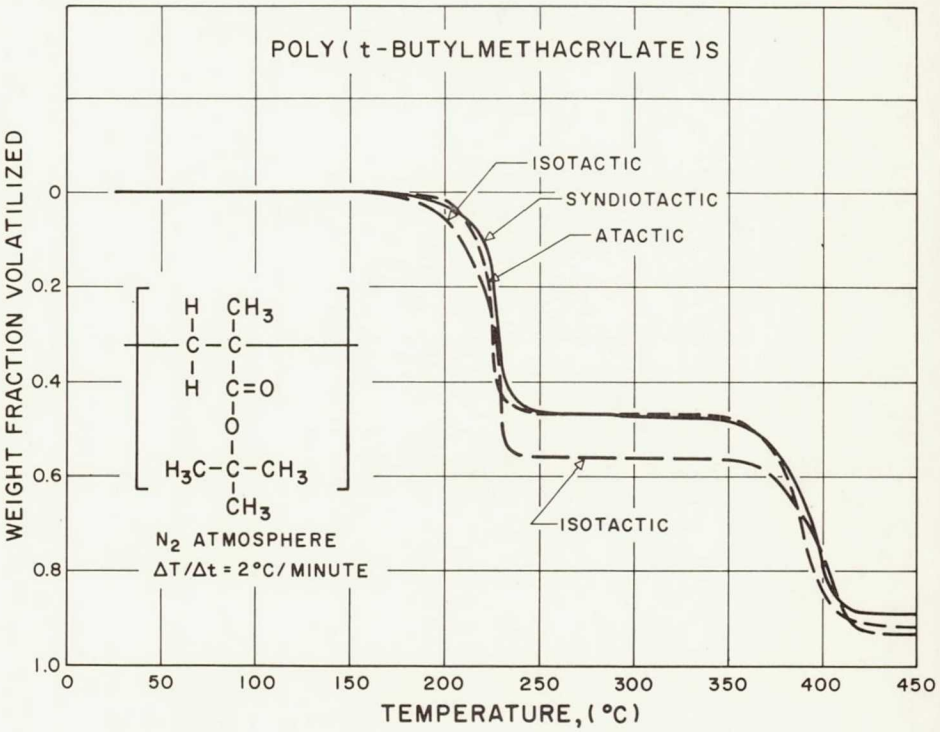

FIG. 2. Thermogravimetric analyses of poly(t-butyl methacrylate)s.

The general characteristics of the TBA spectra shown in Figs. 3-5 compare well with the dynamic mechanical and dielectric loss spectra which have been published. The spectra indicate that there are two distinct types of motion above −180°C in each polymer which are revealed by the two loss peaks. The sharp peaks at 127°C (~0.2 cps), 115°C (~0.2 cps), and 55°C (~0.3 cps) in syndiotactic, atactic and isotactic PMMA, respectively, are associated with the glass transition temperatures of these polymers and are accompanied by sharp decreases in rigidity. The lower-temperature (glassy-region) loss peak in atactic and syndiotactic PMMA is

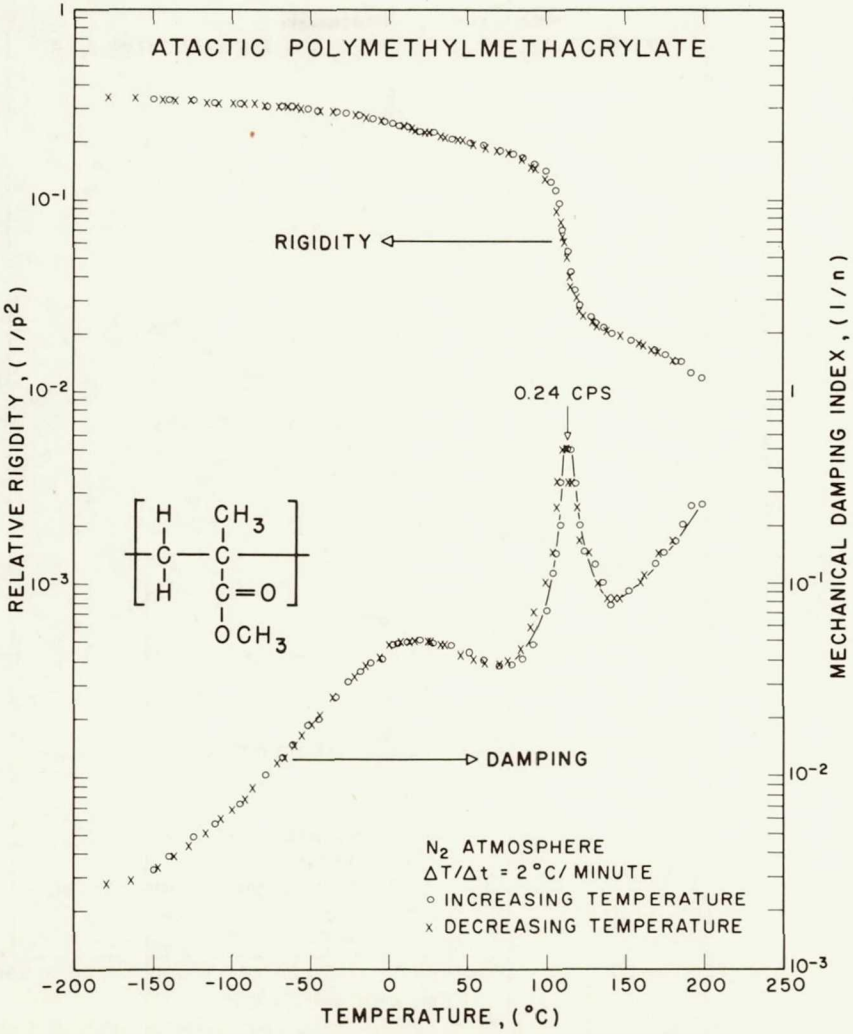

FIG. 3. Thermomechanical spectra of atactic poly(methyl methacrylate).

broad and centered at ~20°C (0.5 cps), and ~25°C (0.5 cps), respectively. In isotactic PMMA, it is not as pronounced and is partially submerged with the glass transition peak. It appears as a shoulder at ~0°C (0.6 cps). These glassy-region loss peaks have been attributed to the motion of ester side groups and/or localized motions of the main chain [1,11-14].

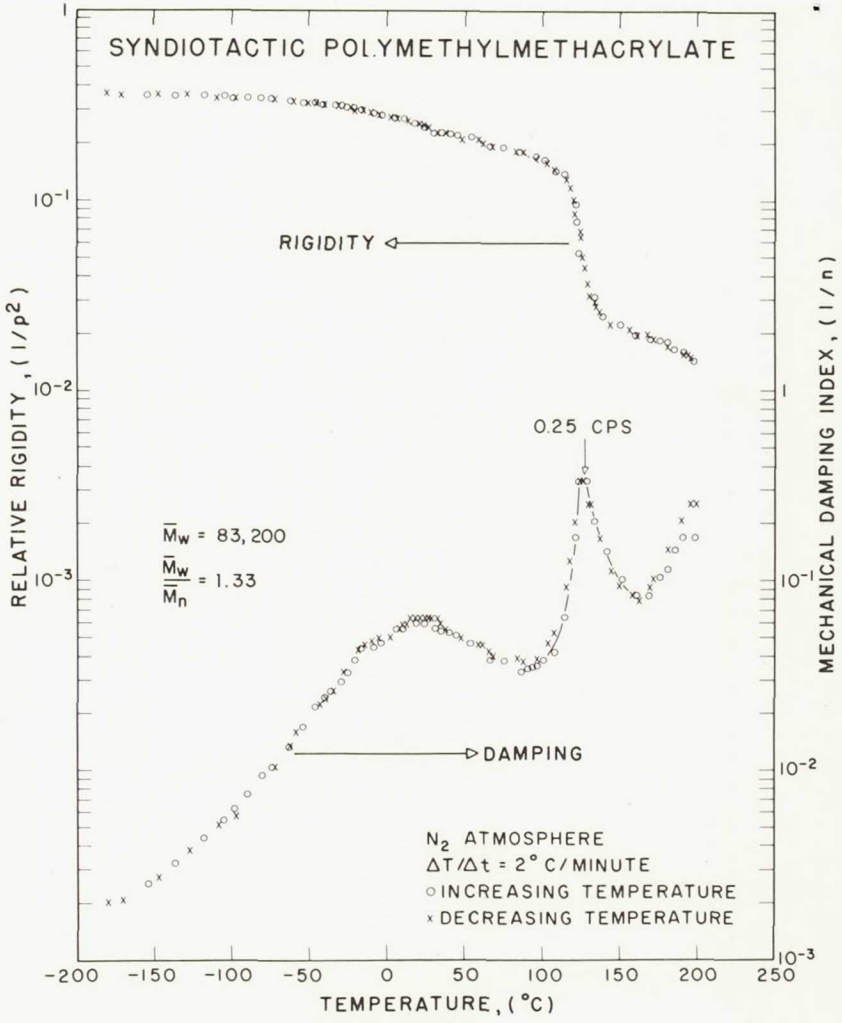

FIG. 4. Thermomechanical spectra of syndiotactic poly(methyl methacrylate).

The T_m of isotactic PMMA is reported to be 160°C [9]; however, the TBA spectra did not display changes that could be associated with the crystallization or melting transitions. The absence of crystallinity in the isotactic PMMA was presumably a consequence of the rate of cooling (2°C/min), i.e., time effects. No change, however, was observed in the subsequent thermomechanical spectra of

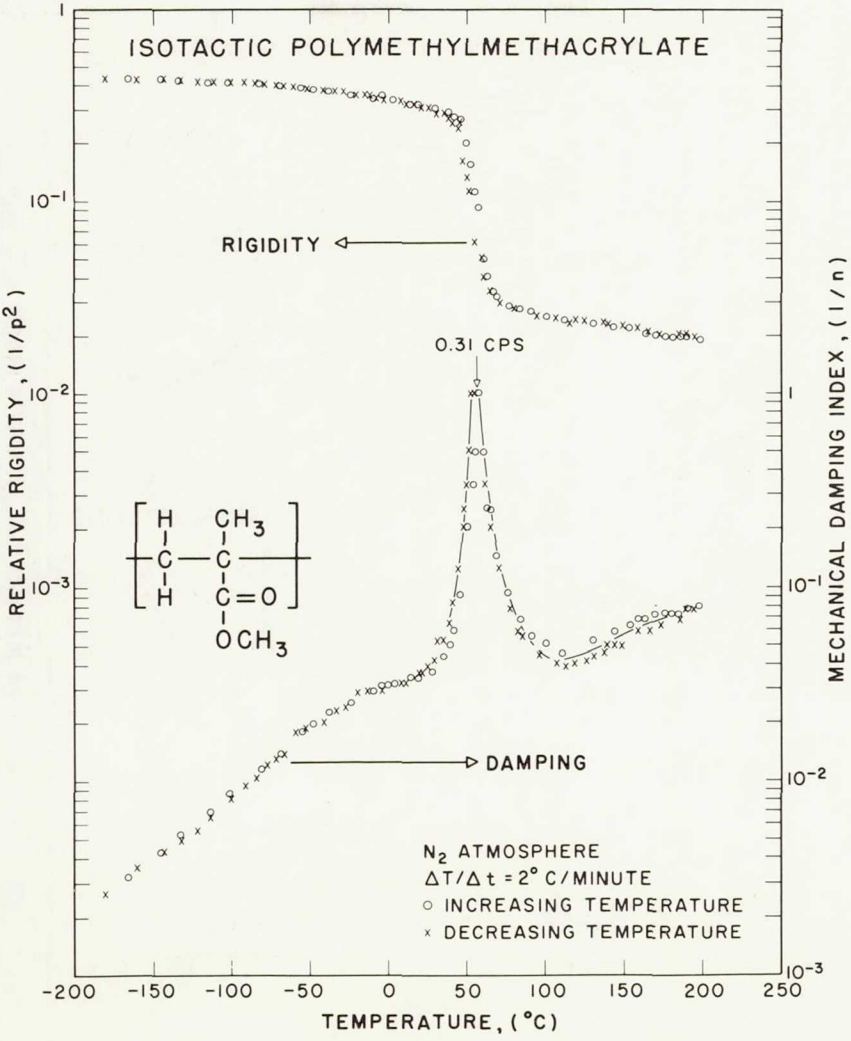

FIG. 5. Thermomechanical spectra of isotactic poly(methyl methacrylate).

a specimen which was left overnight at 120°C to facilitate crystallization. The T_m of syndiotactic PMMA is reported to be above 200°C [9] (which is beyond the upper temperature limit of the present investigation). However, leaving the syndiotactic PMMA overnight at 150°C did not lead to differences in its thermomechanical spectra either. Under these conditions, the isotactic and syndiotactic PMMA

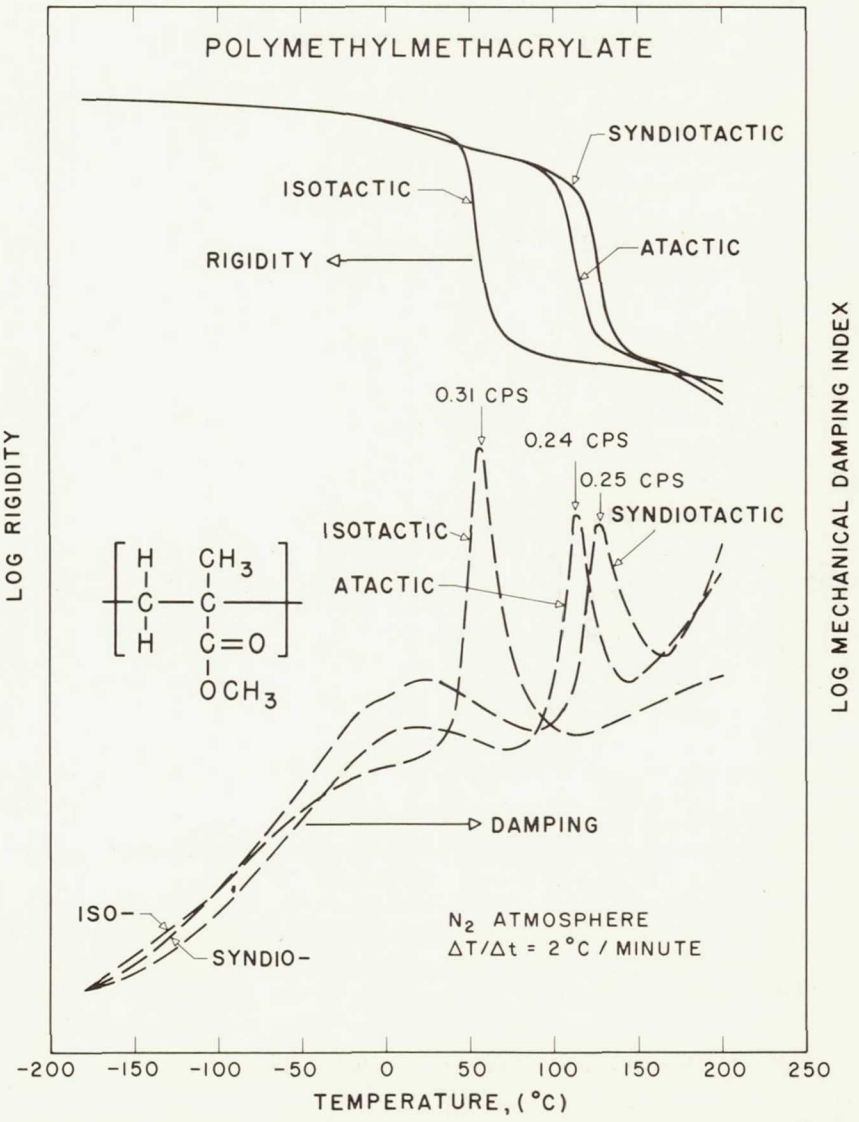

FIG. 6. Thermomechanical spectra of isotactic, syndiotactic, and atactic poly(methyl methacrylate)s.

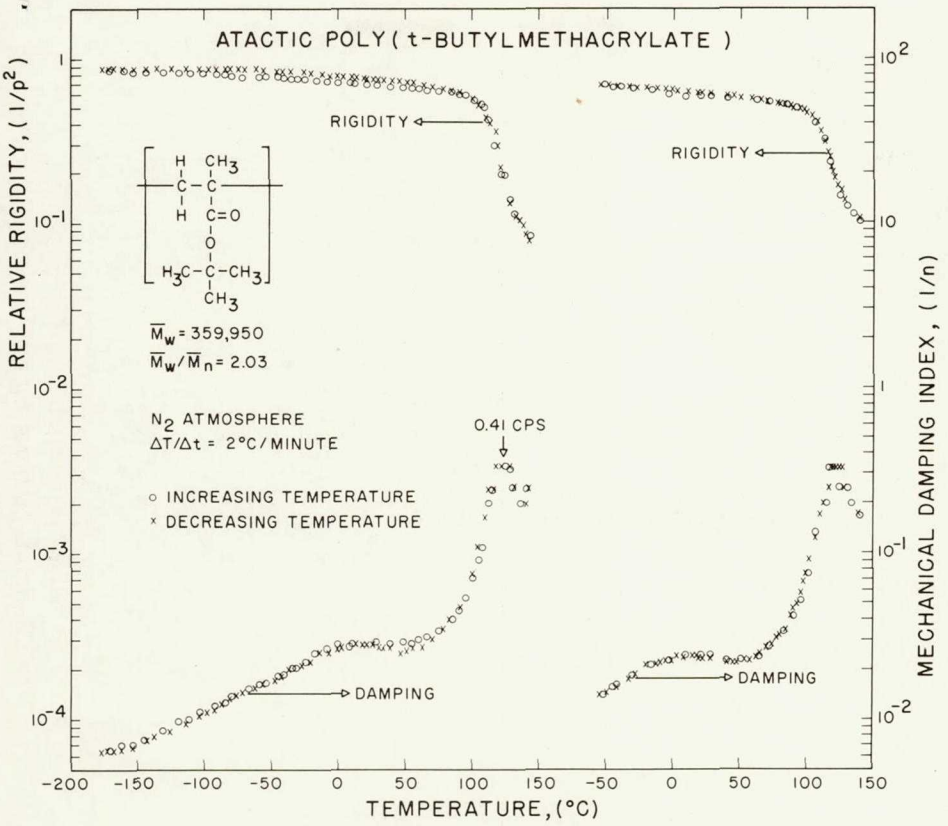

FIG. 7. Thermomechanical spectra of "atactic" poly(t-butyl methacrylate). Thermal cycles: 145°C ⇋ −180°C (left); 145°C ⇋ −50°C (right).

specimens appeared to behave as amorphous materials. The high degree of reproducibility of data (in the direction of both cooling and then heating) provides further evidence for the absence of crystallinity. That isotactic and syndiotactic PMMAs do not crystallize with ease has been indicated also by others [4].

The types of relaxation below T_g that have been reported for PMMAs are side-chain, α-methyl and ester-methyl relaxations. Also, in samples containing moisture, a water peak is observed in the vicinity of −100°C [1].

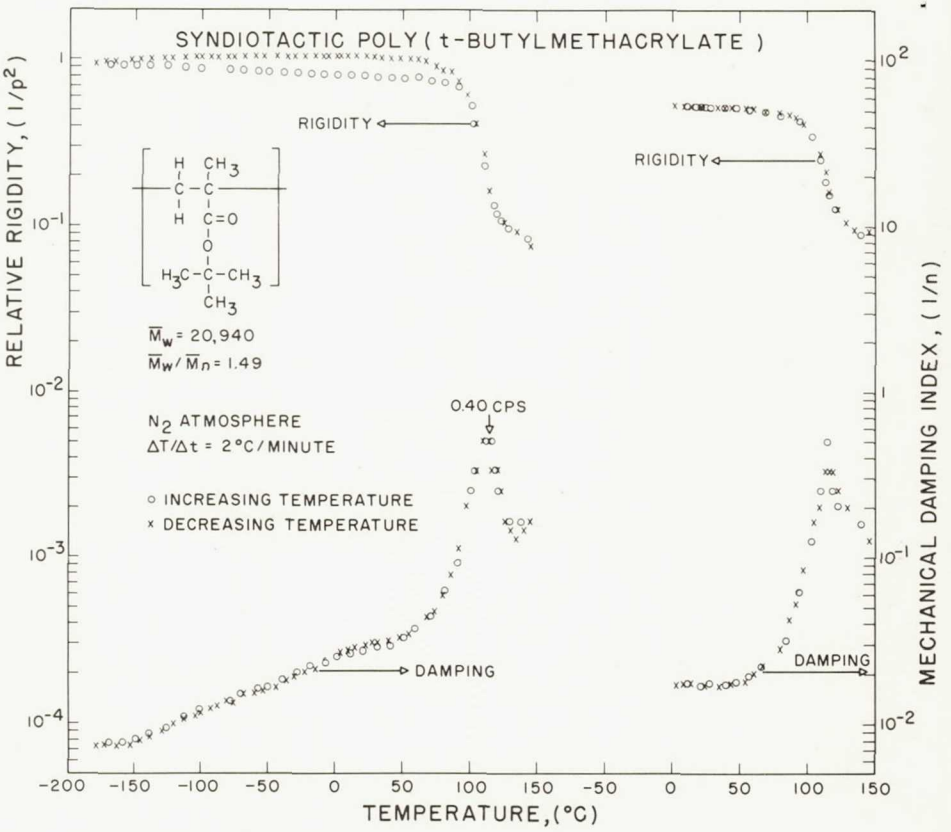

FIG. 8. Thermomechanical spectra of "syndiotactic" poly(t-butyl methacrylate). Thermal cycles: 145°C ≒ − 180°C (left); 145°C ≒ 0° (right).

In the present study, samples were dried, and experiments were carried out in a flowing dried nitrogen atmosphere. The α-methyl and ester-methyl relaxations are reported to occur at very low temperatures [1] which are not accessible by the present apparatus. The one peak observed below T_g is presumably due to the motion of the ester side chains. However, the exact nature of the ester-side chain motion is controversial. It has been suggested that the moving unit in the side chain relaxation involves in addition to the side chain itself, a segment of the backbone chain [11-13]. In another study [14], the motion of ester group was interpreted to be a consequence of the rotational isomeric movement of the O—CH_3 group as well as the rotational isomeric movement of the ester group as a whole. As will be discussed later, the present study indicates that there is a cou-

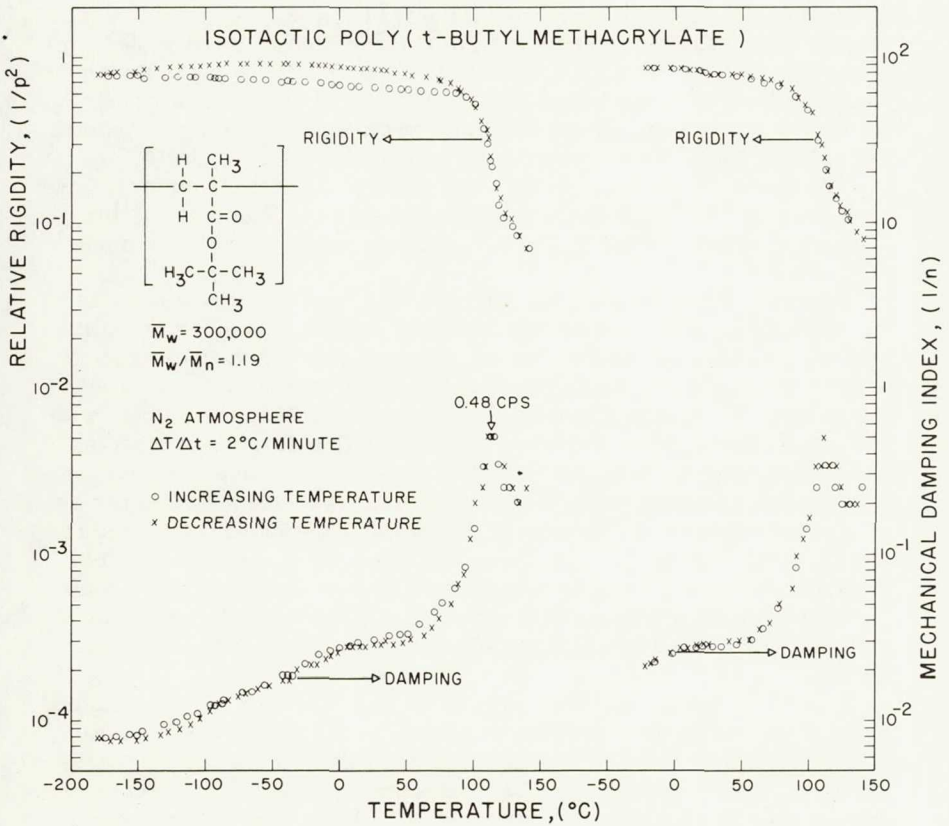

FIG. 9. Thermomechanical spectra of "isotactic" poly-t(butyl methacrylate). Thermal cycles: 145°C ⇋ − 180°C (left); 145°C ⇋ − 25°C (right).

pling of motions which are responsible for the glassy-region transition with the main chain motions which are responsible for the glass transition.

A comparison of the TBA spectra shown in Figs. 3-5 shows the close similarity of the spectra of the atactic and syndiotactic PMMA polymers (Fig. 6). This arises from the high degree of syndiotacticity of the atactic polymer (Table 1). Similarities in the spectra of atactic and syndiotactic PMMA polymers have been observed also in dielectric studies [15].

Poly(methyl methacrylate) is the well-known example where tacticity has a significant effect on the glass transition temperature of the polymer. It has been shown that T_g increases as the syndiotactic

content of the polymer increases (16-18) (Table 2). This phenomenon makes it necessary to report the microtacticities of investigated samples. Otherwise, comparison of published data becomes ambiguous. In fact, even the solvent involved in obtaining the NMR spectra should be noted since disparities have been observed between indices of tacticity found for the same sample in different solvents [6].

The present observations are in accord with the literature in that the polymer with the highest syndiotactic content (Table 1) has the highest T_g (127°C). The T_g for the isotactic polymer (55°C) is some 72°C lower.

To account for the striking differences in the relaxation behavior of syndiotactic versus isotactic forms of PMMA, a number of explanations has been proposed. One of the earliest observations of such a difference was noted in a study of the dielectric behavior in dilute solutions [19]. It was observed that isotactic PMMA, in contrast with the syndiotactic form, displayed higher molar polarization, shorter relaxation time and narrower spread of relaxation times. A plausible explanation (although noted to be inadequate) was suggested in terms of a higher degree of freedom to rotate about the main chain bonds in the isotactic polymer. In another study [20], the greater peak width of NMR absorption lines arising from α-methyl and methoxyl group protons (in 12% solution in chloroform) in predominantly syndiotactic polymer was also attributed to differences in freedom of molecular motion.

It is to be noted that these arguments are based on solution studies and utilize intramolecular factors alone. That intramolecular factors will still be the only operating factors in the bulk state is questionable. It has been argued [18] that since estimation of the cohesive energy density of stereoregular forms of PMMA does not indicate a large difference [21], intermolecular interactions in the solid should not be an important source of the different behavior. However, it must be pointed out that the determination of the cohesive energy densities from intrinsic viscosity data, or for that matter from swelling experiments, depends upon the solution behavior of the polymer segments and a direct extension of bulk behavior must be exercized with caution.

The glass transition is a bulk property and it is generally believed to be a manifestation of longer range motions of the polymer backbones. It has been observed that in a number of vinyl polymers of type $-(CH_2\text{-}CXY)_n-$, T_g varies with tacticity when neither of the two different substituents (X and Y) is hydrogen [22,23]. This difference has been interpreted in terms of a larger difference in energy levels between rotational isomers in the syndiotactic chain (which apparently arises only when the two different substituents, X and Y, are

not hydrogen). Theoretical investigations of the dependence of conformational energy potentials as a function of angles of internal rotation around C—C bonds of the main chain of stereoregular PMMA are reported to show that isotactic PMMA structure leads to broad and flat minima, whereas the minima in syndiotactic PMMA are narrow and a small change in the angle of rotation corresponds to a high potential [24]. It was also concluded from these observations that isotactic PMMA is more flexible (can undergo twisting motions) than syndiotactic PMMA.

That the glass transition temperature of isotactic PMMA is lower than that of syndiotactic PMMA implies that submolecular motions occur more readily in the former than in the latter. Therefore, it has been natural to look for explanations in terms of intramolecular effects such as chain flexibility which could account for this observation. The above-cited arguments all point out that the isotactic chain is perhaps less stiff than the syndiotactic chain and can therefore undergo motion more readily. However, measurements of θ-dimensions and small-angle X-ray scattering data are reported to show that the flexibility difference between the tactic configurations is so small that it cannot be the main reason for the large difference in transitions [25,26]. Furthermore, explanations which have been presented in the literature neglect the peculiar fact that the density of amorphous isotactic PMMA is greater than that of the amorphous syndiotactic PMMA [1,4,10,27,28]. (At 30°C, $\rho_{\text{amorphous, iso}} = 1.22$ g/cc; $\rho_{\text{amorphous, syndio}} = 1.19$ g/cc [10,27]. In one study [29] this fact was realized with concern, but no interpretations were advanced. As discussed below, this difference in density offers another explanation for the differences in the transitions of the isotactic versus syndiotactic PMMA samples in terms of an intermolecular (geometrical interlocking) argument.

The fact that the density of isotactic PMMA is greater than that of syndiotactic PMMA indicates that packing must be more efficient in the isotactic polymer. This would imply (other things being equal) that electrostatic forces are greater in the isotactic polymer. One might therefore expect a higher glass transition temperature for the isotactic polymer which is, in fact, not the case. The factors responsible for the low T_g of isotactic polymer must be the inherent flexibility of the single molecule and/or more geometrical interlocking with the syndiotactic polymer. Although, as discussed above, the literature indicates that isotactic polymer is a more flexible molecule, there is evidence that the predominating factor in determining the glass transition temperature can be the geometrical interlocking of the polymer molecules [30,31]. It must be noted that interlocking does not necessarily lead to greater density; there is a

distinction between packing and interlocking. A pack of pencils, for example, represents an efficient (i.e., dense) packing without interlocking. By analogy, the lower T_g of the isotactic PMMA, despite its higher density compared with the syndiotactic PMMA, can be interpreted in terms of less geometrical interlocking in the isotactic polymer. In the syndiotactic PMMA, main chain motions would then be hindered more by the geometrical intermolecular interlocking of the side groups.

One consequence of the difference in packing is a smaller free volume for the side groups in the isotactic polymer. Therefore, it would be reasonable to assume that the side-group motions in the isotactic polymer cannot take place as intensely as in the syndiotactic polymer, not at least until T_g is approached. This assumption is substantiated by the much smaller intensity of the glassy-region loss peak in the isotactic PMMA (Fig. 6). The onset of the intensified side-group motions as T_g is approached may be the reason for the enhanced intensity of the T_g peak in the isotactic PMMA (Fig. 6). Hitherto, it was assumed that the shallow nature of the glassy-region loss peak in the isotactic polymer was because it was submerged with the glass transition [1]. The present argument, however, indicates that this can be a consequence of the efficient packing in the isotactic polymer. A similar argument based on differences in density and packing was proposed in 1961, but only to justify a failure to observe the glassy-region transition in the isotactic PMMA [32]. Additional support for the interpretation of the glassy-region relaxation behavior in terms of a "packing" hypothesis comes from the observation that in stereoblock PMMA polymers (synthesized according to published procedures [4,9]) there occurs a splitting of the secondary dielectric loss peak; the splitting being more pronounced in the sample with the higher syndiotactic content [12,17]. Assuming that the syndiotactic PMMA is bulkier (i.e., less efficiently packed) than the isotactic form, it was argued that an isotactic sequence which lies between syndiotactic sequences in a stereoblock PMMA should have a larger free volume, (bulky syndiotactic groups acting as "spacers") [12,17]. Thus, the relaxation time for the isotactic peak becomes shorter, shifting the isotactic peak to a higher frequency and leading therefore to the observed splitting. No splitting of the glass transition peak is observed since it involves longer-range motions (i.e., the unit for segmental motion is much longer than the isotactic and the syndiotactic sequences in the stereoblock PMMA).

If one were to interpret the glassy-region relaxation in the PMMA polymers as being due to a simple side-group motion, then the free-volume arguments based on packing differences presented above

would predict the location of this relaxation peak to be at a lower temperature in the syndiotactic PMMA than in the isotactic PMMA. This is because the free volume for the side groups will be favorable for their freer motion in the syndiotactic polymer; syndiotactic groups of one chain act as "spacers" for the syndiotactic groups of neighboring chains. That the relaxation peak in the syndiotactic polymer appears to occur at a higher temperature (~25°C) is indicative of either a longer range or more restricted motion which can be attributed to the nature of the motion responsible for this relaxation peak; it apparently incorporates a segment of the main chain whose motion is hindered by geometrical interlocking and thus shifted to higher temperatures.

Table 3 shows the ratios of the glassy-region relaxation temperature (T_β) to the glass transition temperature (T_g) in the PMMA and

TABLE 3

Transition Temperatures of the PMMA and P-t-BMA Polymers

Polymer	T_g (K)	T_β (K)	T_β/T_g
Atactic PMMA	388 (~0.2 cps)	~293 (0.5 cps)	0.76
Syndiotactic PMMA	400 (~0.2 cps)	~298 (0.5 cps)	0.75
Isotactic PMMA	328 (~0.3 cps)	~273 (0.6 cps)	0.83
Atactic P-t-BMA	397 (~0.4 cps)	~293 (~0.85 cps)	0.74
Syndiotactic P-t-BMA	388 (~0.4 cps)	~293 (~0.25 cps)	0.76
Isotactic P-t-BMA	385 (~0.5 cps)	~293 (~0.85 cps)	0.76

P-t-BMA polymers as obtained in the present study. It is to be noted that the ratio is a constant (~0.75), except for the isotactic PMMA. The constancy of T_β/T_g implies a common glass transition mechanism in these polymers except for the isotactic PMMA. The mechanism of the glass transition in the isotactic PMMA could be different in that, as stated earlier, geometrical intermolecular interlocking does not appear to be as significant with this polymer, and hence a β-process, in the sense of freeing the localized motions to free the chains from intermolecular interactions, is not such a major precursor for the onset of longer-range cooperative motions of the main chain. It follows that the β-relaxation for the syndiotactic polymer incorporates the motions of the ester side group with the main chain to a greater extent than is the case for the isotactic polymer.

The following trends are of importance:

(1) In the syndiotactic PMMA, the β-process (~25°C) involves, in addition to the side groups, a segment of the main chain and is thus coupled with the glass transition process. Both processes are influenced by geometrical interlocking. The T_β/T_g ratio is 0.75 which is displayed by the majority of the methacrylate polymers in the present study.

(2) In the isotactic PMMA, as a consequence of efficient packing with this polymer, the β-process is influenced by the glass transition process in the sense that side group motions take place more readily as T_g is approached. However, neither process is as influenced by intermolecular geometrical factors since these are not as significant with this polymer. The T_β/T_g ratio is 0.83.

The conclusion of these observations is that the T_β/T_g ratio is not only a measure of the degree of coupling of the T_β and T_g processes, but also of the degree to which intermolecular factors, simultaneously or independently, influence these processes. It is evident that coupling of the processes increases the ratio. But, coupling in the absence of major intermolecular interactions as in the case of isotactic PMMA increases the ratio even more. This is not surprising. In fact, if coupling of the β-process with the T_g process were to take place in the total absence of intermolecular interactions (i.e., limit of isolated chains), the ratio should become 1.0 since in such a case the onset of the β-process would mean the onset of the main chain motions. On this basis, in linear amorphous polyethylene where there are no polar forces, no geometrical interlocking, but high flexibility, since no motion which does not involve a segment of the main chain is feasible, there is perfect coupling of local and main chain motions and the glass transition process should occur with the β-process. Furthermore, it is interesting to note that amorphous polyisobutylene $\{CH_2 - C(CH_3)_2\}_n$ and amorphous poly(2-methyl-1-butene) $\{CH_2 - C(CH_3)(C_2H_5)\}_n$ which are nonpolar, cannot interlock geometrically [31] and are stiff, do not show a β-process [33]. These observations imply that the β-process perhaps involves freeing of intermolecular interactions and its observance is dependent upon the type and degree to which these are present.

The foregoing discussions point out that intermolecular effects, such as packing and geometrical interlocking, should be considered to be important factors in influencing transitions in polymers, and in particular those of the poly(methyl methacrylate)s.

Poly(t-Butyl Methacrylate)s

P-t-BMA polymers have received little attention compared to PMMAs. The limited published data on the transitions is summar-

ized in Table 4. It is to be noted that microtacticities of the P-t-BMA samples were not reported in these earlier studies. The present study is therefore of special interest.

As can be seen from the NMR microtacticity assignments in Table 1, the syndiotactic content of the atactic P-t-BMA sample is greater than its heterotactic content, whereas the heterotactic content of the syndiotactic P-t-BMA sample is greater than its syndiotactic content. The reason for the designated nomenclature is that the P-t-BMA polymer, which is designated as "atactic" despite its higher syndiotactic content, when converted to methyl methacrylate polymer, displayed an NMR spectrum which was similar to that of conventional PMMA (see Table 1). It is interesting to note, however, that the P-t-BMA polymer with the highest degree of syndiotacticity displayed the highest glass transition temperature, as in the case of PMMA polymers (Table 1).

Figures 7-9 show the TBA spectra for the P-t-BMAs when subjected to two different thermal cycles. They show that, like PMMAs, P-t-BMAs also display two distinct types of motion in the temperature range investigated. The high-temperature relaxations of the glass transition are observed around 124 (~0.4 cps), 115 (~0.4 cps), and 112°C (~0.5 cps) in atactic, syndiotactic, and isotactic P-t-BMAs, respectively. It is to be noted that the difference in values of T_g between syndiotactic and isotactic polymer is not as pronounced as in PMMAs. The lower-temperature β peaks are centered around 20°C. The smaller intensity of these glassy-region loss peaks in P-t-BMAs compared to PMMAs is presumably due to the bulky nature of the tertiary butyl groups. The forms of the thermomechanical spectra are those to be expected of amorphous polymers.

Unlike the TBA spectra of PMMAs, the spectra in P-t-BMAs display acute irreversibilities at low temperatures. This is evidenced by the hysteresis loops in rigidity. Furthermore, on cooling, the rigidity displays an apparent decrease in magnitude as −180°C is approached. This is indicative of cracking. Repetition of the experiments by impregnating the braids in less-concentrated (5% instead of 10%) solutions did not eliminate the occurrence of these phenomena. This brittle character in P-t-BMA polymers is a likely consequence of the bulky t-butyl side groups which presumably weaken cohesive forces. It is displayed to a lesser extent by PMMAs [34]. Similarly, whereas polyisobutylene gives reversible TBA spectra, poly 2-methyl-1-butene displays irreversibilities [30]. TBA spectra of polystyrene also display irreversibilities [34].

Experiments in which samples were cooled to temperatures where the side-group motions are presumably only slowed down rather than being frozen out, as inferred from the location of the low-temperature loss peaks, did not display such irreversibilities (Figs. 7-9).

TABLE 4

Transitions in Poly(t-butyl methacrylate)s: Literature Data

Designation*	Microtacticity	Density in g/cc, (°C)	Transition Temperatures					Temp. range °C	Ref.
			T_m °C	T_g, °C, (cps)	Method**	T_β, °C (cps)	Method**		
a	—	1.02 (—)	—	104 (—)	1	—	—	—	39
a	—	—	—	105 (—)	2	—	—	—	40
a	—	—	—	140 (60)	3	~65 (60)	3	0→150	41
a	—	—	—	—	—	~20 (1)	1	−50→100	41
a	—	1.02 (—)	—	130 (—), 118	3,5	—	—	—	5
s	—	—	—	114 (—)	5	—	—	—	5
i	—	1.02 (—)	—	97 (—), 70	3,5	—	—	—	5
a	—	—	—	132 (1)	1	~20 (1)	1	−180→150	29
a	—	—	—	160 (200)	3	~60 (200)	3	−40→180	42
i	—	—	—	130 (200)	3	~0 (200)	3	−40→180	42

*Designation: a, atactic; s, syndiotactic; i, isotactic.

**Methods: 1, mechanical; 2, volume-temperature; 3, dielectric; 4, differential thermal analysis; 5, photoelelastic.

Cooling the atactic polymer to ~—50°C, which is below the location of the maximum in its secondary loss peak, was sufficient to slow down the motions of side groups to such a degree that internal stresses developed and a small, yet observable, hysteresis loop was observed (Fig. 7). In the syndiotactic and isotactic polymers, specimens were cooled to ~0°C and ~—25°C, respectively, so as not to go too far below the location of the maximum of the secondary loss peaks. Reversibility appeared to be complete in the latter cases (Fig. 8 and 9). These observations demonstrate that internal stress generation and, in consequence, brittleness in these polymers is due to change in the degree of mobility of the bulky side groups with temperature and becomes especially significant when motions of the side groups are frozen out.

Internal stress development and brittleness in polymers have been shown to be strongly dependent upon the nature of the side groups in a number of different contexts [35-38]. For example, in a comparative study of the radiation-induced gelation of aqueous polymer solutions, it was observed that syneresis (shrinkage of the network and liberation of water) and eventually breakdown into smaller fragments of the gels occur sooner in polymers with bulkier side groups [35,36]. For example, poly(vinylpyrrolidone) undergoes syneresis before poly(vinyl alcohol) which in turn shows syneresis before poly(ethylene oxide). In another study, a correlation between brittle fracture and molecular structure of polymers involved the molecular cross-sectional area [37,38]. The systematic variation in the critical tensile breaking stress of polymers was argued to be a consequence of variations in the distance between adjacent molecules caused by bulky side groups and other steric factors.

The present observations in P-t-BMAs provide further evidence for the influence of bulky side groups and show that brittleness of polymers is connected to immobilization of side groups.

Acknowledgments

This work was supported by NASA Research Grant NGR-31-001-221 and the Textile Research Institute, Princeton, N. J.

REFERENCES

[1] N. G. McCrum, B. E. Read, and G. Williams, *Anelastic and Dielectric Effects in Polymeric Solids*, Wiley, New York, 1967.

[2] J. K. Gillham, *Encyc. Polym. Sci. Tech.* (N. Bikales, ed.), Vol. 14, Wiley-Interscience, New York, 1971, p. 76.

[3] W. R. Sorenson and T. W. Campbell, *Preparative Methods of Polymer Chemistry*, 2nd ed., Interscience, New York, 1968.

[4] W. E. Goode et al., *J. Polym. Sci.*, **46**, 317 (1960).
[5] Z. A. Azimov, S. P. Mitsengendler, and A. A. Korotkov, *Polym. Sci. USSR*, **1**, 929 (1965).
[6] E. P. Chlanda and L. G. Donaruma, *J. Appl. Polym. Sci.*, **15**, 1195 (1971).
[7] F. Arndt, *Organic Synthesis*, Coll. Vol. *II*, 165 (1943).
[8] R. F. Boyer, *Polym. Eng. Sci.*, **8** (3), 161 (1968).
[9] T. G. Fox et al., *J. Am. Chem. Soc.*, **80**, 1768 (1958).
[10] J. D. Stroupe and R. E. Hughes, *J. Am. Chem. Soc.*, **80**, 2341 (1958).
[11] Y. Kawamura et al., *J. Polym. Sci., Part A-2*, **7**, 1559 (1969).
[12] Y. Ishida, *J. Polym. Sci., Part A-2*, **7**, 1835 (1969).
[13] Yu. V. Zelenev and A. G. Novikov, *Polym. Sci. USSR*, **11** (10), 2632 (1969).
[14] T. V. Belopol'skaya and O. N. Trapeznikova, *Polym. Sci. USSR*, **13** (5), 1259 (1971).
[15] G. P. Mikhaelov and T. I. Borisova, *Polym. Sci. USSR*, **2**, 387 (1961).
[16] E. V. Thompson, *J. Polym. Sci., Part A2*, **4**, 199 (1966).
[17] Y. Ishida, S. Togami, and K. Yamafuji, *Kolloid Z.*, **222**, 16 (1968).
[18] S. Bywater and P. M. Toporowski, *Polymer*, **13**, 94 (1972).
[19] H. A. Pohl, R. Bacskai, and W. P. Purcell, *J. Phys. Chem.*, **64**, 1701 (1960).
[20] S. Brownstein and D. M. Wiles, *Can. J. Chem.*, **44**, 153 (1966).
[21] J. M. G. Cowie, *Polymer*, **10** (8), 708 (1969).
[22] F. E. Karasz, H. E. Bair, and J. M. O'Reilly, *J. Phys. Chem.*, **69**, 2657 (1965).
[23] F. E. Karasz and W. J. MacKnight, *Macromol.*, **1** (6), 537 (1968).
[24] F. P. Grigor'eva and Yu. Ya. Gotlib, *Polym. Sci. USSR*, **10**, 396 (1968).
[25] W. Wunderlich, Private Communication, letters to J. K. Gillham dated November 3, 1972 and March 14, 1973. See E. Kiran, Ph.D. Thesis, Princeton Univ., 1973.
[26] R. G. Kriste, *Makromol. Chem.*, **101**, 91 (1967).
[27] J. A. Shetter, *Polymer Letters*, **1**, 209 (1963).
[28] J. F. Johnson and R. S. Porter, in *The Stereochemistry of Macromolecules* (A. D. Ketley, ed.), Vol. 1, Dekker, New York, 1968, p. 213.
[29] J. Heijboer, in *Physics of Non-Crystalline Solids* (J. A. Prins, ed.), North Holland, Amsterdam, 1965, p. 231.
[30] J. R. Martin, Ph.D. Thesis, Dept. of Chemical Eng., Princeton University, Princeton, N.J., 1972.
[31] J. R. Martin and J. K. Gillham, *J. Appl. Polym. Sci.*, **16**, 2091 (1972).
[32] W. G. Gall and N. G. McCrum, *J. Polym. Sci.*, **50**, 489 (1961).
[33] A. Hiltner et al., *J. Macromol. Sci.—Phys.*, B9, 255 (1974).
[34] S. J. Stadnicki, Ph.D. Thesis, Princeton Univ., 1974.
[35] E. Kiran and F. Rodriguez, *23rd Int. Cong. Pure Appl. Chem.*, Vol. 8, Butterworths, London, 1971, p. 175.
[36] E. Kiran and F. Rodriguez, *J. Macromol. Sci.—Phys.*, B7, 209 (1973).
[37] P. I. Vincent, *Nature*, **233** (40), 104 (1971).
[38] P. I. Vincent, *Polymer*, **13**, 558 (1972).
[39] E. A. W. Hoff, D. W. Robinson, and A. H. Willbourn, *J. Polym. Sci.*, **18**, 161 (1955).
[40] S. S. Rogers and L. Mandelkern, *J. Phys. Chem.*, **61**, 985 (1957).
[41] J. Heijboer, *Makromol. Chem.*, 35A (1960).
[42] G. P. Mihailov, in *Physics of Non-Crystalline Solids* (J. A. Prins, ed.), North-Holland, Amsterdam, 1965, p. 270.

Received by Editor January 12, 1973
Accepted by Editor April 17, 1973